Disentangling supercohomology symmetry-protected topological phases in three spatial dimensions

Yu-An Chen,[1,*] Tyler D. Ellison,[2,†] and Nathanan Tantivasadakarn[3,‡]
[1]California Institute of Technology, Pasadena, CA 91125, USA
[2]University of Washington, Seattle, WA 98195, USA
[3]Harvard University, Cambridge, MA 02138, USA
(Dated: August 14, 2020)

We build exactly solvable lattice Hamiltonians for fermionic symmetry-protected topological (SPT) phases in $(3+1)$D classified by group supercohomology. A central benefit of our construction is that it produces an explicit finite-depth quantum circuit (FDQC) that prepares the ground state from an unentangled symmetric state. The FDQC allows us to clearly demonstrate the characteristic properties of supercohomology phases - namely, symmetry fractionalization on fermion parity flux loops – predicted by continuum formulations. By composing the corresponding FDQCs, we also recover the stacking relations of supercohomology phases. Furthermore, we derive topologically ordered gapped boundaries for the supercohomology models by extending the protecting symmetries, analogous to the construction of topologically ordered boundaries for bosonic SPT phases. Our approach relies heavily on dualities that relate certain bosonic 2-group SPT phases with supercohomology SPT phases. We develop physical motivation for the dualities in terms of explicit lattice prescriptions for gauging a 1-form symmetry and for condensing emergent fermions. We also comment on generalizations to supercohomology phases in higher dimensions and to fermionic SPT phases outside of the supercohomology framework.

CONTENTS

* E-mail: yuanchen718@gmail.com
† E-mail: ellisont@uw.edu
‡ E-mail: ntantivasadakarn@g.harvard.edu

I. INTRODUCTION

Symmetry-protected topological (SPT) phases of matter are classified by quantized invariants that capture a characteristic response to probing with symmetry defects [1–14]. SPT phases built from fermionic degrees of freedom (d.o.f.) must conserve fermion parity, and the associated fermion parity symmetry defects can be used to probe the system. Consequently, the classification of fermionic SPT (fSPT) phases, where the constituent d.o.f. may be fermions, is notably distinct from the classification of bosonic SPT (bSPT) phases, composed of only bosonic d.o.f.. In particular, in three spatial dimensions and with unitary internal symmetries, the bSPT phases are believed to be classified by group cohomology, while the fSPT phases are only *partially* classified by the more rich, group supercohomology theory [6, 12, 15–17].

The algebraic data of group cohomology can be used to construct an exactly solvable model belonging to a bSPT phase [15]. The celebrated group cohomology models yield a transparent connection between the quantized invariant - namely, a group cocycle ν - and a lattice Hamiltonian. Another feature of these models is that a finite-depth quantum circuit (FDQC) [18] that prepares the ground state from a tensor product state can be written expressly in terms of ν. Further, in Ref. [19], it was shown that the group cohomology data could be used to identify symmetric topologically ordered gapped boundaries for the group cohomology models, by enlarging the protecting symmetry group on the boundary.

In this work, we construct exactly solvable models for $(3+1)$D fSPT phases directly from the group supercohomology data that characterizes the phases. The resulting supercohomology models describe fSPT phases protected by finite unitary internal symmetries of the form $G_f = G \times \mathbb{Z}_2^f$, where $\mathbb{Z}_2^f$ denotes the fermion parity symmetry. The supercohomology data can be written as a certain pair of G-dependent functions (ρ, ν), where heuristically, ν corresponds to the data that characterizes the bSPT phases, while ρ captures a response that is intrinsic to fSPT phases [13, 14]. With this, our principal contributions can be stated as follows. For any choice of supercohomology data (ρ, ν) characterizing a $(3+1)$D fSPT phase:

(i) We construct a representative fSPT Hamiltonian with mutually commuting un-frustrated terms and verify that the quantized responses of the model correspond to the data (ρ, ν) - by explicitly computing the G-symmetry fractionalization on fermion parity fluxes.

(ii) We identify a FDQC that prepares the ground state from a symmetric product state and determine the stacking rules for supercohomology phases from the composition of the FDQCs.

(iii) We use an extension of the symmetry to build symmetric topologically ordered gapped boundaries for the supercohomology model.

Our strategy is largely motivated by the spacetime formulation in Ref. [20], wherein fSPT phases are related to particular 2-group bSPT phases through a process of bosonization. More specifically, our construction can be broken down into the three succinct steps outlined below, and shown schematically in Fig. 1.

(1) Starting with a choice of supercohomology data (ρ, ν), we first build an auxiliary bSPT model with a 2-group symmetry. The 2-group symmetry contains a $\mathbb{Z}_2$ 1-form symmetry as a subgroup.

(2) We gauge the $\mathbb{Z}_2$ 1-form subgroup by minimally coupling the model to a 2-form gauge field. This produces a symmetry-enriched $\mathbb{Z}_2$ gauge theory with an emergent fermion, referred to as the 'shadow model' [21].

(3) Finally, we pair the emergent fermion with a physical fermion and condense the composite excitation: the $\mathbb{Z}_2$ gauge theory is dual to a fermionic theory [22]. The result is a model for a fSPT phase characterized by the supercohomology data (ρ, ν).

Relation to previous work:

Our work can be viewed as a generalization of the exactly solvable supercohomology models in $(2+1)$D, described in Refs. [21, 23, 24]. Similarly, the first step is to construct an auxiliary bSPT model from the supercohomology data. In the case discussed here, however, the auxiliary bSPT phase is protected by a higher-form symmetry.

In the pioneering work of Ref. [16], representative wave functions for supercohomology phases were identified by studying re-triangulation invariant non-linear σ models on a discrete spacetime manifold. Later, Ref. [17] provided a comprehensive classification of fSPT phases on a spatial lattice, by solving for consistent domain wall decorations. Our work builds on these results by constructing an explicit parent Hamiltonian for their fixed point wave functions along with FDQCs that prepare the ground states from a product state. Within our framework, we are also able to demonstrate that the supercohomology models indeed exhibit the universal responses to symmetry fluxes captured by the supercohomology data (ρ, ν).

Our strategy for constructing the supercohomology models mirrors the methods employed at the level of spacetime partition functions in Refs. [20, 25, 26]. In particular, Ref. [25] studies supercohomology phases by constructing a Lagrangian for the associated shadow model. However, we go beyond studying the shadow model and explicitly implement the fermionization duality to establish supercohomology data as quantized invariants of lattice Hamiltonians. In recent work, Ref. [26] constructed gapped boundaries for spacetime models of supercohomology phases using a symmetry extension. We employ a similar symmetry extension to construct the supercohomology Hamiltonians on a manifold with boundary.

We note that many of the models constructed in this text describe intrinsically interacting fSPT phases [7, 8]. That is, there are neither interacting bosonic counterparts nor free-fermionic representations of the phases. Hence, in particular, our work falls outside of the scope of Refs. [27–29].

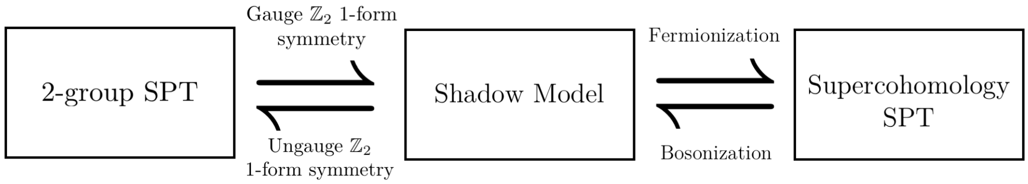

FIG. 1. To construct a $G_f = G \times \mathbb{Z}_2^f$ supercohomology SPT model we start with a model for a particular 2-group SPT phase determined by the supercohomology data (ρ, ν). Next, we gauge the $\mathbb{Z}_2$ 1-form symmetry of the 2-group to build the shadow model. We then condense the fermion in the shadow model, or apply the fermionization duality, to obtain a model for the supercohomology SPT phase corresponding to (ρ, ν).

Structure of the paper:

In Section II, we define the quantized invariants of supercohomology phases and present our supercohomology models in terms of the associated data. Subsequently, we describe the derivation of the bulk supercohomology models in Sections III and IV. In Section III, we give an example of our construction, for the case where the protecting symmetry is simply $G_f = \mathbb{Z}_2^f$. We use the opportunity to introduce the notation of cohomology on a manifold M, which is used throughout the text. Furthermore, in Section III B and Section III C, we detail a lattice prescription for gauging a 1-form symmetry and condensing an emergent fermion, respectively. Section IV describes the construction of the supercohomology models more generally, where the protecting symmetry is $G_f = G \times \mathbb{Z}_2^f$. We show that the lattice Hamiltonians are indeed characterized by the supercohomology data and recover the additive group structure of supercohomology phases under the operation of stacking by composing the corresponding FDQCs in Section IV D. Section V presents the symmetry extension method for constructing symmetric gapped boundaries for the supercohomology models; we leave the detailed derivation to Appendix K. In Appendix A, we compile the notation used in the text. We discuss spin structure and the bosonization duality of Ref. [22] in Appendix F. In Appendices I and J, we give a concise review the construction of supercohomology models in $(2+1)$D and 2-group gauge theory, respectively. Lastly, Appendix L gives an example of the symmetry extensions used to construct the models with a boundary. The remaining appendices provide the technical details and explicit calculations used in the derivation of our models.

II. SUPERCOHOMOLOGY MODELS

Before discussing the construction of the supercohomology models in Sections III and IV, we give a concise description of the models themselves. We begin with a definition for the supercohomology data (ρ, ν), and we assume familiarity with group cohomology. The group cohomology notation used here is summarized in Appendix A 1. In Section II B, we then review the group cohomology models of Ref. [15]. We finish with Section II C, where we define the more general supercohomology models and describe the stacking rules for the supercohomology phases, derived from the composition of FDQCs.

A. Supercohomology data

The supercohomology data gives quantized invariants for $(3+1)$D fSPT phases protected by a finite onsite[1] unitary $G_f = G \times \mathbb{Z}_2^f$ symmetry. To streamline the discussion, we refer to Appendix A 1 for a review of the notation from group cohomology. We freely use the notion of group cochains, the coboundary operator δ, and the cup-n products $\cup_n$ with $n \in \{0, 1, 2\}$ in the discussion below.

For a finite group G, the supercohomology data is given by a pair of group cochains (ρ, ν) belonging to:

$$(\rho, \nu) \in C^3(G, \mathbb{Z}_2) \times C^4(G, \mathbb{R}/\mathbb{Z}). \tag{1}$$

Furthermore, ρ and ν satisfy the relations [16]:

$$\delta\rho = 0, \quad \delta\nu = \frac{1}{2}\rho \cup_1 \rho. \tag{2}$$

Note that if $\rho = 0$, then ν is a group cocycle ($\delta\nu = 0$). In this case, the supercohomology data reduces to the data that characterizes bSPT phases within the group cohomology framework [15].

The supercohomology data is further organized into equivalence classes. Two sets of supercohomology data (ρ, ν) and (ρ', ν') are considered equivalent if there exists:

$$\beta \in C^2(G, \mathbb{Z}_2), \quad \eta \in C^3(G, \mathbb{R}/\mathbb{Z}), \tag{3}$$

such that:

$$\begin{aligned} \rho' &= \rho + \delta\beta \\ \nu' &= \nu + \delta\eta + \frac{1}{2}\beta \cup \beta + \frac{1}{2}\beta \cup_1 \delta\beta + \frac{1}{2}\rho \cup_2 \delta\beta. \end{aligned} \tag{4}$$

In Section IV D, we give physical motivation for the equivalence relation, by showing that (ρ, ν) and (ρ', ν') are equivalent if and only if the corresponding supercohomology models belong to the same fSPT phase.[2]

---

[1] An onsite representation of a 0-form G symmetry is a representation of G in which, for all $g \in G$ the representation $V(g)$ is a tensor product of linear representations of G on each site.

[2] We emphasize that we assume $G_f = G \times \mathbb{Z}_2^f$ for a unitary G.

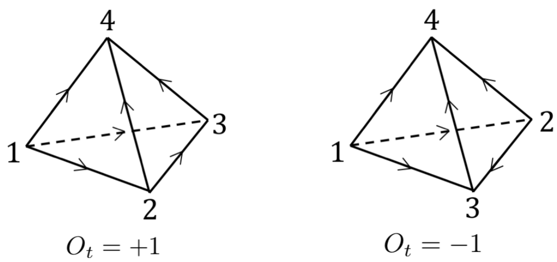

FIG. 2. A branching structure determines an ordering of the vertices of a tetrahedron. The vertices are ordered by the number of edges oriented towards the vertex. The branching structure also gives an orientation of each tetrahedron relative to the orientation of M. We use the convention that the tetrahedron pictured on the left is positively oriented ($O_t = +1$), and the tetrahedron to the right is negatively oriented ($O_t = -1$).

Throughout the text, we use the convention that group cochains are homogeneous. Therefore, in what follows, we take ρ and ν to be functions:

$$\begin{aligned} \rho &: G^4 \to \mathbb{Z}_2 = \{0,1\}, \\ \nu &: G^5 \to \mathbb{R}/\mathbb{Z} = [0,1), \end{aligned} \tag{5}$$

which are homogeneous, i.e., for any $h \in G$:

$$\begin{aligned} \rho(g_0,g_1,g_2,g_3) &= \rho(hg_0,hg_1,hg_2,hg_3), \\ \nu(g_0,g_1,g_2,g_3,g_4) &= \nu(hg_0,hg_1,hg_2,hg_3,hg_4). \end{aligned} \tag{6}$$

B. Review of group cohomology models

When ρ is zero, the supercohomology data is equivalent to the familiar group cohomology data, which characterizes $(3+1)$D bSPT phases with a finite onsite unitary G symmetry. As a consequence, the corresponding group cohomology models are a special case of the supercohomology models. We build up to the supercohomology models in Section II C by first reviewing the group cohomology models of Ref. [15].

The group cohomology models are defined on an arbitrary triangulation of an orientable closed 3-manifold M. The triangulation of M gives a decomposition of M into vertices, edges, faces, and tetrahedra. We further require that the triangulation is equipped with a branching structure – an assignment of an orientation to each edge in such a way that there are no cycles around any of the faces. A branching structure yields both an ordering of the vertices of each tetrahedron as well as an orientation $O_t \in \{-1,+1\}$ of any tetrahedron t relative to the orientation of M (see Fig. 2).

The Hilbert spaces for the group cohomology models are formed by placing a G d.o.f. on each vertex of M (Fig. 3). A basis for the $|G|$ dimensional Hilbert space at vertex v is given by states $|g_v\rangle$ labeled by elements of G. Furthermore, a basis for the full Hilbert space is given by product states of the form $|\{g_v\}\rangle$, in which, the state at vertex v is $|g_v\rangle$. The G symmetry is represented using the regular representation, i.e.,

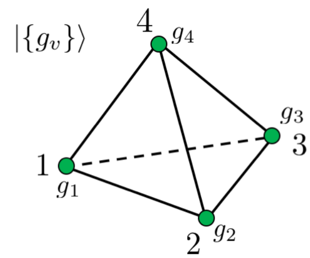

FIG. 3. The group cohomology models are defined on a Hilbert space consisting of a G d.o.f. on every vertex. The configuration states $|\{g_v\}\rangle$ form a basis for the Hilbert space.

for any $h \in G$, h is represented by:

$$V(h) \equiv \sum_{\{g_v\}} |\{hg_v\}\rangle\langle\{g_v\}|. \tag{7}$$

The group cohomology models can be built from a G-paramagnet Hamiltonian – a Hamiltonian belonging to the trivial SPT phase. The G-paramagnet Hamiltonian is given by:

$$H^G \equiv -\sum_v \mathcal{P}_v, \tag{8}$$

where the sum is over vertices in M, and $\mathcal{P}_v$ is a projector onto a symmetric state at the vertex v, i.e.:

$$\mathcal{P}_v \equiv \frac{1}{|G|}\left(\sum_{g_v}|g_v\rangle\right)\left(\sum_{g_v}\langle g_v|\right). \tag{9}$$

The ground state $|\Psi^G\rangle$ of the G-paramagnet Hamiltonian is a tensor product of a symmetric state at each vertex. This can be written as an equal amplitude superposition over all $\{g_v\}$ configurations:

$$|\Psi^G\rangle \equiv \sum_{\{g_v\}} |\{g_v\}\rangle. \tag{10}$$

Here, as elsewhere in the text, we omit the normalization of the state for notational convenience.

We build the group cohomology model corresponding to the group cocycle ν by conjugating H^G by a FDQC $\mathcal{U}_b$. $\mathcal{U}_b$ is defined in terms of the data ν as [15]:

$$\mathcal{U}_b \equiv \sum_{\{g_v\}} \prod_{t=\langle 1234\rangle} e^{2\pi i O_t \nu(1,g_1,g_2,g_3,g_4)} |\{g_v\}\rangle\langle\{g_v\}|, \tag{11}$$

where the product is over all tetrahedra in M, the vertices specifying the tetrahedron $\langle 1234\rangle$ are ordered according to the branching structure, and 1, in the argument of ν, denotes the identity in G. To simplify the notation, we introduce an operator $\hat{\boldsymbol{\nu}}(\langle 1234\rangle)$, for each tetrahedron $\langle 1234\rangle$ in M:

$$\hat{\boldsymbol{\nu}}(\langle 1234\rangle) \equiv \sum_{\{g_v\}} \nu(1,g_1,g_2,g_3,g_4)|\{g_v\}\rangle\langle\{g_v\}|. \tag{12}$$

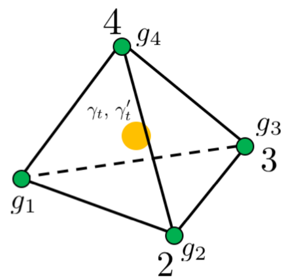

FIG. 4. Our model for a fSPT phase is defined on a Hilbert space with G d.o.f. on the vertices of a triangulation of M and a single spinless complex fermion at the center of each tetrahedron.

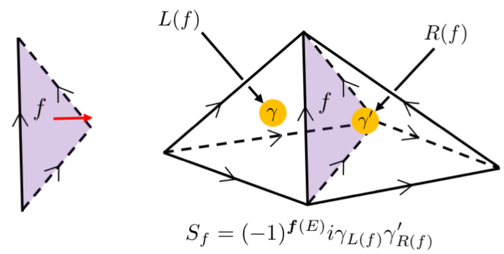

FIG. 5. The orientation of a face f (red vector) is determined by the branching structure. The orientation of f points out of the tetrahedron $L(f)$ and into the tetrahedron $R(f)$. The hopping operator S_f acts with γ on the complex fermion Hilbert space at $L(f)$ and γ' on the site at $R(f)$.

With this, $\mathcal{U}_b$ can be written more compactly as:

$$\mathcal{U}_b = \prod_t e^{2\pi i O_t \hat{\boldsymbol{\nu}}(t)}. \tag{13}$$

The Hamiltonian for the group cohomology model is then:

$$H_b \equiv \mathcal{U}_b H^G \mathcal{U}_b^\dagger, \tag{14}$$

with the unique ground state:

$$\begin{aligned} |\Psi_b\rangle &\equiv \mathcal{U}_b |\Psi^G\rangle \\ &= \sum_{\{g_v\}} \prod_{t=\langle 1234\rangle} e^{2\pi i O_t \nu(1,g_1,g_2,g_3,g_4)} |\{g_v\}\rangle. \end{aligned} \tag{15}$$

The Hamiltonian H_b indeed describes a bSPT phase. This is because the Hamiltonian is both symmetric and has a unique short-range entangled (SRE) ground state. The symmetry of the Hamiltonian follows from the fact that $\mathcal{U}_b$ is symmetric, which can be shown using the property $\delta\nu = 0$. The ground state is SRE, since it can be prepared from a product state by the FDQC $\mathcal{U}_b$.[3] Furthermore, the group cohomology models exhibit the characteristic responses encoded by ν, as can be checked by introducing symmetry defects or gauging the G symmetry and analyzing the properties of the symmetry fluxes [9, 12].

C. Definition of supercohomology models

We now generalize the discussion to supercohomology models, which describe fSPT phases. We leave the explicit derivation of the models from a choice of supercohomology data (ρ, ν) to Sections III and IV. Similar to the group cohomology models, the supercohomology models are prepared from a Hamiltonian in a trivial SPT phase by conjugation with a FDQC. Further, the FDQCs for (ρ, ν) and (ρ', ν') can be used to recover the stacking laws for supercohomology phases, discussed at the end of this section.

The supercohomology models are defined on a Hilbert space with G d.o.f. at the vertices of M, as in the previous section, along with a fermionic d.o.f. at each tetrahedron. Specifically, we place a single spinless complex fermion at the center of each tetrahedron and label the two Majorana operators at the tetrahedron t by γ_t and γ'_t (see Fig. 4). The fermion parity at t is then given by:

$$P_t \equiv -i\gamma_t\gamma'_t, \tag{16}$$

and we also introduce a "hopping" operator S_f that changes the fermion parity on either side of the face f:

$$S_f \equiv (-1)^{\boldsymbol{f}(E)} i\gamma_{\mathrm{L}(f)}\gamma'_{\mathrm{R}(f)}. \tag{17}$$

Here, $L(f)$ and $R(f)$ are the tetrahedra neighboring f such that the orientation of f points out of the tetrahedron $L(f)$ and into the tetrahedron $R(f)$ (see Fig. 5). $\boldsymbol{f}(E) \in \{0,1\}$ corresponds to a choice of spin-structure and is determined by the branching structure of the triangulation of M. We refer to Appendix F and Ref. [30] for the explicit form of $\boldsymbol{f}(E)$. As before, the G symmetry is represented with the regular representation, and here the global fermion parity symmetry is generated by $\prod_t P_t$.

The supercohomology models are built from a Hamiltonian belonging to a trivial fSPT phase - namely, an atomic insulator with a decoupled G-paramagnet. The trivial fSPT Hamiltonian is explicitly:

$$H^G_{\mathrm{AI}} \equiv -\sum_t P_t - \sum_v \mathcal{P}_v. \tag{18}$$

The ground state $|\Psi^G_{\mathrm{AI}}\rangle$ of H^G_{AI} is a product state with zero fermion occupancy at each tetrahedron and a symmetric state at each vertex.

Given a choice of supercohomology data (ρ, ν), we prepare the supercohomology model from H^G_{AI} by conjugation with the FDQC $\mathcal{U}_f$:

$$\mathcal{U}_f \equiv \prod_t e^{2\pi i O_t \hat{\boldsymbol{\nu}}(t)} \xi_\rho(M) \prod_f S_f^{\hat{\boldsymbol{\rho}}(f)} \prod_t P_t^{\int \hat{\boldsymbol{\rho}} \cup_2 \boldsymbol{t}}. \tag{19}$$

---

[3] We note that, although $\mathcal{U}_b$ is symmetric, this does not imply that the state $|\Psi_b\rangle$ in Eq. (15) belongs to the trivial SPT phase. This is only the case if $\mathcal{U}_b$ can additionally be expressed as a FDQC composed of symmetric local unitaries.

Let us unpack the notation used in the definition of $\mathcal{U}_f$. First of all, the $\hat{\boldsymbol{\nu}}(t)$ term is analogous to the FDQC $\mathcal{U}_b$ in Section II B, tensored with the identity on the fermionic d.o.f.. Second, the product over hopping operators in Eq. (19) depends on a choice of ordering for the faces $f \in M$, since not all hopping operators commute. However, $\xi_\rho(M)$ is an order dependent sign that compensates for the choice of ordering. Therefore, in the end, the FDQC is independent of the choice of ordering for the faces in M. We give the explicit form of $\xi_\rho(M)$ in Section IV D.[4] $\hat{\boldsymbol{\rho}}(f)$ is the ρ-dependent operator:

$$\hat{\boldsymbol{\rho}}(\langle 123\rangle) \equiv \sum_{\{g_v\}} \rho(1, g_1, g_2, g_3)|\{g_v\}\rangle\langle\{g_v\}|, \tag{20}$$

for an arbitrary face $\langle 123\rangle$ and implicitly tensored with the identity on the fermionic d.o.f.. Finally, for a tetrahedron $t = \langle 1234\rangle$, $\int \hat{\boldsymbol{\rho}} \cup_2 \boldsymbol{t}$ is shorthand for:

$$\int \hat{\boldsymbol{\rho}} \cup_2 \boldsymbol{t} = \hat{\boldsymbol{\rho}}(\langle 123\rangle) + \hat{\boldsymbol{\rho}}(\langle 134\rangle). \tag{21}$$

The exactly-solvable fermionic Hamiltonian produced by conjugating H^G_{AI} by $\mathcal{U}_f$ is thus:

$$H_f \equiv \mathcal{U}_f H^G_{\text{AI}} \mathcal{U}_f^\dagger, \tag{22}$$

which has the unique ground state $|\Psi_f\rangle$:

$$|\Psi_f\rangle \equiv \mathcal{U}_f |\Psi^G_{\text{AI}}\rangle. \tag{23}$$

H_f describes a system in a $G\times\mathbb{Z}_2^f$ fermionic SPT phase, because (i) H_f is symmetric and (ii) it has a unique, SRE ground state [Eq. (23)]. The Hamiltonian in Eq. (22) is symmetric, since both H^G_{AI} and $\mathcal{U}_f$ are invariant under the symmetry – we argue that $\mathcal{U}_f$ is symmetric in Section IV D. The ground state is unique and SRE, because H_f is unitarily equivalent to a trivial fSPT Hamiltonian with a unique ground state and the unitary is a FDQC.

Most importantly, H_f belongs to the fSPT phase characterized by the corresponding supercohomology data (ρ, ν). We show this in Section IV D, by gauging the fermion parity symmetry of H_f. This results in a G-symmetry-enriched $\mathbb{Z}_2$ gauge theory, where the G symmetry fractionalizes on the fermion parity flux loops, as determined by ρ. The appropriate responses to G-symmetry defects follow from the bosonic, group cohomology case.

We can gain intuition for the fSPT Hamiltonian by inserting the right hand side of Eq (18) into the expression for H_f:

$$H_f = -\sum_t \left(\mathcal{U}_f P_t \mathcal{U}_f^\dagger\right) - \sum_v \left(\mathcal{U}_f \mathcal{P}_v \mathcal{U}_f^\dagger\right). \tag{24}$$

[4] We note that while $\xi_\rho(M)$ depends on a global ordering of the faces in M, it can nonetheless be implemented by a FDQC. This can be seen from the derivation of $\xi_\rho(M)$ in Appendix H 2.

By commuting the hopping operators of $\mathcal{U}_f$ past the parity operator P_t and using that $\delta\rho = 0$, the tetrahedron terms become:

$$-\sum_t \left(\mathcal{U}_f P_t \mathcal{U}_f^\dagger\right) = -\sum_{t=\langle 1234\rangle} (-1)^{\rho(g_1,g_2,g_3,g_4)} P_t. \tag{25}$$

In the ground state, the fermion occupancy depends on the $\{g_v\}$-configuration. For a $\{g_v\}$-configuration $|\{g_v\}\rangle$, it is energetically preferable for the fermion occupancy at the tetrahedron $\langle 1234\rangle$ to be equal to $\rho(g_1, g_2, g_3, g_4)$. In this way, complex fermions are bound to junctions of symmetry domains. The vertex terms of H_f, on the other hand:

$$-\sum_v \left(\mathcal{U}_f \mathcal{P}_v \mathcal{U}_f^\dagger\right), \tag{26}$$

are more difficult to compute, in general. Heuristically, they fluctuate the G d.o.f. and create, move, and annihilate fermions without affecting the tetrahedron terms in Eq. (25). The ground state is thus a weighted superposition of $\{g_v\}$-configurations with the fermion occupancy at each tetrahedron $\langle 1234\rangle$ equal to $\rho(g_1, g_2, g_3, g_4)$. This is in agreement with the fixed point wave functions in Ref. [17].

Stacking rules for supercohomology phases:

With this, we can deduce the stacking rules for supercohomology phases. We recall that two states can be stacked by taking the tensor product. Given two G-SPT states $|\Psi_{\text{SPT}_1}\rangle$ and $|\Psi_{\text{SPT}_2}\rangle$, the stacked state $|\Psi_{\text{SPT}_1}\rangle \otimes |\Psi_{\text{SPT}_2}\rangle$ also belongs to a G-SPT phase. Thus, the stacking of G-SPT states induces an operation $\boxtimes$ at the level of the SPT phases.

In Ref. [23], it was argued that the stacking operation $\boxtimes$ on SPT phases can be determined from the composition of FDQCs. To state the result from Ref. [23], we define $\mathcal{U}_{\text{SPT}_1}$ and $\mathcal{U}_{\text{SPT}_2}$ to be symmetric FDQCs that prepare the G-SPT states $|\Psi_{\text{SPT}_1}\rangle$ and $|\Psi_{\text{SPT}_2}\rangle$, respectively, from a symmetric product state. According to Ref. [23], if $|\Psi_{\text{SPT}_1}\rangle$ and $|\Psi_{\text{SPT}_2}\rangle$ belong to the same Hilbert space, then the composition of the FDQCs $\mathcal{U}_{\text{SPT}_1}$ and $\mathcal{U}_{\text{SPT}_2}$ prepares a state belonging to the same G-SPT phase as $|\Psi_{\text{SPT}_1}\rangle \otimes |\Psi_{\text{SPT}_2}\rangle$.

With this, we determine the group law under stacking for $(3+1)$D supercohomology phases by composing the FDQCs $\mathcal{U}_f$ defined in Eq. (19). Given two sets of supercohomology data (ρ, ν) and (ρ', ν') both characterizing fSPT phases with a $G \times \mathbb{Z}_2^f$ symmetry, we consider stacking the ground states of the corresponding supercohomology models, denoted by $|\Psi_f^{\rho\nu}\rangle$ and $|\Psi_f^{\rho'\nu'}\rangle$, respectively. The result from Ref. [23] tells us that the stacked state $|\Psi_f^{\rho\nu}\rangle \otimes |\Psi_f^{\rho'\nu'}\rangle$ belongs to the same phase as the state prepared by applying $\mathcal{U}_f^{\rho'\nu'}\mathcal{U}_f^{\rho\nu}$ to a symmetric product state. Here, $\mathcal{U}_f^{\rho\nu}$ and $\mathcal{U}_f^{\rho'\nu'}$ are the FDQCs from Eq. (19) that prepare $|\Psi_f^{\rho\nu}\rangle$ and $|\Psi_f^{\rho'\nu'}\rangle$ from an unentangled symmetric state, respectively. In Appendix H 3, we show that the composition $\mathcal{U}_f^{\rho'\nu'}\mathcal{U}_f^{\rho\nu}$ is equivalent to a FDQC $\mathcal{U}_f^{\rho''\nu''}$ corresponding to a set of supercohomology data (ρ'', ν''):

$$(\rho'', \nu'') = (\rho + \rho', \nu + \nu' + \frac{1}{2}\rho \cup_2 \rho'). \tag{27}$$

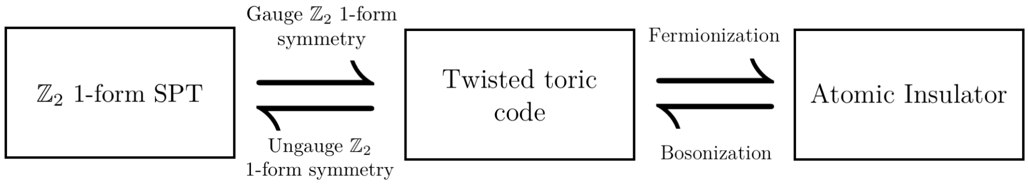

FIG. 6. In the case of $G_f = \mathbb{Z}_2^f$, the construction of a fermionic model starts with a model for a certain $\mathbb{Z}_2$ 1-form SPT phase. We then gauge the $\mathbb{Z}_2$ 1-form symmetry to obtain a twisted toric code. Lastly, we fermionize the twisted toric code, and the result is a model for an atomic insulator.

Therefore, at the level of the supercohomology data, the stacking operation $\boxtimes$ is:

$$(\rho, \nu) \boxtimes (\rho', \nu') = (\rho + \rho', \nu + \nu' + \frac{1}{2}\rho \cup_2 \rho'), \tag{28}$$

in agreement with Ref. [16].

III. BULK CONSTRUCTION: $G_f = \mathbb{Z}_2^f$

We begin by illustrating our construction of exactly-solvable models for fSPT phases in the simplest possible case – for fSPT phases protected by only fermion parity symmetry $\mathbb{Z}_2^f$. While the resulting fSPT model is trivial (an atomic insulator), we nonetheless find this example instructive in demonstrating the general strategy. Moreover, we use this as an opportunity to introduce notation used throughout the paper.

To start, we describe a model for a certain bosonic SPT phase protected by a $\mathbb{Z}_2$ 1-form symmetry in (3+1)D. The special property of this bosonic SPT is that, upon gauging the $\mathbb{Z}_2$ 1-form symmetry, we obtain a $\mathbb{Z}_2$ gauge theory with an emergent fermion. We refer to this $\mathbb{Z}_2$ gauge theory as the *twisted* toric code. In the final step, we employ the fermionization duality of Ref. [31] to map the twisted toric code to a model with a fundamental fermion. The construction is shown schematically in Fig. 6, for the case of $G_f = \mathbb{Z}_2^f$.

A. 1-form SPT and notation

SPT phases protected by higher form symmetries, including 1-form symmetries, were first introduced in Ref. [32]. Subsequently, fixed point Hamiltonians for 1-form SPT phases were described in detail in Refs. [33] and [34]. We note that the Hamiltonian discussed in this section agrees with the model in Ref. [34] and is closely related to the $\mathbb{Z}_2 \times \mathbb{Z}_2$ 1-form SPT model of Ref. [33].[5]

Our model for a nontrivial $\mathbb{Z}_2$ 1-form SPT phase can be defined on an arbitrary triangulation of an oriented closed 3-manifold M equipped with a branching structure, as described

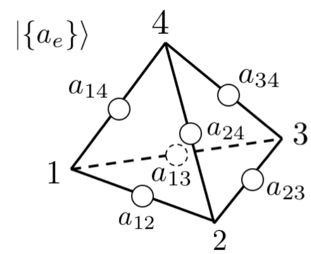

FIG. 7. The 1-form SPT model is defined on a triangulation where each edge hosts a $\mathbb{Z}_2$ d.o.f. (represented by a circle). A state in the configuration basis is given by a value $a_e \in \{0, 1\}$ chosen for each edge e. We have suppressed the branching structure for clarity.

in Section II B. We define a Hilbert space on M using the triangulation of the manifold – at each edge of the triangulation, we place a single $\mathbb{Z}_2$ degree of freedom. Correspondingly, a basis for the Hilbert space at edge e is given by states $|a_e\rangle$ with a_e valued in $\{0, 1\}$. The Pauli Z and Pauli X operators at each e act as:

$$Z_e|a_e\rangle = (-1)^{a_e}|a_e\rangle, \quad X_e|a_e\rangle = |a_e + 1\rangle, \tag{29}$$

where addition is taken modulo 2. A basis for the total Hilbert space consists of states $|\{a_e\}\rangle$ labeled by configurations $\{a_e\}$ (Fig. 7). Here, the state $|\{a_e\}\rangle$ denotes a product state with the d.o.f. at edge e in the state $|a_e\rangle$.

The $\mathbb{Z}_2$ 1-form symmetry acts on closed codimension-1 submanifolds of the dual lattice. In particular, we represent the symmetry action on a closed surface Σ of the dual lattice with the operator:

$$A_\Sigma \equiv \prod_{e \perp \Sigma} X_e, \tag{30}$$

where the product is over edges intersected by the surface Σ (see Fig. 8).

We construct our model for the nontrivial SPT phase starting with a Hamiltonian for a $\mathbb{Z}_2$ 1-form paramagnet. The Hamiltonian for the 1-form paramagnet is given by:

$$H_0 = -\sum_e X_e. \tag{31}$$

H_0 is certainly symmetric, as it commutes with A_Σ for every surface Σ of the dual lattice. Further, the unique ground state

[5] Specifically, our model is equivalent to the model in Ref. [33] on a four-colorable triangulation and upon restricting to the diagonal $\mathbb{Z}_2$ of the $\mathbb{Z}_2 \times \mathbb{Z}_2$ symmetry.

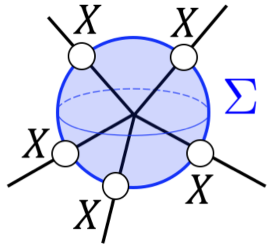

FIG. 8. The 1-form symmetry operators act on closed surfaces in the dual lattice. Pauli X operators are applied to each edge intersected by the surface. The figure shows a surface Σ (blue) that encloses a single vertex.

of H_0 is a product state with the $+1$ eigenstate of X_e at each edge e. This state can be expressed in the configuration basis as:

$$|\Psi_0\rangle \equiv \sum_{\{a_e\}} |\{a_e\}\rangle, \tag{32}$$

with the sum over all configurations $\{a_e\}$.

Now, our model for the nontrivial $\mathbb{Z}_2$ 1-form SPT phase is built from the 1-form paramagnet in Eq. (31) by conjugation with the FDQC:

$$\mathcal{U}_1 \equiv \sum_{\{a_e\}} \prod_{t=\langle 1234\rangle} (-1)^{a_{12}(a_{23}+a_{34}+a_{24})} |\{a_e\}\rangle\langle\{a_e\}|. \tag{33}$$

Specifically, the Hamiltonian of the nontrivial $\mathbb{Z}_2$ 1-form SPT model is:

$$H_1 \equiv \mathcal{U}_1 H_0 \mathcal{U}_1^\dagger = -\sum_e \mathcal{U}_1 X_e \mathcal{U}_1^\dagger. \tag{34}$$

Indeed, H_1 describes a *nontrivial* $\mathbb{Z}_2$ 1-form SPT phase. In the next section, we show this by gauging the the 1-form symmetry. The 1-form paramagnet H_0 is mapped to a $\mathbb{Z}_2$ gauge theory with an emergent boson - the usual 3D toric code, while H_1 is mapped to a $\mathbb{Z}_2$ gauge theory with an emergent fermion - a “twisted toric code”.

For now, we note that the model in Eq. (34) is symmetric and exactly solvable. In Appendix B, we show that $\mathcal{U}_1$ is symmetric under the $\mathbb{Z}_2$ 1-form symmetry. Consequently, H_1 is also symmetric. Furthermore, the model is exactly solvable, since by construction, the terms in H_1 are mutually commuting and unfrustrated. The unique ground state is then expressly:

$$\begin{aligned} |\Psi_1\rangle &\equiv \mathcal{U}_1|\Psi_0\rangle \\ &= \sum_{\{a_e\}} \prod_{t=\langle 1234\rangle} (-1)^{a_{12}(a_{23}+a_{34}+a_{24})} |\{a_e\}\rangle. \end{aligned} \tag{35}$$

To further motivate this model, we recount the spacetime construction of the $\mathbb{Z}_2$ 1-form SPT phase in Ref. [34]. We consider a partition function for the SPT phase on the cone of M, denoted CM, which is the $(3+1)$D spacetime formed by connecting a single spacetime vertex to each vertex of the closed manifold M as shown in Fig. 9. This produces a manifold with a boundary equal to M. We refer to the edges connected to the additional spacetime point as “time-like” edges and extend the branching structure so that the time-like edges have an orientation pointing away from the additional spacetime vertex. Then, the partition function for the 1-form SPT model is [34]:[6]

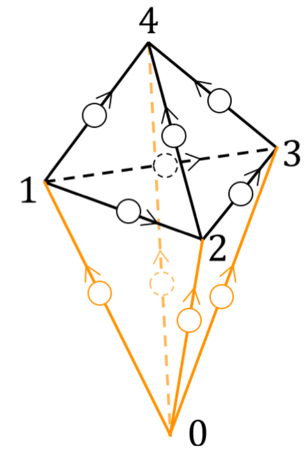

FIG. 9. The cone of M is constructed by connecting the vertices of M to an additional spacetime point labeled by 0. A tetrahedron of the spatial manifold M is shown in black. The time-like edges (orange) are oriented away from the 0 vertex. The 1-form SPT partition function is defined on CM with $\mathbb{Z}_2$ d.o.f. on the time-like edges (orange circles). Due to the re-triangulation invariance of the partition function, a_{01}, a_{02}, and a_{03} can be set to 0.

$$\mathcal{Z}_1 = \sum_{\{a_e\}} \prod_{\langle 01234\rangle} (-1)^{(a_{01}+a_{12}+a_{02})(a_{23}+a_{34}+a_{24})}, \tag{36}$$

with the product over spacetime 4-simplices. The amplitude for a fixed configuration $\{a_e\}$:

$$\Psi_1(\{a_e\}) \equiv \prod_{\langle 01234\rangle} (-1)^{(a_{01}+a_{12}+a_{02})(a_{23}+a_{34}+a_{24})}, \tag{37}$$

is topological in the sense that it is invariant under re-triangulations of the spacetime manifold. Through re-triangulations, it can be seen that the values of a_e on the time-like edges do not affect the amplitude. Therefore, we may set their value to 0, for simplicity. As a result, the amplitude for a configuration $\{a_e\}$ on M reduces to:

$$\Psi_1(\{a_e\}) \equiv \prod_{t=\langle 1234\rangle} (-1)^{a_{12}(a_{23}+a_{34}+a_{24})}, \tag{38}$$

where the product is over tetrahedra $t = \langle 1234\rangle$ in the boundary of CM. This gives the amplitude $\Psi_1(\{a_e\})$ for a wave

[6] Using notation introduced later in the text, the expression:

$$(a_{01} + a_{12} + a_{02})(a_{23} + a_{34} + a_{24}),$$

can be written as $\delta\boldsymbol{a}_e \cup \delta\boldsymbol{a}_e(\langle 01234\rangle)$. $\delta\boldsymbol{a}_e \cup \delta\boldsymbol{a}_e$ is a nontrivial $\mathbb{Z}_2$ 1-form cocycle that has been pulled back to CM.

function on M with the configuration $\{a_e\}$, as in Eq. (35). We remark that this construction parallels the approach for building 0-form SPT Hamiltonians in Ref. [15].

$\mathbb{Z}_2$ cohomology on M

At this point, we find it convenient to introduce the language of $\mathbb{Z}_2$ cohomology on M. The cohomology notation allows for compact expressions and, in our opinion, more transparent calculations. Here, we only describe the necessary ingredients, and we leave a more thorough summary to Appendix A 2. In the process of introducing concepts from $\mathbb{Z}_2$ cohomology on M, we re-express the 1-form SPT model using the corresponding notation. In particular, we aim to write H_1 in an explicit form.

To begin, we define a p-cochain as a linear, $\mathbb{Z}_2$-valued function of p-simplices in M. For example, we can consider the 1-cochain $\boldsymbol{e}$ defined by:

$$\boldsymbol{e}(e') = \begin{cases} 1 & e' = e \\ 0 & \text{otherwise.} \end{cases} \tag{39}$$

In words, $\boldsymbol{e}$ evaluates to 1 on the edge e and 0 on all other edges. More general 1-cochains can be formed from linear combinations of 1-cochains of the form in Eq. (39). Specifically, for each configuration $\{a_e\}$ we can define a corresponding 1-cochain $\boldsymbol{a}_e$ as:

$$\boldsymbol{a}_e \equiv \sum_{\boldsymbol{e}} a_e \boldsymbol{e}. \tag{40}$$

Evaluating $\boldsymbol{a}_e$ on an edge e' gives:

$$\boldsymbol{a}_e(e') = \sum_{\boldsymbol{e}} a_e \boldsymbol{e}(e') = a_{e'}. \tag{41}$$

Given the correspondence between 1-cochains and configurations $\{a_e\}$ in Eq. (40), we can label a configuration state $|\{a_e\}\rangle$ by the 1-cochain $\boldsymbol{a}_e$:

$$|\{a_e\}\rangle \to |\boldsymbol{a}_e\rangle. \tag{42}$$

In this notation, a Pauli Z operator at edge e' acts on the state $|\boldsymbol{a}_e\rangle$ as:

$$Z_{e'}|\boldsymbol{a}_e\rangle = (-1)^{\boldsymbol{a}_e(e')}|\boldsymbol{a}_e\rangle, \tag{43}$$

and an $X_{e'}$ operator acts as:

$$X_{e'}|\boldsymbol{a}_e\rangle = |\boldsymbol{a}_e + \boldsymbol{e}'\rangle. \tag{44}$$

Moreover, the action of the 1-form symmetry operator A_Σ on a configuration state is:

$$A_\Sigma|\boldsymbol{a}_e\rangle = \prod_{e\perp\Sigma} X_e|\boldsymbol{a}_e\rangle = |\boldsymbol{a}_e + \sum_{e\perp\Sigma}\boldsymbol{e}\rangle = |\boldsymbol{a}_e + \boldsymbol{\Sigma}\rangle, \tag{45}$$

where we have defined the 1-cochain $\boldsymbol{\Sigma}$ as:

$$\boldsymbol{\Sigma} \equiv \sum_{e\perp\Sigma} \boldsymbol{e}. \tag{46}$$

Next, we introduce the coboundary operator δ, which is a linear map taking p-cochains to $(p+1)$-cochains. Specifically, it maps a p-cochain $\boldsymbol{c}$ to the $(p+1)$-cochain $\delta\boldsymbol{c}$ for which:

$$\delta\boldsymbol{c}(s) = \boldsymbol{c}(\partial s), \tag{47}$$

where s is any $(p+1)$-simplex and ∂s denotes a formal sum of p-simplices in the boundary of s. Simply put, the $(p+1)$-cochain $\delta\boldsymbol{c}$ is evaluated on a $(p+1)$-simplex s by evaluating $\boldsymbol{c}$ on the boundary components of s. The coboundary of $\boldsymbol{a}_e$, for example, is a 2-cochain satisfying:

$$\begin{aligned}\delta\boldsymbol{a}_e(\langle 123\rangle) &= \boldsymbol{a}_e(\langle 12\rangle + \langle 23\rangle + \langle 13\rangle) \\ &= \boldsymbol{a}_e(\langle 12\rangle) + \boldsymbol{a}_e(\langle 23\rangle) + \boldsymbol{a}_e(\langle 13\rangle) \\ &= a_{12} + a_{23} + a_{13},\end{aligned} \tag{48}$$

for a face $\langle 123\rangle$.

If the coboundary of a p-cochain is 0, we call the p-cochain closed. The 1-cochain $\boldsymbol{\Sigma}$ in Eq. (46) is closed, i.e.:

$$\delta\boldsymbol{\Sigma} = 0. \tag{49}$$

This is because Σ is a closed surface of the dual lattice. As such, for any face f, the boundary of f contains an even number of edges intersected by Σ.

Further, we define the cup product $\cup$. The cup product maps a p-cochain $\boldsymbol{c}$ and a q-cochain $\boldsymbol{d}$ to a $(p+q)$-cochain $\boldsymbol{c}\cup\boldsymbol{d}$. Specifically, $\boldsymbol{c}\cup\boldsymbol{d}$ evaluated on a $(p+q)$-simplex $\langle 0,\dots,p+q\rangle$ is:

$$\boldsymbol{c}\cup\boldsymbol{d}(\langle 0,\dots,p+q\rangle) = \boldsymbol{c}(\langle 0,\dots,p\rangle)\boldsymbol{d}(\langle p,\dots,p+q\rangle). \tag{50}$$

$\boldsymbol{c}$ is evaluated on the p-simplex formed by the first $p+1$ vertices, while $\boldsymbol{d}$ is evaluated on q-simplex formed by the last $q+1$ vertices.

A suggestive example of the cup product comes from considering $\boldsymbol{a}_e\cup\delta\boldsymbol{a}_e$. $\boldsymbol{a}_e\cup\delta\boldsymbol{a}_e$ evaluated on a tetrahedron $\langle 1234\rangle$ gives:

$$\begin{aligned}\boldsymbol{a}_e\cup\delta\boldsymbol{a}_e(\langle 1234\rangle) &= \boldsymbol{a}_e(\langle 12\rangle)\delta\boldsymbol{a}_e(\langle 234\rangle) \\ &= a_{12}(a_{23}+a_{34}+a_{24}).\end{aligned} \tag{51}$$

Referring to Eq. (33), we see that the FDQC $\mathcal{U}_1$ can be written as:

$$\mathcal{U}_1 = \sum_{\boldsymbol{a}_e}\prod_t (-1)^{\boldsymbol{a}_e\cup\delta\boldsymbol{a}_e(t)}|\boldsymbol{a}_e\rangle\langle\boldsymbol{a}_e|, \tag{52}$$

with the sum over all 1-cochains.

To simplify the notation, we use the shorthand:

$$\int_N \boldsymbol{c} \equiv \sum_{s\in N}\boldsymbol{c}(s), \tag{53}$$

where $\boldsymbol{c}$ is a p-cochain, N is a p-dimensional manifold, and the sum is over p-simplices s in N. Throughout the text, unless specified otherwise, it should be assumed that the integral is over the manifold M. In particular, we can make the replacement:

$$\int \boldsymbol{a}_e \cup \delta \boldsymbol{a}_e = \sum_{t\in M} \boldsymbol{a}_e \cup \delta \boldsymbol{a}_e(t). \tag{54}$$

With this, the circuit $\mathcal{U}_1$ is:

$$\mathcal{U}_1 = \sum_{\boldsymbol{a}_e} (-1)^{\int \boldsymbol{a}_e \cup \delta \boldsymbol{a}_e} |\boldsymbol{a}_e\rangle\langle \boldsymbol{a}_e|, \tag{55}$$

and the ground state in Eq. (35) is:

$$|\Psi_1\rangle = \sum_{\boldsymbol{a}_e} (-1)^{\int \boldsymbol{a}_e \cup \delta \boldsymbol{a}_e} |\boldsymbol{a}_e\rangle. \tag{56}$$

Lastly, we introduce the cup-1 product $\cup_1$. Although abstract, the cup-1 product allows for a convenient form of the Hamiltonian H_1 and is key to our analysis of the twisted toric code in the subsequent section. The cup-1 product takes a p-cochain $\boldsymbol{c}$ and a q-cochain $\boldsymbol{d}$ to a $(p+q-1)$-cochain $\boldsymbol{c} \cup_1 \boldsymbol{d}$. Explicitly, $\boldsymbol{c} \cup_1 \boldsymbol{d}$ evaluated on a $(p+q-1)$-simplex $\langle 0, \dots, p+q-1\rangle$ is:

$$\begin{aligned} &\boldsymbol{c} \cup_1 \boldsymbol{d}(\langle 0, \dots, p+q-1\rangle) = \\ &\sum_{i=0}^{p-1} \boldsymbol{c}(\langle 0, \dots, i, q+i, \dots, p+q-1\rangle)\boldsymbol{d}(\langle i, ..., q+i\rangle). \end{aligned} \tag{57}$$

A useful example, relevant to our expression for H_1, is the cup-1 product of $\boldsymbol{f}$ and $\delta\boldsymbol{e}$. Here, $\boldsymbol{f}$ is the 2-cochain that evaluates to 1 on the face f and 0 for all other faces:

$$\boldsymbol{f}(f') = \begin{cases} 1 & f' = f \\ 0 & \text{otherwise}. \end{cases} \tag{58}$$

The 3-cochain $\boldsymbol{f} \cup_1 \delta\boldsymbol{e}$ evaluated on a tetrahedron $\langle 1234\rangle$ is [using Eq. (57)]:

$$\begin{aligned} \boldsymbol{f} \cup_1 \delta\boldsymbol{e}(\langle 1234\rangle) = \boldsymbol{f}(\langle 134\rangle)\delta\boldsymbol{e}(\langle 123\rangle) \\ +\boldsymbol{f}(\langle 124\rangle)\delta\boldsymbol{e}(\langle 234\rangle). \end{aligned} \tag{59}$$

Now, with the notation from $\mathbb{Z}_2$ cohomology on M, we can express H_1 in Eq. (34) in a compact form. In Appendix B, we show that:

$$H_1 = -\sum_e \Big(X_e \prod_f W_f^{\int \boldsymbol{f} \cup_1 \delta \boldsymbol{e}} \Big). \tag{60}$$

Above, we have used W_f to denote the product of Z_e around the face f:

$$W_f \equiv \prod_{e\subset f} Z_e. \tag{61}$$

While the product in Eq. (60) is over all faces in M, the Hamiltonian is indeed local. This is because $\boldsymbol{f} \cup_1 \delta \boldsymbol{e}(t) = 0$, if the face f and edge e do not both belong to the tetrahedron t. Heuristically, X_e is "dressed" with loops of Pauli Z operators around certain faces near e [Fig. 10].

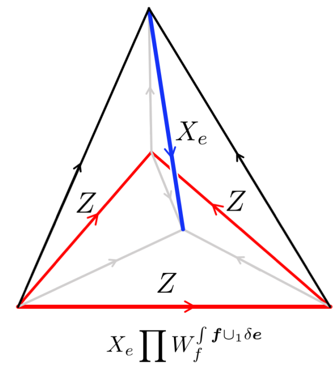

FIG. 10. Pictured above is an example of a term in H_1 associated to an edge e with three tetrahedra meeting at e. The operator acts with X_e on e (blue) and with Pauli Z operators on edges nearby (shown in red). The placement of the Pauli Z operators depends on the branching structure through the exponent $\int \boldsymbol{f} \cup_1 \delta\boldsymbol{e}$.

B. Twisted toric code

The twisted toric code is constructed from H_1 in Eq. (60) by gauging the $\mathbb{Z}_2$ 1-form symmetry. In this section, we provide a physical description of the gauging procedure following the steps outlined in Ref. [1]. In Appendix C, we discuss the subtleties of the procedure and describe the process at the level of states, as in Ref. [33]. After gauging the 1-form symmetry of H_1, we show that the resulting twisted toric code admits localized excitations with fermionic statistics.

The prescription for gauging a $\mathbb{Z}_2$ 0-form symmetry in Ref. [1] naturally generalizes to gauging a $\mathbb{Z}_2$ 1-form symmetry. In particular, the 1-form symmetry is gauged according to the following steps.

1. We introduce $\mathbb{Z}_2$ d.o.f. on faces corresponding to 2-form gauge fields. We denote the Pauli Z and Pauli X operators at the face f by Z_f and X_f, respectively.

2. We impose a gauge constraint at each edge e:

$$X_e \prod_{f\supset e} X_f = 1, \tag{62}$$

where the product is over faces containing e. This constraint can be interpreted as a 1-form Gauss law. We note that the operator $X_e \prod_{f\supset e} X_f$ defines a local action of the 1-form symmetry. That is, a product of $X_e \prod_{f\supset e} X_f$ over edges intersected by a closed surface Σ in the dual lattice yields the 1-form symmetry operator A_Σ.

3. To make coupling to the gauge field in the subsequent step unambiguous, we energetically enforce a "no flux condition". The point-like 1-form gauge flux can be detected by the operator W_t, where W_t is a product of Z_f operators around a tetrahedron t:

$$W_t \equiv \prod_{f\subset t} Z_f. \tag{63}$$

Model with $\mathbb{Z}_2$ 1-form symmetry	Model with dual $\mathbb{Z}_2$ 1-form symmetry
X_e	$\prod_{f \supset e} X_f$
$W_f = \prod_{e \subset f} Z_e$	Z_f
$A_\Sigma = \prod_{e \perp \Sigma} X_e,\ \delta \boldsymbol{\Sigma} = 0$	1
1	$M_\sigma = \prod_{f \subset \sigma} Z_f,\ \partial \sigma = 0$

TABLE I. In the process of gauging the 1-form symmetry, the generators of local, 1-form symmetric operators are mapped according to the duality above. The symmetry operators A_Σ are mapped to the identity in the dual theory. The system on the right-hand side has a $\mathbb{Z}_2$ 1-form symmetry, generated by membrane operators M_σ, where σ is a closed 2D surface on the direct lattice.

Therefore, the no flux condition is enforced by adding to the Hamiltonian the term:

$$-\sum_t W_t. \tag{64}$$

In addition, we conjugate each Hamiltonian term by a local projector onto the zero flux subspace in the vicinity of the term. That is, for a Hamiltonian term whose support[7] is contained in the bounded region R, we conjugate by a projector:

$$\mathcal{P}_R^{\text{0-flux}} \equiv \prod_{t \in R} \frac{(1+W_t)}{2}, \tag{65}$$

where the product is over tetrahedra in R.

4. We then minimally couple the $\mathbb{Z}_2$ 1-form symmetric model to the gauge fields, so as to make the model invariant under the gauge constraint. In particular, W_f is coupled to the gauge field as:

$$W_f \rightarrow W_f Z_f. \tag{66}$$

5. We fix a gauge by mapping gauge invariant states to representative states in which the eigenvalue of Z_e is 1 at every edge e[8]. This gauge fixed Hilbert space is equivalent to a Hilbert space with only the gauge field d.o.f. on the faces. The action of X_e on gauge invariant states is replaced by $\prod_{f \supset e} X_f$ after fixing the gauge, and $W_f Z_f$ in Eq. (66) becomes equivalent to Z_f in the gauge fixed Hilbert space. Therefore, the gauge invariant operators X_e and $W_f Z_f$ are mapped according to:

$$X_e \rightarrow \prod_{f \supset e} X_f, \quad W_f Z_f \rightarrow Z_f. \tag{68}$$

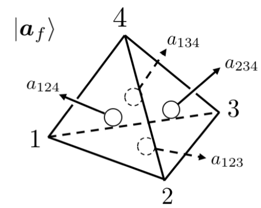

FIG. 11. We define the twisted toric code on a triangulation with $\mathbb{Z}_2$ d.o.f. at each face (represented by a circle). A configuration state is given by a value $a_f \in \{0, 1\}$ chosen for each face f.

We remark that, operationally, the gauging procedure is equivalent to a certain operator duality. In particular, the duality maps the 1-form symmetric operators X_e and W_f according to:

$$X_e \rightarrow \prod_{f \supset e} X_f, \quad W_f \rightarrow Z_f. \tag{69}$$

We have summarized the corresponding operator duality in Table I, and we refer to Appendix C for further details.

As a result of applying steps 1-5 above to our model for the nontrivial 1-form SPT phase, we obtain the twisted toric code. The twisted toric code is defined on a Hilbert space composed of $\mathbb{Z}_2$ d.o.f. attached to each face of the triangulation of M (Fig. 11). Further, a basis for the Hilbert space is given by the product states $|\{a_f\}\rangle$, where the state at the face f is $|a_f\rangle$ (with $a_f \in \{0, 1\}$). In analogy to Eq. (42), a configuration state $|\{a_f\}\rangle$ can be labeled by a 2-cochain $\boldsymbol{a}_f$:

$$\boldsymbol{a}_f \equiv \sum_f a_f \boldsymbol{f}. \tag{70}$$

With this notation, the Pauli Z and Pauli X operators acting on the face f' can be written as:

$$Z_{f'} |\boldsymbol{a}_f\rangle = (-1)^{\boldsymbol{a}_f(f')} |\boldsymbol{a}_f\rangle, \quad X_{f'} |\boldsymbol{a}_f\rangle = |\boldsymbol{a}_f + \boldsymbol{f}'\rangle. \tag{71}$$

By gauging the 1-form symmetry of H_1 [Eq. (60)], we find the twisted toric code Hamiltonian:

$$H_{\text{ttc}} \equiv -\sum_e \bar{G}_e - \sum_t W_t, \tag{72}$$

[7] The support of an operator is the set of sites on which the operator acts non-identically.

[8] More precisely, we can form an over-complete basis for the gauge invariant Hilbert space by projecting configuration basis states to the gauge invariant subspace with the operator:

$$\prod_e \left(1 + X_e \prod_{f \supset e} X_f \right). \tag{67}$$

Each gauge invariant state in this (over-complete) basis is a superposition of configuration states and includes exactly one state for which the eigenvalue of Z_e is 1 at every edge. By gauge fixing, we mean that the over-complete basis states are mapped to the "representative" state with the eigenvalue of Z_e equal to 1 at each edge. The representative states form a basis for the gauge fixed Hilbert space.

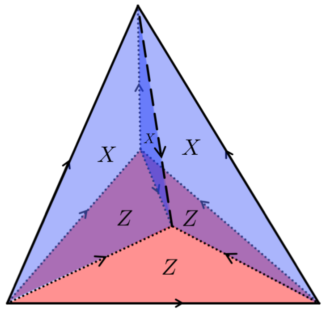

FIG. 12. An example of $\bar{G}_e$ for the edge e (dashed line) is shown above. Pauli X operators act on the faces (shaded blue) adjoined at e and Pauli Z operators (shaded red) act on nearby faces according to $\int \boldsymbol{f} \cup_1 \delta\boldsymbol{e}$.

where $\bar{G}_e$ is:

$$\bar{G}_e \equiv \prod_{f\supset e} X_f \prod_f Z_f^{\int \boldsymbol{f}\cup_1\delta\boldsymbol{e}}. \tag{73}$$

An example of the term $\bar{G}_e$ is shown in Fig 12. For simplicity, we have omitted the local projectors from step 3 of the gauging procedure. They do not affect the discussion in this section. The terms of H_{ttc} are all mutually commuting, since the gauging procedure preserves the commutation relations. We show in Appendix D that a ground state of the model is:

$$|\Psi_{\text{ttc}}\rangle \equiv \sum_{\boldsymbol{a}_e} (-1)^{\int \boldsymbol{a}_e\cup\delta\boldsymbol{a}_e} |\delta\boldsymbol{a}_e\rangle. \tag{74}$$

Note that while the expression for $|\Psi_{\text{ttc}}\rangle$ has a sum over 1-cochains $\boldsymbol{a}_e$, there are no d.o.f. on the edges. Rather, by summing over 1-cochains $\boldsymbol{a}_e$, $|\Psi_{\text{ttc}}\rangle$ is a ground state of H_{ttc} with trivial holonomy.

Excitations in the twisted toric code:

There are two types of excitations of the twisted toric code. The first, is a line-like $\mathbb{Z}_2$ 1-form gauge charge corresponding to violations of the edge terms $\bar{G}_e$. A small loop of gauge charge around the face f is created by acting with the face operator Z_f. A larger loop of gauge charge can be created by acting with Z_f on all faces contained in a 2D membrane σ of the direct lattice:

$$M_\sigma \equiv \prod_{f\subset\sigma} Z_f. \tag{75}$$

We think of the gauge charge as lying along the boundary of σ, since the membrane operator M_σ anti-commutes with the edge terms $\bar{G}_e$ for which e is in the boundary of σ.

The second type of excitation of H_{ttc} is a point-like $\mathbb{Z}_2$ 1-form gauge flux corresonding to a violation of a W_t term. A pair of gauge fluxes can be created at neighboring tetrahedra

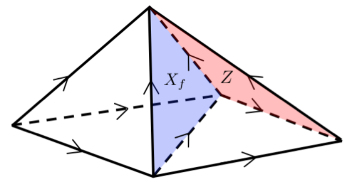

FIG. 13. The operator $\bar{U}_f$ applies a Pauli X operator at f (blue) and Pauli Z operators on certain faces of the neighboring tetrahedra (red). For a tetrahedron $t = \langle 1234\rangle$, the cup-1 product of $\boldsymbol{f}$ and $\boldsymbol{f}'$ evaluates to $\boldsymbol{f}\cup_1\boldsymbol{f}'(t) = \boldsymbol{f}(\langle 134\rangle)\boldsymbol{f}'(\langle 123\rangle) + \boldsymbol{f}(\langle 124\rangle)\boldsymbol{f}'(\langle 234\rangle)$. In the figure above, f is the $\langle 124\rangle$ face of the tetrahedron $\langle 1234\rangle$ on the right. Thus, $\bar{U}_f$ applies a Pauli Z to $f' = \langle 234\rangle$.

by the short string operator:[9]

$$\bar{U}_f \equiv X_f \prod_{f'} Z_{\boldsymbol{f}'}^{\int \boldsymbol{f}\cup_1\boldsymbol{f}'}, \tag{76}$$

pictured in Fig. 13. $\bar{U}_f$ anticommutes with the tetrahedron terms W_t on either side of the face f. Thus, we interpret the gauge fluxes as living at the centers of tetrahedra. The Pauli Z operators in Eq. (76) ensure that for any f and any e, $\bar{U}_f$ commutes with $\bar{G}_e$. The short string operators satisfy the commutation relations [22]:

$$\bar{U}_f\bar{U}_{f'} = (-1)^{\int(\boldsymbol{f}'\cup_1\boldsymbol{f}+\boldsymbol{f}\cup_1\boldsymbol{f}')}\bar{U}_{f'}\bar{U}_f, \tag{77}$$

for any faces f and f'.

Longer string operators can be formed by composing the short string operators in Eq. (76). However, a simple product of $\bar{U}_f$ operators along a path p in the dual lattice is ambiguous. This is because, given the commutation relations in Eq. (77), a product of $\bar{U}_f$ operators is generically order dependent. To remove the ambiguity, we define the following notation. For any set F of faces, we define an order independent product of $\bar{U}_f$ by:

$$\overline{\prod_{f\in F}}\bar{U}_f \equiv \prod_{f\in F}\left(\prod_{f'} Z_{\boldsymbol{f}'}^{\int \boldsymbol{f}\cup_1\boldsymbol{f}'}\right)\prod_{f\in F} X_f. \tag{78}$$

Here, all of the Pauli Z operators from the definition of $\bar{U}_f$ appear to the left of the Pauli X operators. We can then unambiguously define a gauge flux string operator $\mathcal{S}_p$ along a path p in the dual lattice by:

$$\mathcal{S}_p \equiv \overline{\prod_{f\in F_{\perp p}}}\bar{U}_f, \tag{79}$$

[9] To avoid confusion with the operator $U_f \equiv X_f \prod_{f'} Z_{\boldsymbol{f}'}^{\int \boldsymbol{f}'\cup_1\boldsymbol{f}}$ in Ref. [22], we use $\bar{U}_f$.

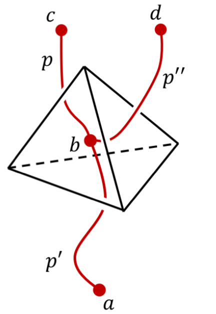

FIG. 14. The paths p, p', and p'' share a single common endpoint b inside of a tetrahedron t. Furthermore, the paths intersect distinct faces of t. Other details of the paths are unimportant in the computation of the statistics of the gauge fluxes.

where $F_{\perp p}$ denotes the set of faces intersected by p.

Remarkably, the gauge fluxes are emergent fermions. To see this, we use the methods developed in Refs. [35] and [36] for computing the statistics of anyons from microscopic models. We consider three paths p, p', and p'' along the dual lattice sharing a common endpoint, as in Fig. 14. The statistics of the gauge fluxes can be deduced by comparing the product $\mathcal{S}_p\mathcal{S}_{p'}\mathcal{S}_{p''}$ to $\mathcal{S}_{p''}\mathcal{S}_{p'}\mathcal{S}_p$.

To gain intuition for this comparison, we imagine gauge fluxes at a and b in Fig. 14. In the first process $\mathcal{S}_p\mathcal{S}_{p'}\mathcal{S}_{p''}$, the gauge flux at b is moved to c and the gauge flux at a is moved to d. Whereas, in the second process $\mathcal{S}_{p''}\mathcal{S}_{p'}\mathcal{S}_p$, the gauge flux at b is moved to d and the gauge flux at a is moved to c. The final configurations of the gauge fluxes differ by an interchange of the position of the gauge fluxes. Consequently, the difference between $\mathcal{S}_p\mathcal{S}_{p'}\mathcal{S}_{p''}$ and $\mathcal{S}_{p''}\mathcal{S}_{p'}\mathcal{S}_p$ determines the statistics of the gauge fluxes.

It can be shown that the gauge flux string operator satisfies:

$$\mathcal{S}_p\mathcal{S}_{p'}\mathcal{S}_{p''} = -\mathcal{S}_{p''}\mathcal{S}_{p'}\mathcal{S}_p. \tag{80}$$

This follows from an explicit computation using the commutation relations of the operators $\bar{U}_f$ in Eq. (77).[10] Therefore, the gauge fluxes are emergent fermions. We note that this is equivalent to saying that the twisted toric code has an anomalous $\mathbb{Z}_2$ 2-form symmetry [20, 22]. The 2-form symmetry, which, by definition, acts on closed codimension-2 subspaces, is generated by loops of the emergent fermion string operator. It is called anomalous, simply because the gauge fluxes have fermionic statistics.

Before leveraging our understanding of the twisted toric code to construct a model of physical fermions, we would like to point out that the emergent fermion string operator is not unique. In fact, we can define an alternative emergent fermion

[10] More precisely, this can be checked by explicitly computing the sign for each possible intersection at a tetrahedron. The sign for only four of the possible orientations of the tetrahedron needs to be verified, as the others follow from symmetries of the calculation.

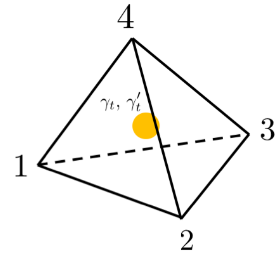

FIG. 15. The atomic insulator is defined on a Hilbert space with a single complex fermion d.o.f. (yellow circle) at each tetrahedron. The operator algebra at the tetrahedron $t = \langle 1234 \rangle$ is generated by the Majorana operators γ_t and γ_t'.

string operator built from the short segments:

$$\tilde{U}_f \equiv \bar{U}_f W_{R(f)}, \tag{81}$$

with $R(f)$ denoting the tetrahedron neighboring f in the direction of the orientation of f (see Fig. 5). The corresponding string operator along a path p in the dual lattice is:

$$\tilde{\mathcal{S}}_p \equiv \overline{\prod_{f\in F_{\perp p}} \bar{U}_f} \prod_{f\in F_{\perp p}} W_{R(f)}. \tag{82}$$

An important observation moving forward is that $\bar{G}_e$ is equivalent to a small loop of $\tilde{\mathcal{S}}_p$ string around the edge e (see Appendix E):

$$\bar{G}_e = \tilde{\mathcal{S}}_{p_e}, \tag{83}$$

where the path p_e intersects only the faces adjoined at e. Therefore, the $\bar{G}_e$ operators are local generators of an anomalous $\mathbb{Z}_2$ 2-form symmetry. Since $\bar{G}_e$ commutes with H_{ttc}, we see explicitly that the twisted toric code has an anomalous 2-form symmetry.

C. Atomic insulator

The last step of our $G = \mathbb{Z}_2^f$ example is to convert the twisted toric code into a model with physical fermions. This can be accomplished by applying the $(3+1)$D fermionization duality introduced in Ref. [22], reviewed in Appendix F. In this section, we instead opt to describe the fermionization process in terms of fermion condensation [23, 37]. That is, we construct the fermionic model by pairing emergent fermions with physical fermions and condensing the composite bosonic excitations. The fermion condensation procedure, described below, can be interpreted as a generalization of Refs. [1] and [38] to gauging an anomalous 2-form symmetry. Although an anomalous symmetry typically implies an obstruction to gauging the symmetry, we bypass the obstruction by employing fermionic d.o.f. for the gauge fields.

Our prescription for fermion condensation starts by introducing a spinless complex fermion d.o.f. at the center of each tetrahedron (Fig. 15). Thus, to prepare for the discussion of

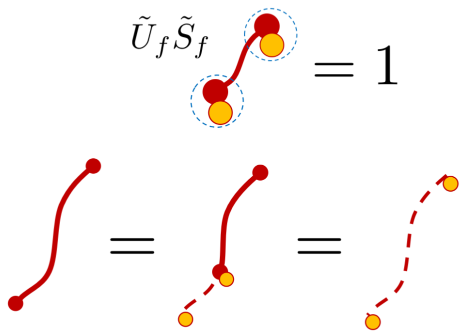

FIG. 16. To condense the emergent fermion, we impose the gauge constraint $\tilde{U}_f \tilde{S}_f = 1$. Acting on the vacuum, $\tilde{U}_f$ creates a pair of emergent fermions (red) and $\tilde{S}_f$ creates a pair of physical fermions (yellow). The composite excitation (dashed blue circle) has bosonic statistics, so it may be condensed. Heuristically, emergent fermions can be replaced with physical fermions in the constrained Hilbert space.

fermion condensation, we recall the notation for the operators on the fermionic Hilbert space, defined in Section II C. The fermion parity operator at t is:

$$P_t = -i\gamma_t \gamma'_t, \tag{84}$$

and the hopping operator S_f across the face f is:

$$S_f = (-1)^{\boldsymbol{f}(E)} i\gamma_{\mathrm{L}(f)}\gamma'_{\mathrm{R}(f)}. \tag{85}$$

$L(f)$ and $R(f)$ are defined below Eq. (17), and E is a formal sum of 2-simplices that amounts to a choice of spin-structure; see Appendix F for the explicit form of E. The hopping operators satisfy the commutation relations:

$$S_f S_{f'} = (-1)^{\int (\boldsymbol{f}' \cup_1 \boldsymbol{f} + \boldsymbol{f} \cup_1 \boldsymbol{f}')} S_{f'} S_f, \tag{86}$$

which we note matches the commutation relations of $\bar{U}_f$ in Eq. (77). Lastly, we define an alternative hopping operator $\tilde{S}_f$, instrumental for the fermion condensation prescription below:

$$\tilde{S}_f \equiv P_{L(f)} S_f. \tag{87}$$

With notation for the fermionic d.o.f. defined, we can describe the fermion condensation procedure. Our procedure applies to any Hamiltonian with an emergent fermion created by the string operator $\tilde{\mathcal{S}}_p$ in Eq. (82). In other words, the fermion condensation procedure applies to any Hamiltonian with an anomalous $\mathbb{Z}_2$ 2-form symmetry locally represented by the operators $\bar{G}_e$. Fermion condensation then proceeds as follows.

1. We introduce a spinless complex fermion d.o.f. at each tetrahedron. In terms of gauging the 2-form symmetry, the anomalous nature requires that the "3-form gauge fields" are fermionic d.o.f..

2. We impose a gauge constraint:

$$\tilde{U}_f \tilde{S}_f = 1, \tag{88}$$

for each face f. This constraint enforces a proliferation (or condensation) of composite excitations composed of an emergent fermion and a physical fermion. This is because $\tilde{U}_f$ is a short segment of emergent fermion string operator [Eq. (82)], which creates emergent fermions at the tetrahedra on either side of f, while $\tilde{S}_f$ creates physical fermions at the corresponding tetrahedra (Fig. 16). Importantly, the constraints at different faces commute, due to the matching commutation relations of $\tilde{U}_f$ and $\tilde{S}_f$ (see Appendix E). We note that the gauge constraint in Eq. (88) is a local action of the $\mathbb{Z}_2$ anomalous 2-form symmetry, in the sense that the product of $\tilde{U}_f \tilde{S}_f$ around an edge returns $\bar{G}_e$; this is guaranteed by the spin structure dependent sign in the definition of the hopping operator.

3. To make the Hamiltonian gauge invariant, i.e., commute with the constraints in Eq. (88), we couple the Hamiltonian to the fermionic d.o.f.. Since the Hamiltonian commutes with $\bar{G}_e$, it can be expressed in terms of $\bar{U}_f$ and W_t operators [22]. We couple $\bar{U}_f$ operators and W_t operators to the gauge fields as:

$$\bar{U}_f \to \bar{U}_f P_{L(f)}, \quad W_t \to W_t P_t. \tag{89}$$

To avoid possible ambiguity, we require that the coupling preserves the locality of the Hamiltonian. Any local, gauge invariant operators can be expressed in terms of the operators $\bar{U}_f P_{L(f)}$ and $W_t P_t$.

4. We fix a gauge in which the eigenvalue of Z_f is 1 at each face f. The action of $\bar{U}_f P_{L(f)}$ on the constrained space is replaced by S_f in the gauge fixed Hilbert space.[11] Further, the gauge invariant operator $W_t P_t$ becomes P_t after fixing the gauge. The generators of local, gauge invariant operators are thus mapped according to:

$$\bar{U}_f P_{L(f)} \to S_f, \quad W_t P_t \to P_t. \tag{90}$$

The mapping in Eq. (90) produces a fermionic Hamiltonian defined on a Hilbert space with a single spinless complex fermion d.o.f. at each tetrahedron, as depicted in Fig. 15.

By condensing the emergent fermion in the twisted toric code, we obtain a model for an atomic insulator. More specifically, applying the fermion condensation procedure to H_{ttc} yields the atomic insulator Hamiltonian (Appendix E):

$$H_{\text{AI}} \equiv -\sum_t P_t. \tag{91}$$

[11] This can be seen by multiplying $\bar{U}_f P_{L(f)}$ by $\tilde{U}_f \tilde{S}_f = 1$. We obtain:
$$\bar{U}_f P_{L(f)} = \bar{U}_f P_{L(f)} \tilde{U}_f \tilde{S}_f = \bar{U}_f P_{L(f)} \bar{U}_f W_{R(f)} P_{L(f)} S_f = W_{R(f)} S_f.$$
$W_{R(f)}$ acts as the identity in the fixed gauge.

Model with emergent fermions	Model with even fermion parity
$\bar{U}_f$	S_f
$W_t = \prod_{f \subset t} Z_f$	P_t
$\bar{G}_e$	1
1	$\prod_t P_t$

TABLE II. Fermion condensation implements an operator duality, wherein operators describing a model with an emergent fermion (commute with $\bar{G}_e$) are mapped to operators that act on a fermionic Hilbert space and have even fermion parity (commute with $\prod_t P_t$). For simplicity, we have only listed the local generators $\bar{G}_e$ of the anomalous 2-form symmetry.

This Hamiltonian has a unique ground state $|\Psi_{\mathrm{AI}}\rangle$, a product state with zero fermion occupancy at each tetrahedron. Excitations are physical fermions, where P_t has eigenvalue -1.

The process of gauging a non-anomalous symmetry, such as the 1-form symmetry in Section III B, can be stated as an operator duality [1]. Likewise, the fermion condensation procedure can be implemented by a mapping of operators. We summarize the corresponding duality in Table II and provide more details in Appendix F. Notably, the duality corresponding to fermion condensation maps:

$$\bar{U}_f \to S_f, \quad W_t \to P_t. \tag{92}$$

Combining Eqs. (89) and (90), we see that the duality is functionally the same as the fermion condensation procedure outlined above.

IV. BULK CONSTRUCTION: $G_f = G \times \mathbb{Z}_2^f$

We now generalize the discussion of Section III to construct fSPT models protected by a $G_f = G \times \mathbb{Z}_2^f$ symmetry. In this case, we require a choice of supercohomology data (ρ, ν). Therefore, before outlining the construction of the fSPT models, we first review the supercohomology data (ρ, ν), and introduce corresponding cochains on the manifold M. Then, we use the supercohomology data to build a 2-group SPT model, which, loosely speaking is protected by an interdependent 1-form and 0-form symmetry. Next, we gauge the 1-form symmetry of the 2-group to obtain the so-called shadow model – a symmetry-enriched twisted toric code. The shadow model is such that fermion condensation produces a model for the fSPT phase corresponding to the supercohomology data (ρ, ν). The construction is shown schematically in Fig. 1.

A. Supercohomology data on M

In Section II A, we introduced the supercohomology data (ρ, ν) as homogeneous functions:

$$\rho : G^4 \to \mathbb{Z}_2, \quad \nu : G^5 \to \mathbb{R}/\mathbb{Z}, \tag{93}$$

which, as group cochains, satisfy the relations:

$$\delta\rho = 0, \quad \delta\nu = \frac{1}{2}\rho \cup_1 \rho. \tag{94}$$

In what follows, we find it convenient to work with cochains on M – functions of simplices in the triangulation of M. Therefore, in this section, we describe how functions of G variables, can be pulled back to cochains on M.

We use the functions $\bar{\rho}$, $\bar{\rho}^h$, and $\bar{\nu}$ as examples for describing the pull back of functions to cochains on M. $\bar{\rho}$, $\bar{\rho}^h$, and $\bar{\nu}$ are defined by:

$$\bar{\rho}(g_1, g_2, g_3) \equiv \rho(1, g_1, g_2, g_3), \tag{95}$$
$$\bar{\rho}^h(g_1, g_2) \equiv \rho(1, h^{-1}, g_1, g_2), \tag{96}$$
$$\bar{\nu}(g_1, g_2, g_3, g_4) \equiv \nu(1, g_1, g_2, g_3, g_4), \tag{97}$$

with 1 denoting the identity in G. The pull backs of these functions play an important role in the construction of the supercohomology models below. We note that the functions are not group cochains, since they fail to be homogeneous.

To define cochains on M, corresponding to $\bar{\rho}$, $\bar{\rho}^h$, and $\bar{\nu}$, we assign an element of G to each vertex in the triangulation of M. We refer to the set of G labels $\{g_v\}$ as a $\{g_v\}$-configuration. With G labels on the vertices of M, functions of G^p can be pulled back to p-cochains on M. For each $\{g_v\}$-configuration, we define the cochains $\bar{\boldsymbol{\rho}}_{\{g_v\}}$, $\bar{\boldsymbol{\rho}}^h_{\{g_v\}}$, and $\bar{\boldsymbol{\nu}}_{\{g_v\}}$ on M satisfying:

$$\bar{\boldsymbol{\rho}}_{\{g_v\}}(\langle 123\rangle) \equiv \bar{\rho}(g_1, g_2, g_3), \tag{98}$$
$$\bar{\boldsymbol{\rho}}^h_{\{g_v\}}(\langle 12\rangle) \equiv \bar{\rho}^h(g_1, g_2), \tag{99}$$
$$\bar{\boldsymbol{\nu}}_{\{g_v\}}(\langle 1234\rangle) \equiv \bar{\nu}(g_1, g_2, g_3, g_4), \tag{100}$$

for an arbitrary face $\langle 123\rangle$, edge $\langle 12\rangle$, and tetrahedron $\langle 1234\rangle$.

The Hamiltonians discussed below are defined on triangulated manifolds with a G d.o.f. at every vertex, such as in Figs. 3 and 4, and a set of basis states can be labeled by $\{g_v\}$-configurations. Hence, to simplify the notation in the construction of the supercohomology models, we introduce diagonal operators for each $\{g_v\}$-dependent cochain on M. The operator associated to the $\{g_v\}$-dependent p-cochain $\boldsymbol{c}_{\{g_v\}}$ and a p-simplex s is defined as:

$$\hat{\boldsymbol{c}}(s) \equiv \sum_{\{g_v\}} \boldsymbol{c}_{\{g_v\}}(s) |\{g_v\}\rangle\langle\{g_v\}|. \tag{101}$$

The operators associated to $\bar{\boldsymbol{\rho}}_{\{g_v\}}$, $\bar{\boldsymbol{\rho}}^h_{\{g_v\}}$, and $\bar{\boldsymbol{\nu}}_{\{g_v\}}$ are thus:

$$\hat{\bar{\boldsymbol{\rho}}}(f) \equiv \sum_{\{g_v\}} \bar{\boldsymbol{\rho}}_{\{g_v\}}(f) |\{g_v\}\rangle\langle\{g_v\}| \tag{102}$$

$$\hat{\bar{\boldsymbol{\rho}}}^h(e) \equiv \sum_{\{g_v\}} \bar{\boldsymbol{\rho}}^h_{\{g_v\}}(e) |\{g_v\}\rangle\langle\{g_v\}| \tag{103}$$

$$\hat{\bar{\boldsymbol{\nu}}}(t) \equiv \sum_{\{g_v\}} \bar{\boldsymbol{\nu}}_{\{g_v\}}(t) |\{g_v\}\rangle\langle\{g_v\}| \tag{104}$$

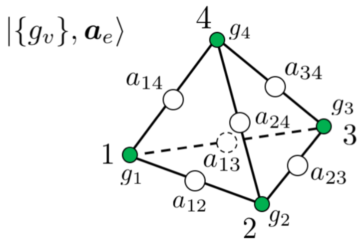

FIG. 17. The Hilbert space for the 2-group SPT model has G d.o.f. on vertices and $\mathbb{Z}_2$ d.o.f. on edges. We have labeled the states at the edges by the value of $\boldsymbol{a}_e(e) = a_e$.

for a choice of face f, edge e, and tetrahedron t. Unless otherwise stated, it should be assumed that the operators are tensored with the identity on any other d.o.f. in the model.

The coboundary operator and cup products can naturally be extended to the operators at the cochain level. For example, the coboundary of $\hat{\overline{\boldsymbol{\rho}}}$ is the operator:[12]

$$\delta\hat{\overline{\boldsymbol{\rho}}}(t) = \sum_{\{g_v\}} \delta\overline{\boldsymbol{\rho}}_{\{g_v\}}(t)|\{g_v\}\rangle\langle\{g_v\}|, \tag{105}$$

where t is an arbitrary tetrahedron. Similarly, the cup-1 product $\hat{\overline{\boldsymbol{\rho}}} \cup_1 \boldsymbol{f}(t)$ should be interpreted as:

$$\hat{\overline{\boldsymbol{\rho}}} \cup_1 \boldsymbol{f} = \sum_{\{g_v\}} \overline{\boldsymbol{\rho}}_{\{g_v\}} \cup_1 \boldsymbol{f}(t)|\{g_v\}\rangle\langle\{g_v\}|. \tag{106}$$

Using these operators we now build a Hamiltonian describing a certain 2-group SPT phase.

B. 2-group SPT

In this section, we construct a model for a 2-group SPT phase, given a set of supercohomology data (ρ, ν). The particular 2-group symmetry is dependent upon G and the group cochain ρ. For simplicity, we describe the relevant 2-group symmetry in terms of its representation on a lattice. More details on 2-groups including a formal definition can be found in Appendix J. Our model for the 2-group SPT phase is based on a Euclidean spacetime picture presented in Ref. [20], and we elaborate on the connection to this perspective at the end of this section.

The model for the 2-group SPT phase is defined on a Hilbert space consisting of a $\mathbb{Z}_2$ d.o.f. at each edge and a G d.o.f. at each vertex of a triangulation of M (see Fig. 17). As described in the previous section, a basis for the G d.o.f. is given by configuration states $|\{g_v\}\rangle$, and as in section III A, a basis for the edge d.o.f. can be formed by states $|\boldsymbol{a}_e\rangle$ labeled by $\mathbb{Z}_2$ 1-cochains $\boldsymbol{a}_e$. Thus, we use the collection of states of the form $|\{g_v\}, \boldsymbol{a}_e\rangle$ as a basis for the total Hilbert space.

The 2-group symmetry has both a $\mathbb{Z}_2$ 1-form symmetry and a certain 0-form symmetry parameterized by elements of G. Similar to Section III A, we represent the 1-form symmetry using the operators:

$$A_\Sigma = \prod_{e \perp \Sigma} X_e, \tag{107}$$

where the product is over edges intersected by the closed surface Σ on the dual lattice. The action of the 1-form symmetry operator on a basis state is explicitly:

$$A_\Sigma|\{g_v\}, \boldsymbol{a}_e\rangle = |\{g_v\}, \boldsymbol{a}_e + \boldsymbol{\Sigma}\rangle, \tag{108}$$

for a closed 1-cochain $\boldsymbol{\Sigma}$ corresponding to Σ [see Eq. (45)].

We represent the 0-form symmetry action associated to $h \in G$ as:

$$V_\rho(h) \equiv V(h) \prod_e X_e^{\hat{\overline{\boldsymbol{\rho}}}^h(e)}. \tag{109}$$

Here, $V(h)$ acts by (left) group multiplication of h on the vertex d.o.f.:

$$V(h) \equiv \sum_{\{g_v\}, \boldsymbol{a}_e} |\{hg_v\}, \boldsymbol{a}_e\rangle\langle\{g_v\}, \boldsymbol{a}_e|. \tag{110}$$

Therefore, the action of the 0-form symmetry operator $V_\rho(h)$ on a basis state is:

$$V_\rho(h)|\{g_v\}, \boldsymbol{a}_e\rangle = |\{hg_v\}, \boldsymbol{a}_e + \overline{\boldsymbol{\rho}}^h_{\{g_v\}}\rangle. \tag{111}$$

We now construct a model for an SPT phase protected by the 2-group symmetry generated by the operators in Eqs. (107) and (109). We start with the 1-form paramagnet Hamiltonian H_0 in Section III A and the decoupled G paramagnet H^G from Section II B:

$$H_0^G \equiv H_0 + H^G. \tag{112}$$

The 2-group SPT Hamiltonian is prepared from H_0^G by conjugation with the FDQC $\mathcal{U}_2$, which is a composition of two FDQC:

$$\mathcal{U}_2 = \mathcal{U}_2' \mathcal{U}_1. \tag{113}$$

$\mathcal{U}_1$ is the FDQC from Section III A – it prepares a 1-form SPT model from a 1-form paramagnet:

$$\mathcal{U}_1 = \sum_{\{g_v\}, \boldsymbol{a}_e} (-1)^{\int \boldsymbol{a}_e \cup \delta \boldsymbol{a}_e} |\{g_v\}, \boldsymbol{a}_e\rangle\langle\{g_v\}, \boldsymbol{a}_e|. \tag{114}$$

$\mathcal{U}_2'$ is a FDQC that couples the vertex d.o.f. to the edge d.o.f. and ensures that the model is 2-group symmetric. Explicitly, $\mathcal{U}_2'$ is:

$$\mathcal{U}_2' \equiv \prod_t \left[e^{2\pi i O_t\left[\hat{\overline{\nu}}(t) + \frac{1}{2}\hat{\overline{\boldsymbol{\rho}}} \cup_1 \hat{\overline{\boldsymbol{\rho}}}(t)\right]} \prod_{f \subset t} W_f^{\hat{\overline{\boldsymbol{\rho}}} \cup_1 \boldsymbol{f}(t)} \right]. \tag{115}$$

[12] In fact, $\delta\hat{\overline{\boldsymbol{\rho}}}$ is equivalent to the operator $\hat{\boldsymbol{\rho}}$, corresponding to the cochain $\boldsymbol{\rho}_{\{g_v\}}$ and the function ρ in the natural way. This follows from the coboundary relation in Eq. (94). We note that, although $\delta\overline{\boldsymbol{\rho}}_{\{g_v\}}$ is indeed equal to $\boldsymbol{\rho}_{\{g_v\}}$, this does not imply that ρ is a group coboundary. The equality holds for cochains on M. Lacking homogeneity, $\bar{\rho}$ is not a group cochain.

Here, the O_t is the orientation of each tetrahedron, defined in Fig. 2, the second product is over the faces in the boundary of t, and W_f is given in Eq. (61) . The 2-group SPT Hamiltonian H_2 is thus:

$$H_2 \equiv \mathcal{U}_2 H_0^G \mathcal{U}_2^\dagger. \tag{116}$$

In Appendix G, we prove that H_2 is indeed invariant under the 2-group symmetry operators in Eqs. (107) and (109).

The important property of this 2-group SPT Hamiltonian is revealed after gauging the 1-form symmetry of the total 2-group symmetry. In the next section, we show that the remaining 0-form G symmetry "fractionalizes" on the loop-like 1-form gauge charges according to the group cochain ρ. This property is key to characterizing the fSPT phase that results from this construction.

Before gauging the 1-form symmetry, however, we motivate the 2-group SPT model from the spacetime construction in Ref. [20]. The spacetime model is defined on CM, the cone of the closed 3-manifold M. We orient the time-like edges, those connected to the additional spacetime point, towards the vertices of M (Fig. 9). We also place a G d.o.f. on the additional spacetime point of CM as well as a $\mathbb{Z}_2$ d.o.f. on each time-like edge. The partition function for the 2-group SPT phase is taken to be:

$$\mathcal{Z}_2 \equiv \sum_{\{g_v\},\boldsymbol{a}_e} \prod_{\Delta_4} e^{2\pi i O_{\Delta_4} \boldsymbol{\alpha}_{\{g_v\}}(\Delta_4)}, \tag{117}$$

where the product is over 4-simplices Δ_4, and $\boldsymbol{\alpha}_{\{g_v\}}$ is a certain $\{g_v\}$-dependent $\mathbb{R}/\mathbb{Z}$ valued cochain on M. In particular, $\boldsymbol{\alpha}_{\{g_v\}}$ is defined in terms of the supercohomology data (ρ,ν) as:

$$\boldsymbol{\alpha}_{\{g_v\}} \equiv \boldsymbol{\nu}_{\{g_v\}} + \frac{1}{2}\boldsymbol{\rho}_{\{g_v\}} \cup_1 \boldsymbol{\epsilon}_{\{g_v\}} + \frac{1}{2}\boldsymbol{\epsilon}_{\{g_v\}} \cup \boldsymbol{\epsilon}_{\{g_v\}}. \tag{118}$$

To define $\boldsymbol{\alpha}_{\{g_v\}}$, we have introduced the cochains $\boldsymbol{\rho}_{\{g_v\}}$, $\boldsymbol{\nu}_{\{g_v\}}$, and $\boldsymbol{\epsilon}_{\{g_v\}}$. $\boldsymbol{\rho}_{\{g_v\}}$ is the $\mathbb{Z}_2$ 3-cochain given by:

$$\boldsymbol{\rho}_{\{g_v\}}(\langle 0123\rangle) \equiv \rho(g_0,g_1,g_2,g_3), \tag{119}$$

for any 3-simplex $\langle 0123\rangle$, and $\boldsymbol{\nu}_{\{g_v\}}$ is the $\mathbb{R}/\mathbb{Z}$ valued 4-cochain:

$$\boldsymbol{\nu}_{\{g_v\}}(\langle 01234\rangle) \equiv \nu(g_0,g_1,g_2,g_3,g_4), \tag{120}$$

where $\langle 01234\rangle$ is an arbitrary 4-simplex. Lastly, $\boldsymbol{\epsilon}_{\{g_v\}}$ denotes the 2-cochain:

$$\boldsymbol{\epsilon}_{\{g_v\}} \equiv \overline{\boldsymbol{\rho}}_{\{g_v\}} + \delta \boldsymbol{a}_e. \tag{121}$$

As elaborated on in Appendix J, $\boldsymbol{\alpha}_{\{g_v\}}$ is the pullback of a 2-group cocycle [20]:

$$\alpha \equiv \nu + \frac{1}{2}\rho \cup_1 \epsilon + \frac{1}{2}\epsilon \cup \epsilon, \tag{122}$$

which acts on the 2-group classifying space.

To write down the SPT state, we consider the amplitude for a fixed configuration:

$$\Psi_2\left(\{g_v\},\boldsymbol{a}_e\right) \equiv \prod_{\Delta_4} e^{2\pi i O_{\Delta_4} \boldsymbol{\alpha}_{\{g_v\}}(\Delta_4)}. \tag{123}$$

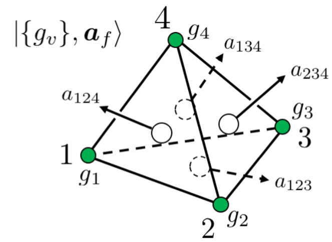

FIG. 18. The Hilbert space for the shadow model consists of G d.o.f. on vertices and $\mathbb{Z}_2$ d.o.f. on faces. In the state $|\{g_v\},\boldsymbol{a}_f\rangle$, the values of the $\mathbb{Z}_2$ d.o.f. at the faces are given by $\boldsymbol{a}_f(f) = a_f$.

The amplitude is invariant under re-triangulations of CM, so by a series of re-triangulations, we can remove both the dependence on the G d.o.f. at the additional spacetime point and the dependence on the $\mathbb{Z}_2$ d.o.f. at the time-like edges. Therefore, without affecting the amplitude, the additional d.o.f. can be set to the identity state. It can be checked that the resulting amplitude gives precisely the wave function for the ground state of the 2-group SPT Hamiltonian H_2.

C. Shadow model

The next step in our construction is to build the shadow model. We start by gauging the $\mathbb{Z}_2$ 1-form symmetry of the 2-group SPT Hamiltonian H_2. Then, we perform a change of basis to ensure that the remaining 0-form symmetry forms an onsite representation of G. The result is the shadow model – a G-symmetry-enriched twisted toric code, where the G symmetry fractionalizes on the loop-like 1-form gauge charges. We compute the symmetry fractionalization on the loop-like excitations explicitly, and show that the fractionalization is governed by the group cochain ρ in the supercohomology data (ρ,ν). In the subsequent section, we condense the emergent fermion in the shadow model to complete the construction of the $G\times\mathbb{Z}_2^f$ fSPT model corresponding to the supercohomology data (ρ,ν).

We gauge the 1-form symmetry of H_2 following the discussion in Section III B and Appendix C. As described earlier in the text, the procedure for gauging the 1-form symmetry is functionally equivalent to applying a duality that maps the 1-form symmetric operators X_e and W_f according to:

$$X_e \to \prod_{f\supset e} X_f, \quad W_f \to Z_f. \tag{124}$$

For the the 2-group SPT model, the gauging procedure maps to a Hilbert space composed of $\mathbb{Z}_2$ d.o.f. on faces and G d.o.f. on vertices (Fig. 18). A basis for this Hilbert space is given by states of the form $|\{g_v\},\boldsymbol{a}_f\rangle$, where we have used notation from Section III B to label a configuration of the face d.o.f. with a 2-cochain $\boldsymbol{a}_f$.

To apply the operator duality in Eq. (124) to H_2, we rewrite

H_2 as:

$$H_2 = \mathcal{U}_2' \left(\mathcal{U}_1 H_0^G \mathcal{U}_1^\dagger\right) \mathcal{U}_2'^\dagger, \tag{125}$$

and map $\mathcal{U}_1 H_0^G \mathcal{U}_1^\dagger$ and $\mathcal{U}_2'$ independently. $\mathcal{U}_1$ prepares the 1-form SPT model in Section III A from H_0^G, so gauging the 1-form symmetry of $\mathcal{U}_1 H_0^G \mathcal{U}_1^\dagger$ yields H_{ttc}^G, a twisted toric code with a decoupled G paramagnet:

$$H_{\text{ttc}}^G \equiv H_{\text{ttc}} + H_G^0. \tag{126}$$

Importantly, we retain the local projectors $\mathcal{P}_R^{\text{0-flux}}$ in Eq. (65) from the gauging procedure (for appropriate choices of regions R). They are needed to ensure that the shadow model is G symmetric.[13]

We next apply the duality to $\mathcal{U}_2'$. Before doing so, however, we multiply $\mathcal{U}_2'$ by the identity:[14]

$$1 = \prod_t \Big(\prod_{f\subset t} W_f\Big)^{\int \hat{\bar{\boldsymbol{\rho}}}\cup_2 \boldsymbol{t}}. \tag{127}$$

Here, we have used the cup-2 product $\cup_2$, defined in Appendix A 2. The $\cup_2$ product of $\hat{\bar{\boldsymbol{\rho}}}$ and $\boldsymbol{t}$ evaluated on the tetrahedron $\langle 1234\rangle$ is:

$$\hat{\bar{\boldsymbol{\rho}}} \cup_2 \boldsymbol{t}(\langle 1234\rangle) = \left[\hat{\bar{\boldsymbol{\rho}}}(\langle 123\rangle) + \hat{\bar{\boldsymbol{\rho}}}(\langle 134\rangle)\right] \boldsymbol{t}(\langle 1234\rangle). \tag{128}$$

After multiplying by the operator in Eq. (127), $\mathcal{U}_2'$ becomes:

$$\mathcal{U}_2' \equiv \prod_t \left[e^{2\pi i O_t\left[\hat{\bar{\boldsymbol{\nu}}}(t) + \frac{1}{2}\hat{\bar{\boldsymbol{\rho}}}\cup_1\hat{\bar{\boldsymbol{\rho}}}(t)\right]} \prod_{f\subset t} W_f^{\hat{\bar{\boldsymbol{\rho}}}\cup_1 \boldsymbol{f}(t)}\right] \times \prod_t \Big(\prod_{f\subset t} W_f\Big)^{\int \hat{\bar{\boldsymbol{\rho}}}\cup_2 \boldsymbol{t}}. \tag{129}$$

While the modification to $\mathcal{U}_2'$ has no affect on the ground state subspace of the shadow model, it is crucial to the symmetry of the FDQC in Section IV D that prepares the fSPT ground state (see Appendix H 1 for details). After the modification, $\mathcal{U}_2'$ maps to the FDQC $\mathcal{U}_s'$:

$$\mathcal{U}_s' \equiv \prod_t \left[e^{2\pi i O_t\left[\hat{\bar{\boldsymbol{\nu}}}(t) + \frac{1}{2}\hat{\bar{\boldsymbol{\rho}}}\cup_1\hat{\bar{\boldsymbol{\rho}}}(t)\right]} \prod_{f\subset t} Z_f^{\hat{\bar{\boldsymbol{\rho}}}\cup_1 \boldsymbol{f}(t)}\right] \times \prod_t W_t^{\int \hat{\bar{\boldsymbol{\rho}}}\cup_2 \boldsymbol{t}}. \tag{130}$$

The gauging procedure produces the Hamiltonian:

$$H_s' \equiv \mathcal{U}_s' H_{\text{ttc}}^G \mathcal{U}_s'^\dagger. \tag{131}$$

[13] Without the projectors, the shadow model is only guaranteed to be G symmetric up to factors of W_t.

[14] The operator $\prod_{f\subset t} W_f$ is identically 1, since: $\prod_{f\subset t} W_f = \prod_{f\subset t}\prod_{e\subset f} Z_e = \prod_{e\subset t} Z_e^2 = 1$, where the last product is over edges e in t.

H_s' is invariant under a 0-form G symmetry given by applying the gauging duality to the 0-form symmetry of the 2-group [Eq. (109)]. The 0-form symmetry operator corresponding to $h\in G$ is mapped to:

$$V_\rho'(h) \equiv V(h) \prod_{f=\langle 123\rangle} X_f^{\hat{\bar{\boldsymbol{\rho}}}^h(\langle 23\rangle) + \hat{\bar{\boldsymbol{\rho}}}^h(\langle 13\rangle) + \hat{\bar{\boldsymbol{\rho}}}^h(\langle 12\rangle)} \tag{132}$$

$$= \sum_{\{g_v\},\boldsymbol{a}_f} |\{hg_v\}, \boldsymbol{a}_f + \delta\overline{\boldsymbol{\rho}}^h_{\{g_v\}}\rangle\langle\{g_v\},\boldsymbol{a}_f|. \tag{133}$$

We notice that the resulting symmetry $V_\rho'(h)$ is not necessarily onsite. This is because the term $\delta\overline{\boldsymbol{\rho}}^h_{\{g_v\}}(f)$ in the second line of Eq. (132) depends on the $\{g_v\}$-configuration at the vertices of f, in general.

To obtain the shadow model, we make a local change of basis – implemented by a FDQC, which makes the remaining 0-form G symmetry onsite. We implement the change of basis with the unitary operator:

$$\mathcal{R} \equiv \prod_f X_f^{\hat{\bar{\boldsymbol{\rho}}}(f)}. \tag{134}$$

Every state $|\Psi\rangle$ and operator $\mathcal{O}$ is transformed as:

$$|\Psi\rangle \to \mathcal{R}|\Psi\rangle, \quad \mathcal{O} \to \mathcal{R}\mathcal{O}\mathcal{R}^\dagger. \tag{135}$$

Under the transformation above, $V_\rho'(h)$ becomes:

$$\sum_{\{g_v\},\boldsymbol{a}_f} |\{hg_v\}, \boldsymbol{a}_f + \overline{\boldsymbol{\rho}}_{\{hg_v\}} + \delta\overline{\boldsymbol{\rho}}^h_{\{g_v\}}\rangle\langle\{g_v\},\boldsymbol{a}_f + \overline{\boldsymbol{\rho}}_{\{g_v\}}|. \tag{136}$$

It can be shown, using that ρ is a cocycle [Eq. (94)], that $\overline{\boldsymbol{\rho}}_{\{g_v\}}$ and $\overline{\boldsymbol{\rho}}^h_{\{g_v\}}$ are related by:

$$\overline{\boldsymbol{\rho}}_{\{hg_v\}} + \delta\overline{\boldsymbol{\rho}}^h_{\{g_v\}} = \overline{\boldsymbol{\rho}}_{\{g_v\}}. \tag{137}$$

Thus, the operator in Eq. (136) is equivalent to the onsite symmetry action:

$$V(h) \equiv \sum_{\{g_v\},\boldsymbol{a}_f} |\{hg_v\},\boldsymbol{a}_f\rangle\langle\{g_v\},\boldsymbol{a}_f|. \tag{138}$$

We apply the basis transformation $\mathcal{R}$ to H_s' by conjugation. This produces the shadow model:

$$H_s \equiv \mathcal{R}H_s'\mathcal{R}^\dagger = \mathcal{R}\left(\mathcal{U}_s' H_{\text{ttc}}^G \mathcal{U}_s'\right)\mathcal{R}^\dagger = \mathcal{U}_s H_{\text{ttc}}^G \mathcal{U}_s^\dagger, \tag{139}$$

where, in the last line, we have introduced $\mathcal{U}_s$:

$$\mathcal{U}_s \equiv \mathcal{R}\mathcal{U}_s'. \tag{140}$$

The FDQC $\mathcal{U}_s$ is explicitly:

$$\mathcal{U}_s = \prod_f X_f^{\hat{\bar{\boldsymbol{\rho}}}(f)} \prod_t \left[e^{2\pi i O_t\left[\hat{\bar{\boldsymbol{\nu}}}(t) + \frac{1}{2}\hat{\bar{\boldsymbol{\rho}}}\cup_1\hat{\bar{\boldsymbol{\rho}}}(t)\right]} \prod_{f\subset t} Z_f^{\hat{\bar{\boldsymbol{\rho}}}\cup_1 \boldsymbol{f}(t)}\right] \times \prod_t W_t^{\int \hat{\bar{\boldsymbol{\rho}}}\cup_2 \boldsymbol{t}}. \tag{141}$$

The Hamiltonian H_s describes a symmetry-enriched twisted toric code. This is because it is both G symmetric and can be constructed from H_{ttc}^G using the FDQC $\mathcal{U}_s$. The symmetry of H_s follows from the symmetry of the 2-group SPT Hamiltonian H_2 (Appendix G).

Similar to the twisted toric code, H_s admits loop-like excitations as well as point-like excitations with fermionic statistics. In the twisted toric code, the loop-like excitations are created at the boundary of a surface σ using the membrane operator M_σ, defined in Eq. (75). Therefore, the loop-like excitations can be created in the shadow model with the operator:

$$M_\sigma^s \equiv \mathcal{U}_s M_\sigma \mathcal{U}_s^\dagger = \prod_{f\subset\sigma}\left[(-1)^{\hat{\bar{\rho}}(f)} Z_f\right], \tag{142}$$

where in the second equality we have commuted $\mathcal{U}_s$ past the Pauli Z operators in M_σ. Likewise, emergent fermion string operators in the shadow model can be formed by conjugating the twisted toric code string operators $\mathcal{S}_p$ and $\tilde{\mathcal{S}}_p$ by $\mathcal{U}_s$:

$$\mathcal{S}_p^s \equiv \mathcal{U}_s \mathcal{S}_p \mathcal{U}_s^\dagger, \quad \tilde{\mathcal{S}}_p^s \equiv \mathcal{U}_s \tilde{\mathcal{S}}_p \mathcal{U}_s^\dagger. \tag{143}$$

For certain choices of supercohomology data (ρ, ν), the corresponding shadow model describes a *nontrivial*, symmetry-enriched twisted toric code. In particular, the group cochain ρ determines the fractionalization (defined below) of the G symmetry on the loop-like 1-form gauge charges. This symmetry fractionalization partially characterizes the G-symmetry-enriched twisted toric code phase [13].

Symmetry fractionalization on loop-like excitations:

In what follows, we compute the symmetry fractionalization on the loop-like excitations of the shadow model, explicitly. We do so by considering an excited state of H_s obtained by applying M_σ^s to a ground state $|\Psi_s\rangle$ of H_s. The resulting state $M_\sigma^s|\Psi_s\rangle$ has a single loop of 1-form gauge charge along $\partial\sigma$, the boundary of σ. We study the effect of the G-symmetry action on this state to determine the fractionalization of the symmetry on the loop-like excitation.

To set up the computation and make the discussion more precise, we introduce an effective Hilbert space in the vicinity of the 1-form gauge charge. We define the state $|\psi_{\text{ttc}}, \{g_v\}_{\partial\sigma}\rangle$ to be the ground state of the twisted toric code Hamiltonian H_{ttc}^G with fixed G configuration $\{g_v\}_{\partial\sigma}$ at vertices v contained in $\partial\sigma$. The set of states $\big\{|\Psi_{\text{ttc}}, \{g_v\}_{\partial\sigma}\rangle\big\}$ spans a Hilbert space with dimension $|G|^N$, where N is the number of vertices in $\partial\sigma$. The effective Hilbert space is then formed by the states $\big\{|\Psi_s^{\partial\sigma}, \{g_v\}_{\partial\sigma}\rangle\big\}$, where $|\Psi_s^{\partial\sigma}, \{g_v\}_{\partial\sigma}\rangle$ is defined by:

$$|\Psi_s^{\partial\sigma}, \{g_v\}_{\partial\sigma}\rangle \equiv M_\sigma^s \mathcal{U}_s |\Psi_{\text{ttc}}, \{g_v\}_{\partial\sigma}\rangle. \tag{144}$$

We note that, in particular, the state $M_\sigma^s|\Psi_s\rangle$ belongs to the effective Hilbert space:

$$M_\sigma^s|\Psi_s\rangle = \sum_{\{g_v\}_{\partial\sigma}} |\Psi_s^{\partial\sigma}, \{g_v\}_{\partial\sigma}\rangle. \tag{145}$$

Heuristically, a state $|\Psi_s^{\partial\sigma}, \{g_v\}_{\partial\sigma}\rangle$ in the effective Hilbert space resembles the ground state $|\Psi_s\rangle$ far away from $\partial\sigma$[15]. Since $|\Psi_s\rangle$ is symmetric, we expect the symmetry to act as the identity on $|\Psi_s^{\partial\sigma}, \{g_v\}_{\partial\sigma}\rangle$ away from $\partial\sigma$. However, the symmetry may act non-identically on the states in the effective Hilbert space, and we define the projection of the symmetry action to the effective Hilbert space to be the *effective* symmetry action on a 1-form gauge charge. The fractionalization of the G-symmetry action is an obstruction to realizing the effective symmetry action onsite.

We next determine the effective symmetry action on the loop-like excitation by acting on an arbitrary state $|\Psi_s^{\partial\sigma}, \{g_v\}_{\partial\sigma}\rangle$ in the effective Hilbert space with the symmetry operator $V(h)$:

$$V(h)|\Psi_s^{\partial\sigma}, \{g_v\}_{\partial\sigma}\rangle = V(h) M_\sigma^s \mathcal{U}_s |\Psi_{\text{ttc}}, \{g_v\}_{\partial\sigma}\rangle. \tag{146}$$

The expression on the right hand side of Eq. (146) can be evaluated further by commuting $V(h)$ past M_σ^s and $\mathcal{U}_s$. Using the relation in Eq. (137), we find:

$$V(h) M_\sigma^s = \Big[\prod_{e\subset\partial\sigma} (-1)^{\hat{\bar{\rho}}^{h^{-1}}(e)}\Big] M_\sigma^s V(h), \tag{147}$$

and as shown in Appendix H 1, $V(h)$ commutes with $\mathcal{U}_s$ up to factors of $\bar{G}_e$:

$$V(h)\mathcal{U}_s = \mathcal{U}_s \Big[\prod_e \bar{G}_e^{\hat{\bar{\rho}}^{h^{-1}}(e)}\Big] V(h). \tag{148}$$

Therefore, the action of $V(h)$ on a state in the effective Hilbert space is:

$$V(h)|\Psi_s^{\partial\sigma}, \{g_v\}_{\partial\sigma}\rangle = \prod_{e\subset\partial\sigma} (-1)^{\hat{\bar{\rho}}^{h^{-1}}(e)} |\Psi_s^{\partial\sigma}, \{hg_v\}_{\partial\sigma}\rangle, \tag{149}$$

where we have used that $|\Psi_{\text{ttc}}, \{hg_v\}_{\partial\sigma}\rangle$ is a $+1$ eigenstate of $\bar{G}_e$. The effective symmetry action for $h \in G$ is explicitly:

$$\mathcal{V}_{\partial\sigma}(h) \equiv \sum_{\{g_v\}_{\partial\sigma}} \prod_{e\subset\partial\sigma} (-1)^{\hat{\bar{\rho}}^{h^{-1}}(e)} |\Psi_s^{\partial\sigma}, \{hg_v\}_{\partial\sigma}\rangle\langle\Psi_s^{\partial\sigma}, \{g_v\}_{\partial\sigma}|. \tag{150}$$

We identify the fractionalization of the symmetry, or an obstruction to an onsite representation, by considering the effective symmetry action restricted to a connected submanifold ℓ of $\partial\sigma$ (Fig. 19):[16]

$$\mathcal{V}_\ell(h) \equiv \sum_{\{g_v\}_\ell} \prod_{e\subset\ell} (-1)^{\hat{\bar{\rho}}^{h^{-1}}(e)} |\Psi_s^{\partial\sigma}, \{hg_v\}_\ell\rangle\langle\Psi_s^{\partial\sigma}, \{g_v\}_\ell|, \tag{151}$$

---

[15] More concretely, any reduced density matrix of the state $|\Psi_s^{\partial\sigma}, \{g_v\}_{\partial\sigma}\rangle\langle\Psi_s^{\partial\sigma}, \{g_v\}_{\partial\sigma}|$ will agree with the reduced density matrix of $|\Psi_s\rangle\langle\Psi_s|$ on regions far from $\partial\sigma$.

[16] There is some ambiguity in defining the restriction near the boundaries of ℓ. In fact, the calculation is unaffected by the particular choice. For more details, we refer to Ref. [12].

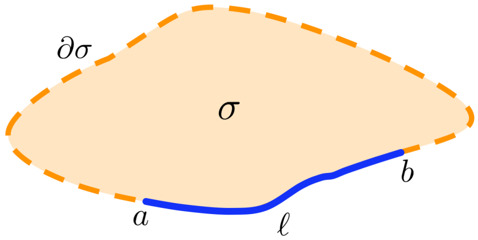

FIG. 19. A loop-like excitation is created at $\partial\sigma$ (dashed orange line) by applying the operator M_σ^s on the surface σ of the direct lattice. ℓ (thick blue line) is a connected submanifold of $\partial\sigma$ used to determine the fractionalization of the symmetry on the gauge charge. a and b label the end points of ℓ.

with $\mathcal{V}_\ell(h)$ acting as the identity on sites in $\partial\sigma$ not contained in ℓ. While $\mathcal{V}_{\partial\sigma}(h)$ satisfies the group law:

$$\mathcal{V}_{\partial\sigma}(h_1)\mathcal{V}_{\partial\sigma}(h_2) = \mathcal{V}_{\partial\sigma}(h_1h_2), \tag{152}$$

$\mathcal{V}_\ell(h)$ only satisfies the group law up to an operator $\Omega(h_1,h_2)$:

$$\mathcal{V}_\ell(h_1)\mathcal{V}_\ell(h_2) = \Omega(h_1,h_2)\mathcal{V}_\ell(h_1h_2). \tag{153}$$

For $\mathcal{V}_\ell(h)$ given in Eq. (151), we find:

$$\Omega(h_1,h_2) = \sum_{g_a,g_b}\Big[(-1)^{\rho(1,h_1,h_1h_2,g_a)+\rho(1,h_1,h_1h_2,g_b)} |\Psi_s^{\partial\sigma},g_a,g_b\rangle\langle\Psi_s^{\partial\sigma},g_a,g_b|\Big], \tag{154}$$

where we have labeled the endpoints of ℓ as a and b, and $\Omega(h_1,h_2)$ acts as the identity on all other sites in $\partial\sigma$. $\Omega(h_1,h_2)$ acts non-trivially only near the endpoints of ℓ. Hence, we can split $\Omega(h_1,h_2)$ into an operator $\Omega_a(h_1,h_2)$ acting at a and an operator $\Omega_b(h_1,h_2)$ acting at b. The decomposition is unique up to a sign,[17] which may depend on h_1 and h_2. For example, we may write:

$$\Omega_a(h_1,h_2) = \sum_{g_a}(-1)^{\rho(1,h_1,h_1h_2,g_a)}|\Psi_b^{\partial\sigma},g_a\rangle\langle\Psi_b^{\partial\sigma},g_a|, \tag{155}$$

which acts as the identity away from the endpoint a. Alternatively, we could modify both $\Omega_a(h_1,h_2)$ and $\Omega_b(h_1,h_2)$ by a sign $(-1)^{\beta(1,h_1,h_1h_2)}$, where β is an arbitrary group cochain in $C^2(G,\mathbb{Z}_2)$.

The symmetry fractionalization can be shown by analyzing the associativity of the restricted group action. The associativity of the $\mathcal{V}_\ell(h)$ operators implies (see Ref. [12]):

$$\Omega(h_1,h_2)\Omega(h_1h_2,h_3) = \mathcal{V}_\ell(h_1)\Omega(h_2,h_3)\mathcal{V}_\ell{}^\dagger(h_1)\Omega(h_1,h_2h_3). \tag{156}$$

If the effective symmetry action can be written as onsite, then Eq. (156) is satisfied independently at endpoints a and b for some choice of β. (This follows from Appendix B of Ref. [12].) On the other hand, if Eq. (156) is not satisfied independently at the endpoints for any choice of β, then there is an obstruction to realizing the effective symmetry action onsite.

For Ω_a in Eq. (155), Eq. (156) only holds up to a G-dependent sign at the endpoint a:

$$\Omega_a(h_1,h_2)\Omega_a(h_1h_2,h_3) = (-1)^{\rho(1,h_1,h_1h_2,h_1h_2h_3)} \times \mathcal{V}_\ell(h_1)\Omega_a(h_2,h_3)\mathcal{V}_\ell{}^\dagger(h_1)\Omega_a(h_1,h_2h_3). \tag{157}$$

The sign $(-1)^{\rho(1,h_1,h_1h_2,h_1h_2h_3)}$ in Eq. (157) captures the symmetry fractionalization on the 1-form gauge charge. Taking into account the ambiguity in defining Ω_a, we see that ρ is well defined up to a group coboundary $\delta\beta$, with β an arbitrary element of $C^2(G,\mathbb{Z}_2)$. In other words, the symmetry fractionalization on the loop-like excitation is described by an element of the group cohomology $H^3(G,\mathbb{Z}_2)$. Therefore, when ρ represents a nontrivial class in $H^3(G,\mathbb{Z}_2)$, there is a nontrivial symmetry fractionalization on the 1-form gauge charges of the shadow model.

The group cohomology class represented by ρ defines a quantized invariant of the symmetry-enriched twisted toric code phase. To make this explicit, we note that any state belonging to the same symmetry-enriched phase can be constructed (approximately) from $|\Psi_s\rangle$ by applying a FDQC built of symmetric local unitaries. If we modify $\mathcal{U}_s$ by a FDQC built of symmetric local unitaries, the calculation above is unchanged. Thus, the symmetry fractionalization on a gauge charge is given by the same group cohomology class for any state in the symmetry-enriched phase.

In the next section, we see that this quantized invariant may be pushed forward to characterize the corresponding fSPT obtained from condensing the emergent fermion in the shadow model.

D. Fermionic SPT

Finally, we condense the emergent fermion in the shadow model to construct a fSPT Hamiltonian corresponding to the supercohomology data (ρ,ν). In the process, we find a FDQC $\mathcal{U}_f$ that prepares the fSPT ground state from a product state. We argue that our models exhibit the expected responses to probing with fermion parity defects, by referring to the properties of the shadow models. Lastly, using the stacking rules for supercohomology phases, we verify the equivalence relation on supercohomology data in Ref. [16].

Fermion condensation, described in Section III C, can be readily applied to any Hamiltonian expressed in terms of the operators $\bar{G}_e$, $\bar{U}_f$, and W_t. The fermion is then condensed by mapping the operators according to:

$$\bar{G}_e \to 1, \quad \bar{U}_f \to S_f, \quad W_t \to P_t. \tag{158}$$

The result is a model defined on a Hilbert space with a single spinless complex fermion at each tetrahedron.

[17] The $\mathbb{Z}_2$ fusion rules of 1-form gauge charges reduce the ambiguity from a general phase to a sign [13].

To apply the fermion condensation duality in Eq. (158) to the shadow model:

$$H_s = \mathcal{U}_s H^G_{\text{ttc}} \mathcal{U}_s^\dagger, \tag{159}$$

we write H^G_{ttc} and $\mathcal{U}_s$ in terms of $\bar{G}_e$, $\bar{U}_f$, and W_t operators. By definition, H^G_{ttc} can be written using $\bar{G}_e$ and W_t. As for $\mathcal{U}_s$, the Pauli X and Pauli Z operators can be commuted to write (see Appendix H 2 for a derivation):

$$\mathcal{U}_s = \prod_t e^{2\pi i O_t \hat{\bar{\boldsymbol{\nu}}}(t)} \xi_\rho(M) \prod_f \bar{U}_f^{\hat{\bar{\boldsymbol{\rho}}}(f)} \prod_t W_t^{\int \hat{\bar{\boldsymbol{\rho}}} \cup_2 \boldsymbol{t}}. \tag{160}$$

Here, we have defined an arbitrary ordering of faces on M:

$$\{f_1, \dots, f_i, \dots\}, \quad (f_1 < \dots < f_i < \cdots), \tag{161}$$

and the product of $\bar{U}_f$ operators is determined by the order of faces in M:

$$\prod_f \bar{U}_f^{\hat{\bar{\boldsymbol{\rho}}}(f)} = \left(\cdots \bar{U}_{f_i}^{\hat{\bar{\boldsymbol{\rho}}}(f_i)} \cdots \bar{U}_{f_1}^{\hat{\bar{\boldsymbol{\rho}}}(f_1)} \right). \tag{162}$$

$\xi_\rho(M)$ in Eq. (160) is a sign that compensates for the order dependence of the product of $\bar{U}_f$ operators, so that $\mathcal{U}_s$ is independent of the choice of ordering. Specifically, $\xi_\rho(M)$ is given by (Appendix H 2):

$$\xi_\rho(M) \equiv \prod_{i,i' | i' < i} (-1)^{\hat{\bar{\boldsymbol{\rho}}}(f_{i'}) \hat{\bar{\boldsymbol{\rho}}}(f_i) \int \boldsymbol{f}_{i'} \cup_1 \boldsymbol{f}_i}. \tag{163}$$

We emphasize that, although $\xi_\rho(M)$ and the product of $\bar{U}_f$ operators depend on a choice of ordering of the faces in M, the FDQC $\mathcal{U}_s$ does *not* depend on the choice of ordering.[18]

With this, we apply the mapping of operators in Eq. (158) to H_s to condense the emergent fermion. First, H^G_{ttc} is mapped to an atomic insulator and a decoupled G paramagnet (Appendix E):

$$H^G_{\text{AI}} \equiv -\sum_t P_t - \sum_v \mathcal{P}_v. \tag{164}$$

Second, $\mathcal{U}_s$ is mapped to a FDQC $\mathcal{U}_f$:

$$\mathcal{U}_f \equiv \prod_t e^{2\pi i O_t \hat{\bar{\boldsymbol{\nu}}}(t)} \xi_\rho(M) \prod_f S_f^{\hat{\bar{\boldsymbol{\rho}}}(f)} \prod_t P_t^{\int \hat{\bar{\boldsymbol{\rho}}} \cup_2 \boldsymbol{t}}. \tag{165}$$

Thus, fermion condensation leads to the exactly-solvable fermionic Hamiltonian:

$$H_f \equiv \mathcal{U}_f H^G_{\text{AI}} \mathcal{U}_f^\dagger. \tag{166}$$

This is precisely the Hamiltonian described in Section II C.

We note that H_f is symmetric due to the symmetry of both H^G_{AI} and $\mathcal{U}_f$. To see that $\mathcal{U}_f$ is symmetric, we consider the bosonic FDQC $\mathcal{U}_s$. $\mathcal{U}_s$ commutes with the symmetry up to factors of $\bar{G}_e$ (see Appendix H 1), and since $\bar{G}_e$ maps to the identity under fermion condensation, $\mathcal{U}_f$ must commute with the symmetry.

[18] The independence on the ordering can be derived from the commutation relations: $\bar{U}_f \bar{U}_{f'} = (-1)^{\int (\boldsymbol{f}' \cup_1 \boldsymbol{f} + \boldsymbol{f} \cup_1 \boldsymbol{f}')} \bar{U}_{f'} \bar{U}_f$, as described in Appendix H 2.

Equivalence relation on supercohomology data:

For each set of supercohomology data, we can now construct a fSPT Hamiltonian H_f. However, the Hamiltonians constructed from two *a priori* different sets of supercohomology data, say (ρ, ν) and (ρ', ν'), may be within the same phase. This motivates imposing an equivalence relation on the supercohomology data, so that two sets of supercohomology data are equivalent if the corresponding Hamiltonians are in the same phase. We argue below that the appropriate equivalence relation $\sim$ on the supercohomology data is:

$$\begin{aligned}(\rho, \nu) \sim \\ (\rho + \delta\beta, \nu + \delta\eta + \frac{1}{2}\beta \cup \beta + \frac{1}{2}\beta \cup_1 \delta\beta + \frac{1}{2}\rho \cup_2 \delta\beta),\end{aligned} \tag{167}$$

which is in agreement with the equivalence relation identified using spacetime methods in Ref. [16]. In the equivalence relation, β and η are arbitrary group cochains:

$$\beta \in C^2(G, \mathbb{Z}_2), \quad \eta \in C^3(G, \mathbb{R}/\mathbb{Z}), \tag{168}$$

and the group cup products can be written explicitly using the general formulas in Appendix A 1. To justify the equivalence relation in Eq. (167), we must show that both (i) equivalent sets of supercohomology data lead to Hamiltonians in the same phase and (ii) inequivalent sets of supercohomology data give rise to Hamiltonians in distinct phases.

In what follows, we exploit the group structure of supercohomology SPT phases under stacking. The operation $\boxtimes$ on induced by stacking can be determined by composing FDQCs, as discussed in Section II C. The stacking operation $\boxtimes$ applied to (ρ, ν) and (ρ', ν') gives:

$$(\rho, \nu) \boxtimes (\rho', \nu') = (\rho + \rho', \nu + \nu' + \frac{1}{2}\rho \cup_2 \rho'). \tag{169}$$

With this, we argue that Hamiltonians constructed using equivalent sets of supercohomology data belong to the same SPT phase. To begin, we notice that the equivalence relation can be phrased in terms of the stacking operation $\boxtimes$. Any two equivalent sets of supercohomology data can be related by stacking a set of supercohomology data:

$$(\rho_0, \nu_0) \equiv (\delta\beta, \delta\eta + \frac{1}{2}\beta \cup \beta + \frac{1}{2}\beta \cup_1 \delta\beta), \tag{170}$$

for some choice of β in $C^2(G, \mathbb{Z}_2)$ and η belonging to $C^3(G, \mathbb{R}/\mathbb{Z})$. This is because stacking (ρ_0, ν_0) with an arbitrary set of supercohomology data (ρ, ν) yields:

$$\begin{aligned}(\rho, \nu) \boxtimes (\delta\beta, \delta\eta + \frac{1}{2}\beta \cup \beta + \frac{1}{2}\beta \cup_1 \delta\beta) = \\ (\rho + \delta\beta, \nu + \delta\eta + \frac{1}{2}\beta \cup \beta + \frac{1}{2}\beta \cup_1 \delta\beta + \frac{1}{2}\rho \cup_2 \delta\beta),\end{aligned} \tag{171}$$

which is equivalent to (ρ, ν) according to Eq. (167). Hamiltonians constructed from supercohomology data (ρ, ν) and any equivalent set of data $(\rho,\nu)\boxtimes(\rho_0,\nu_0)$ are indeed in the same phase. This can be seen by constructing the FDQC $\mathcal{U}_f^{\rho_0\nu_0}$ corresponding to (ρ_0,ν_0). One can show that $\mathcal{U}_f^{\rho_0\nu_0}$ is composed of symmetric local unitaries, for any choice of (ρ_0,ν_0) in Eq. (170); the calculation is analogous to Appendix F of Ref. [23]. Therefore, the composition $\mathcal{U}_f^{\rho_0\nu_0}\mathcal{U}_f^{\rho\nu}$ prepares a state in the same phase as $\mathcal{U}_f^{\rho\nu}$, when applied to an unentangled symmetric state. Thus, equivalent sets of supercohomology data correspond to Hamiltonians in the same phase.

Conversely, we show that Hamiltonians constructed using inequivalent sets of supercohomology data belong to different SPT phases. Suppose (ρ,ν) and (ρ',ν') are inequivalent, or in other words, the stack:

$$(\tilde{\rho},\tilde{\nu})\equiv(\rho,\nu)\boxtimes(\rho',\nu')^{-1} \tag{172}$$

is not equal to (ρ_0,ν_0), for any choice of (ρ_0,ν_0). Here, the inverse in Eq. (172) is taken with respect to the stacking operation. There are two possibilities in which $(\tilde{\rho},\tilde{\nu})$ is not equivalent to any (ρ_0,ν_0), and we address them in turn. The first possibility is that $\tilde{\rho}$ is a nontrivial element of $H^3(G,\mathbb{Z}_2)$, so it cannot be written as $\delta\beta$ for any choice of group cochain $\beta\in C^2(G,\mathbb{Z}_2)$. The second possibility is that $\tilde{\rho}$ is trivial, i.e., it can be written as $\delta\beta$, but $\tilde{\nu}$ is not equal to $\delta\eta+\frac{1}{2}\beta\cup\beta+\frac{1}{2}\beta\cup_1\delta\beta$ for any choice of $\eta\in C^3(G,\mathbb{R}/\mathbb{Z})$.

Case 1. If $\tilde{\rho}$ represents a nontrivial class in $H^3(G,\mathbb{Z}_2)$, then we can use the symmetry fractionalization properties of the shadow model to argue that $(\tilde{\rho},\tilde{\nu})$ must correspond to a nontrivial fSPT phase. To derive a contradiction, suppose that the Hamiltonian $H_f^{\tilde{\rho}\tilde{\nu}}$ built using $(\tilde{\rho},\tilde{\nu})$ is in a trivial fSPT phase. Then, we can find a path of symmetric gapped Hamiltonians connecting $H_f^{\tilde{\rho}\tilde{\nu}}$ to the atomic insulator Hamiltonian H_{AI}^G. For each Hamiltonian in this path, we can gauge the fermion parity symmetry – or "ungauge" the anomalous 2-form symmetry. More precisely, we can map the fermionic operators to bosonic operators according to the duality in Table II. To avoid ambiguity in this ungauging process, we conjugate the bosonic operators by local projectors onto the $\bar{G}_e=1$ subspace and add a term $-\sum_e\bar{G}_e$ to enforce the $\bar{G}_e=1$ constraint. The result of ungauging the anomalous 2-form symmetry is a symmetric gapped path of Hamiltonians connecting the shadow model corresponding to $(\tilde{\rho},\tilde{\nu})$ to the twisted toric code Hamiltonian H_{ttc}^G. This is a contradiction, because the shadow model describes a nontrivial symmetry-enriched twisted toric code when $\tilde{\rho}$ is nontrivial in $H^3(G,\mathbb{Z}_2)$, while H_{ttc}^G is in a trivial symmetry-enriched phase. Therefore, $H_f^{\tilde{\rho}\tilde{\nu}}$ is in a nontrivial SPT phase, and (ρ,ν) and (ρ',ν') must correspond to distinct fSPT phases.

Case 2. In the second case, we assume that $\tilde{\rho}$ is trivial in $H^3(G,\mathbb{Z}_2)$. Then there exists an equivalent set of supercohomology data: $(0,\tilde{\nu}')$, obtained from $(\tilde{\rho},\tilde{\nu})$ by stacking (ρ_0,ν_0) with $\rho_0=\tilde{\rho}$. Further, we can assume that $\tilde{\nu}'$ is a nontrivial cocycle, since it satisfies $\delta\tilde{\nu}'=0$, and by assumption, it cannot be written as ν_0 for any choice of ν_0 in Eq. (170). The data $\tilde{\nu}'$ thus characterizes a bosonic SPT phase with symmetry G and within the group cohomology classification. For a unitary symmetry of the form $G\times\mathbb{Z}_2^f$, the data $(0,\tilde{\nu}')$ also describes a *nontrivial* fermionic SPT phase. To see this, we gauge the fermion parity symmetry following the prescription above and argue that this yields a nontrivial symmetry-enriched twisted toric code.

The fSPT Hamiltonian associated to $(0,\tilde{\nu}')$ is equivalent to a $\tilde{\nu}'$ bSPT Hamiltonian along with a decoupled atomic insulator. Therefore, by gauging the fermion parity symmetry, we obtain a bSPT model corresponding to $\tilde{\nu}'$ stacked with a $\mathbb{Z}_2$ gauge theory (twisted toric code). We show that the stacked system belongs to a nontrivial G-symmetry-enriched twisted toric code phase by computing a quantized invariant using the dimensional reduction methods of Ref. [12].

More specifically, the characteristic group cocycle $\tilde{\nu}'$ of the bSPT phase can be extracted by first acting with the global symmetry on sites within a bounded region R. Given that the SPT state and the twisted toric code are decoupled and that the G symmetry acts as the identity on the twisted toric code d.o.f., the symmetry action on R is equivalent to applying some unitary operator - an effective symmetry action - supported solely on the G d.o.f. near the boundary of R. The quantized invariant can then be deduced from the effective symmetry action according to Ref. [12]. The process is unchanged by acting on the stacked system with any FDQC composed of G-symmetric local unitaries. Therefore, the cocycle $\tilde{\nu}'$ is an indicator that the system is in a nontrivial symmetry-enriched twisted toric code phase. If the fSPT phase with data $(0,\tilde{\nu}')$ can be connected to the trivial phase, then the $\tilde{\nu}'$ SPT phase stacked with a twisted toric code can also be connected to the trivial symmetry-enriched twisted toric code phase. This is a contradiction, and $(0,\tilde{\nu}')$ must describe a nontrivial fermionic SPT phase.

With these two cases, we have shown that $(\tilde{\rho},\tilde{\nu})$ must correspond to a nontrivial fSPT phase if (ρ,ν) and (ρ',ν') in Eq. (172) are inequivalent. Hence, inequivalent supercohomology data correspond to distinct fSPT phases, and the supercohomology data give quantized invariants for lattice Hamiltonians.

We note that the procedure for ungauging an anomalous 2-form symmetry, briefly described above, can be applied to any fermionic model. We emphasize that it is equivalent to gauging the fermion parity symmetry – the point-like 1-form fluxes in the shadow model correspond to fermion parity gauge charges and the loop-like 1-form gauge charges correspond to fermion parity gauge fluxes. We also point out that it was important to analyze the stack of (ρ,ν) and $(\rho',\nu')^{-1}$, since gauging the fermion parity of supercohomology Hamiltonians in distinct phases can yield the same symmetry-enriched twisted toric code.

V. GAPPED BOUNDARIES THROUGH SYMMETRY EXTENSION

The supercohomology models, described in Sections III and IV, characterize the bulk of the SPT phase, i.e., the Hamiltonians are defined on manifolds without boundary. In this section, we consider models on manifolds with boundary. In particular, we describe supercohomology models that feature gapped, topologically ordered boundaries. To get started, we review gapped boundaries for group cohomology models, constructed via a symmetry extension [19]. We then generalize the symmetry extension construction to supercohomology models. Our generalization relies on the connection between 2-group SPT phases and supercohomology phases. We provide the details of the construction, starting from a 2-group SPT model, in Appendix K.

A. Review of gapped boundary construction for group cohomology models

As shown in Ref. [19], symmetric gapped boundaries for group cohomology models can be constructed by first enlarging the symmetry at the boundary. One can then partially gauge the extended symmetry to produce a symmetric, topologically ordered boundary. To illustrate the construction, we consider a $(3+1)$D group cohomology model corresponding to the group cocycle $\nu \in H^4(G, \mathbb{R}/\mathbb{Z})$ with a unitary G symmetry.

We motivate the gapped boundary construction by reviewing the proof that the ground state of the group cohomology model is symmetric on a manifold without boundary. Recall that the ground state of the group cohomology model is:

$$|\Psi_b\rangle = \sum_{\{g_v\}} \Psi_b(\{g_v\}) |\{g_v\}\rangle, \tag{173}$$

with the amplitude $\Psi_b(\{g_v\})$ given by:

$$\Psi_b(\{g_v\}) \equiv \prod_{t=\langle 1234\rangle} e^{2\pi i O_t \nu(1,g_1,g_2,g_3,g_4)}. \tag{174}$$

Applying the symmetry action $V(h)$, for $h \in G$, to $|\Psi_b\rangle$ yields:

$$V(h)|\Psi_b\rangle = \sum_{\{g_v\}} \tilde{\Psi}_b(\{g_v\}) |\{g_v\}\rangle. \tag{175}$$

Here, we have shifted the indices and used the homogeneity of ν to define:

$$\tilde{\Psi}_b(\{g_v\}) \equiv \prod_{t=\langle 1234\rangle} e^{2\pi i O_t \nu(h,g_1,g_2,g_3,g_4)}. \tag{176}$$

We evaluate Eq. (176) further by using the cocycle property of ν, which tells us:

$$\begin{aligned}\nu(h,g_1,g_2,g_3,g_4) &= \nu(1,g_1,g_2,g_3,g_4) - \nu(1,h,g_2,g_3,g_4) \\ &+\nu(1,h,g_1,g_3,g_4) - \nu(1,h,g_1,g_2,g_4) + \nu(1,h,g_1,g_2,g_3).\end{aligned} \tag{177}$$

The last four terms in Eq. (177) each correspond to a face of the tetrahedron $\langle 1234\rangle$. Therefore, in substituting Eq. (177) into Eq. (176), the terms associated to faces cancel in pairs. We are left with: $\tilde{\Psi}_b(\{g_v\}) = \Psi_b(\{g_v\})$, which implies that $|\Psi_b\rangle$ is symmetric.

The cancellation of the face terms in the calculation above relies crucially on the fact that the manifold has no boundary. The wave function in Eq. (173) is not guaranteed to be

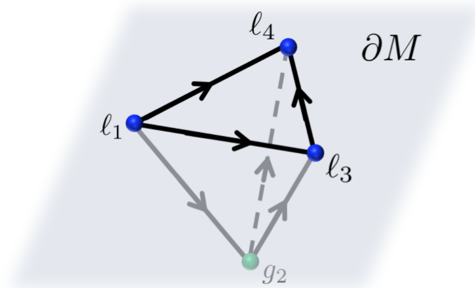

FIG. 20. The L symmetric state $|\Psi_b^L\rangle$ is defined on a Hilbert space with L d.o.f. (blue) on the boundary of M. The vertices on the interior of M host G d.o.f. (green), as in Fig. 3.

symmetric on a manifold M with boundary ∂M, since the terms associated with faces fail to cancel at the boundary. In this case, the symmetry action $V(h)$ on $|\Psi_b\rangle$ leaves a residual phase factor $\mathcal{V}_h(\{g_v\})$ on the boundary of M, i.e.:

$$\tilde{\Psi}_b(\{g_v\}) = \mathcal{V}_h(\{g_v\})\Psi_b(\{g_v\}), \tag{178}$$

where $\mathcal{V}_h(\{g_v\})$ is the phase:

$$\mathcal{V}_h(\{g_v\}) \equiv \prod_{f_\partial=\langle 123\rangle} e^{2\pi i O_{f_\partial} \nu(1,h,g_1,g_2,g_3)}. \tag{179}$$

Here, the product is over faces f_∂ in the boundary of M and $O_{f_\partial} \in \{-1,+1\}$ is -1 if the orientation of f_∂ points out of M and $+1$ otherwise. The residual phase factor is indicative of the anomalous symmetry action at the boundary of the SPT phase [12]. To find a gapped boundary, we search for a modification of $|\Psi_b\rangle$ near the boundary to "saturate" the anomaly.

The key observation, made in Ref. [19], is that the anomaly can be saturated by enlarging the symmetry at the boundary. To make this precise, we define L to be a central extension of G by a group K,[19] giving the short exact sequence:

$$1 \to K \to L \xrightarrow{\pi} G \to 1. \tag{180}$$

The group cocycle ν can then be pulled back by π to form a cocycle $\nu^* \in H^4(L, \mathbb{R}/\mathbb{Z})$:

$$\begin{aligned}&\nu^*(\ell_0,\ell_1,\ell_2,\ell_3,\ell_4) \equiv \\ &\qquad \nu\big(\pi(\ell_0),\pi(\ell_1),\pi(\ell_2),\pi(\ell_3),\pi(\ell_4)\big),\end{aligned} \tag{181}$$

with $\ell_0, \ell_1, \ell_2, \ell_3$, and ℓ_4 in L. According to Refs. [19] and [39], one can always find an extension L such that ν^* is a coboundary, i.e.:

$$\nu^* = \delta\eta, \tag{182}$$

for some η in $C^4(L, \mathbb{R}/\mathbb{Z})$. As described below, the cochain η can be used to absorb the residual phase factor in Eq. (178).

[19] By a central extension, we mean that K belongs to the center of H.

To build a symmetric wave function using η, we extend the global symmetry of the group cohomology model to L by replacing each G d.o.f. on the boundary with an L d.o.f. (see Fig. 20). We denote a configuration of the L and G d.o.f. by $\{\ell_w, g_v\}$, where ℓ_w is an element of L labeling the boundary vertex $w \in \partial M$ and g_v belongs to G and labels a vertex v in the bulk $v \in M \setminus \partial M$. For $h \in L$, the global L symmetry is then represented by:

$$V(\ell) \equiv \sum_{\{\ell_w, g_v\}} |\{\ell\ell_w, \pi(\ell)g_v\}\rangle\langle\{\ell_w, g_v\}|. \tag{183}$$

Heuristically, the symmetry acts as L on the boundary sites and G on the bulk sites.

Now, we consider a modified state built using both ν and η and show that it is invariant under the L symmetry in Eq. (183). In particular, we consider the state $|\Psi_b^L\rangle$ defined as:

$$|\Psi_b^L\rangle \equiv \sum_{\{\ell_w, g_v\}} \Psi_\eta(\{\ell_w\})\Psi_b(\{\pi(\ell_w), g_v\})|\{\ell_w, g_v\}\rangle. \tag{184}$$

Here, $\Psi_\eta(\{\ell_w\})$ is a product of η dependent phase factors corresponding to faces in ∂M:

$$\Psi_\eta(\{\ell_w\}) \equiv \prod_{f_\partial = \langle 123\rangle} e^{-2\pi i O_{f_\partial} \eta(1,\ell_1,\ell_2,\ell_3)}. \tag{185}$$

To see that $|\Psi_b^L\rangle$ is invariant under the L symmetry, we act on the state with $V(\ell)$ in Eq. (183). After shifting the indices and using the homogeneity of ν and η, we find:

$$V(\ell)|\Psi_b^L\rangle = \sum_{\{\ell_w, g_v\}} \tilde{\Psi}_\eta(\{\ell_w\})\tilde{\Psi}_b(\{\pi(\ell_w), g_v\})|\{\ell_w, g_v\}\rangle, \tag{186}$$

where $\tilde{\Psi}_\eta(\{\ell_w\})$ is the phase:

$$\tilde{\Psi}_\eta(\{\ell_w\}) \equiv \prod_{f_\partial = \langle 123\rangle} e^{-2\pi i O_{f_\partial} \eta(\ell,\ell_1,\ell_2,\ell_3)}. \tag{187}$$

The phase factors $\tilde{\Psi}_\eta(\{\ell_w\})$ and $\tilde{\Psi}_b(\{\pi(\ell_w), g_v\})$ can be simplified by using the coboundary relations for ν and η. Similar to Eq. (178), the coboundary relation for ν leads to a residual phase factor:

$$\tilde{\Psi}_b(\{\pi(\ell_w), g_v\}) = \mathcal{V}_\ell(\{\ell_w, g_v\})\Psi_b(\{\pi(\ell_w), g_v\}), \tag{188}$$

with $\mathcal{V}_\ell(\{\ell_w, g_v\})$ given by:

$$\mathcal{V}_\ell(\{\ell_w, g_v\}) \equiv \prod_{f_\partial = \langle 123\rangle} e^{2\pi i O_{f_\partial} \nu^*(1,\ell,\ell_1,\ell_2,\ell_3)}. \tag{189}$$

As for η, the coboundary relation in Eq. (182) tells us:

$$\begin{aligned}\eta(\ell,\ell_1,\ell_2,\ell_3) &= \nu^*(1,\ell,\ell_1,\ell_2,\ell_3) + \eta(1,\ell_1,\ell_2,\ell_3) \\ &- \eta(1,\ell,\ell_2,\ell_3) + \eta(1,\ell,\ell_1,\ell_3) - \eta(1,\ell,\ell_1,\ell_2).\end{aligned} \tag{190}$$

The last three terms correspond to edges in ∂M and cancel pairwise, when substituted into Eq. (187). The ν^* term in the coboundary relation of η produces a phase that precisely cancels the excess phase factor in Eq. (189):

$$\tilde{\Psi}_\eta(\{\ell_w\}) = \mathcal{V}_\ell^{-1}(\{\ell_w, g_v\})\Psi_\eta(\{\ell_w\}). \tag{191}$$

Inserting Eqs. (188) and (191) into the expression for $V(\ell)|\Psi_b^L\rangle$, we see that $|\Psi_b^L\rangle$ is symmetric under the L symmetry. The η-dependent phase factors at the boundary compensates for the failure of the bulk wave function to be symmetric. (We note the similarity with anomalous SPT states introduced in Ref. [40].)

The state $|\Psi_b^L\rangle$ can be prepared from the product state:

$$|\Psi^L\rangle \equiv \sum_{\{\ell_w, g_v\}} |\{\ell_w, g_v\}\rangle \tag{192}$$

by the FDQC $\mathcal{U}_b^L$:

$$\mathcal{U}_b^L \equiv \prod_{f_\partial} e^{-2\pi i O_{f_\partial} \hat{\boldsymbol{\eta}}(f_\partial)} \prod_t e^{2\pi i O_t \hat{\boldsymbol{\nu}}(t)}. \tag{193}$$

Here, $\hat{\boldsymbol{\eta}}(f_\partial)$ is the operator given by:

$$\hat{\boldsymbol{\eta}}(\langle 123\rangle) \equiv \sum_{\{\ell_w, g_v\}} \eta(1,\ell_1,\ell_2,\ell_3)|\{\ell_w, g_v\}\rangle\langle\{\ell_w, g_v\}|, \tag{194}$$

and $\hat{\boldsymbol{\nu}}(t)$ is explicitly:

$$\hat{\boldsymbol{\nu}}(t) = \sum_{\{\ell_w, g_v\}} \overline{\boldsymbol{\nu}}_{\{\pi(\ell_w), g_v\}} |\{\ell_w, g_v\}\rangle\langle\{\ell_w, g_v\}|, \tag{195}$$

with $\overline{\boldsymbol{\nu}}_{\{\pi(\ell_w), g_v\}}$ defined in Eq. (98). $\mathcal{U}_b^L$ can be used to create a gapped parent Hamiltonian for $|\Psi_b^L\rangle$ by conjugating a certain paramagnet Hamiltonian whose ground state is $|\Psi^L\rangle$.

To recover the G symmetry, we can gauge the K subgroup of the L symmetry. This results in a G symmetric system with a K gauge theory at the boundary. The K gauge theory lives only on the boundary d.o.f., because the K subgroup acts as the identity on the bulk sites. We have thus constructed a group cohomology model with a symmetric, topologically ordered gapped boundary.

B. Gapped boundary construction for supercohomology models

We now generalize the construction of gapped boundaries for group cohomology models to build gapped boundaries for $(3+1)$D supercohomology models. The first step of the construction for group cohomology models is to find an extension of the G symmetry to 'trivialize' the cocycle ν. That is, to find an extension L such that the pull back of ν is a coboundary. Similarly, for supercohomology models, we first identify an extension of the G symmetry to an L symmetry that trivializes the supercohomology data (ρ, ν). Here, we say the supercohomology data is trivialized if the pull back (ρ^*, ν^*) is of the form:

$$(\rho^*, \nu^*) = (\delta\beta, \delta\eta + \frac{1}{2}\beta \cup \beta + \frac{1}{2}\beta \cup_1 \delta\beta), \tag{196}$$

for some $\beta \in C^2(L, \mathbb{Z}_2)$ and $\eta \in C^3(L, \mathbb{R}/\mathbb{Z})$. (The trivial supercohomology data in Eq. (196) was identified in Section IV D.) We then use the data (β, η) to build a symmetric, topologically ordered gapped boundary for the supercohomology model. The detailed derivation from a 2-group SPT model is given in Appendix K. In Appendix I 2, we describe a similar construction of gapped, spontaneous symmetry breaking boundaries for $(2+1)$D supercohomology models.

Before defining the supercohomology models on a manifold with boundary using (β, η), we argue that there exists a central extension of G for which the supercohomology data is trivialized, as in Eq. (196). To show that such an extension exists, we make two consecutive extensions of G. The first is given by the short exact sequence:

$$1 \to K_1 \to L' \xrightarrow{\pi_1} G \to 1, \tag{197}$$

and is chosen to trivialize ρ. We denote the pull backs of ρ and ν to L' by ρ' and ν', respectively. By the definition of this extension, ρ' can be written as: $\rho' = \delta\beta'$, for some $\beta' \in C^2(L', \mathbb{Z}_2)$. Using ν' and β', we then construct a cocycle:

$$\nu' + \frac{1}{2}\beta' \cup \beta' + \frac{1}{2}\beta' \cup_1 \delta\beta'. \tag{198}$$

The second extension is defined to trivialize the cocycle in Eq. (198) and corresponds to the short exact sequence:

$$1 \to K_2 \to L \xrightarrow{\pi_2} L' \to 1. \tag{199}$$

Consequently, there exists $\eta \in C^3(L, \mathbb{R}/\mathbb{Z})$ such that:

$$\delta\eta = \nu^* + \frac{1}{2}\beta \cup \beta + \frac{1}{2}\beta \cup_1 \delta\beta, \tag{200}$$

where ν^* and β are the pull backs of ν' and β' by π_2. The extensions in Eqs. (197) and (199) are guaranteed to exist by the arguments presented in Ref. [39]. Since the composition of two central extensions is itself a central extension, there exists an extension:

$$1 \to K \to L \xrightarrow{\pi} G \to 1, \tag{201}$$

which trivializes the supercohomology data (ρ, ν) such that the pull back (ρ^*, ν^*) is:

$$(\rho^*, \nu^*) = (\delta\beta, \delta\eta + \frac{1}{2}\beta \cup \beta + \frac{1}{2}\beta \cup_1 \delta\beta), \tag{202}$$

for $\beta \in C^2(L, \mathbb{Z}_2)$ and $\eta \in C^3(L, \mathbb{R}/\mathbb{Z})$. In Appendix L, we give an example of the trivialization of supercohomology data by extending a $G = \mathbb{Z}_2 \times \mathbb{Z}_4$ symmetry. We also note that the two consecutive extensions above were used in Ref. [26] to construct gapped boundaries for supercohomology models using a spacetime formalism.

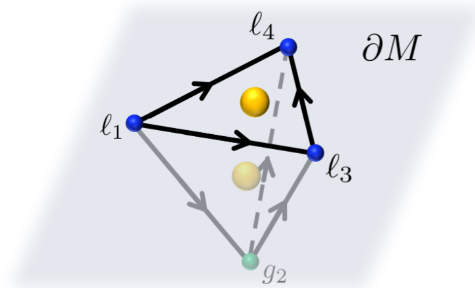

FIG. 21. The Hamiltonian H_f^L acts on a Hilbert space with an L d.o.f. (blue) on each boundary vertex and a spinless complex fermion (yellow) on every face of ∂M. The d.o.f. in the bulk, a G-valued spin (green) at every vertex and a spinless complex fermion on each tetrahedron, are the same as the d.o.f. in Fig. 4.

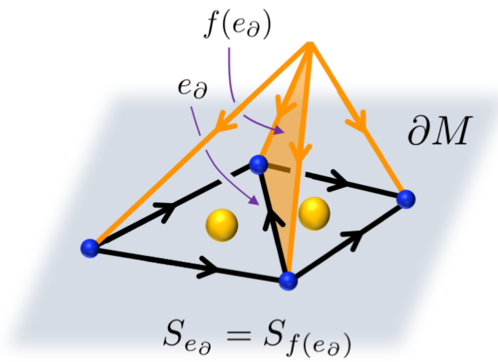

FIG. 22. The hopping operator S_{e_∂} on the boundary is defined by connecting the vertices in the boundary to an artificial vertex. The edges connecting to the artificial vertex are shown in orange and are oriented away from the additional point. The boundary edge e_∂ is associated to the artificial face $f(e_\partial)$ (shaded orange). For clarity the bulk d.o.f. are not pictured.

We now use an extension L of G, given in Eq. (201), and the data (β, η), satisfying Eq. (202), to define supercohomology models with a topologically ordered gapped boundary. To this end, we first build a gapped Hamiltonian H_f^L with an L symmetry and bulk terms that are equivalent to those of a supercohomology model with a G symmetry. The K subgroup of the L symmetry can then be gauged to obtain a G symmetric supercohomology model hosting a K gauge theory at the boundary.

The Hilbert space for the L symmetric Hamiltonian H_f^L can be constructed from the Hilbert space of the bulk supercohomology models. We recall that the supercohomology models on a manifold without boundary are defined on a Hilbert space with a G d.o.f. at each vertex and a single complex fermion on each tetrahedron, as in Fig. 4. For H_f^L on a manifold M with boundary ∂M, we replace the G d.o.f. on the boundary with L d.o.f. and introduce a single spinless complex fermion on each face in ∂M (see Fig. 21). To define the hopping operators on this Hilbert space, we imagine extending the manifold to $\overline{M}$

by connecting all of the boundary vertices to an additional "artificial" vertex. Each fermionic d.o.f. on a boundary face can then be associated to a tetrahedron connected to the artificial vertex, and every boundary edge e_∂ can be assigned a face $f(e_\partial)$ containing the artificial vertex, as pictured in Fig. 22. The trick of adding a vertex allows one to unambiguously determine the spin structure dependent sign in the definition of the hopping operator, discussed in Appendix F. We use S_{e_∂} to denote the hopping operator $S_{f(e_\partial)}$ between ferminionic d.o.f. at boundary faces:

$$S_{e_\partial} \equiv S_{f(e_\partial)}. \tag{203}$$

Similar to Eq. (183), the L symmetry is represented by:

$$V(\ell) = \sum_{\{\ell_w, g_v\}} |\{\ell\ell_w, \pi(\ell)g_v\}\rangle\langle\{\ell_w, g_v\}|, \tag{204}$$

tensored with the identity on the fermionic d.o.f..

The Hamiltonian H_f^L is formed from a trivial Hamiltonian - with a product state ground state - by conjugation with a FDQC. The trivial Hamiltonian H_{AI}^L is an atomic insulator with a decoupled L-paramagnet, defined as:

$$H_{\mathrm{AI}}^L \equiv -\sum_{v\notin\partial M} \mathcal{P}_v^G - \sum_{w\in\partial M} \mathcal{P}_w^L - \sum_{f_\partial\in\partial M} P_{f_\partial} - \sum_{t\in M} P_t. \tag{205}$$

Here, $\mathcal{P}_v^G$ and $\mathcal{P}_w^L$ are projectors onto the symmetric state at the bulk vertex v and boundary vertex w, respectively, and P_{f_∂} is the fermion parity operator at a face f_∂ in ∂M.

We prepare H_f^L from H_{AI}^L by conjugation with the FDQC $\mathcal{U}_f^L$:

$$\begin{aligned} \mathcal{U}_f^L \equiv &\prod_{f_\partial} e^{-2\pi i O_{f_\partial}\hat{\bar{\boldsymbol{\eta}}}(f_\partial)} \chi_\beta(\partial M) \prod_{e_\partial} S_{e_\partial}^{\hat{\bar{\boldsymbol{\beta}}}(e_\partial)} \prod_{f_\partial} P_{f_\partial}^{\int_{\partial M} \boldsymbol{f_\partial}\cup_1\hat{\bar{\boldsymbol{\beta}}}} \\ &\times \prod_t e^{2\pi i O_t \hat{\bar{\boldsymbol{\nu}}}(t)} \xi_\rho(M) \prod_f S_f^{\hat{\bar{\boldsymbol{\rho}}}(f)} \prod_t P_t^{\int_M \hat{\bar{\boldsymbol{\rho}}}\cup_2 \boldsymbol{t}}. \end{aligned} \tag{206}$$

The first line of Eq. (206) is a FDQC supported on the boundary sites, while the second line is the FDQC that prepares the bulk supercohomology model (composed with the projector π on the boundary vertices). The $\hat{\bar{\boldsymbol{\eta}}}$ term in Eq. (206) is the analog of the $\hat{\bar{\boldsymbol{\eta}}}$ term in Eq. (193) for the group cohomology models. In the configuration basis, $\chi_\beta(\partial M)$ is a sign that depends on an ordering of the faces in ∂M and makes up for the order dependence of the product of S_{e_∂} hopping operators; we give the explicit form of $\chi_\beta(\partial M)$ in Eq, (K41) in Appendix K. Furthermore, $\hat{\bar{\boldsymbol{\beta}}}(e_\partial)$ is the diagonal operator:

$$\hat{\bar{\boldsymbol{\beta}}}(\langle 12\rangle) \equiv \sum_{\{\ell_w, g_v\}} \beta(1, \ell_1, \ell_2)|\{\ell_w, g_v\}\rangle\langle\{\ell_w, g_v\}|, \tag{207}$$

defined for an arbitrary edge e_∂ in the boundary of M. With this, H_f^L is the Hamiltonian:

$$H_f^L \equiv \mathcal{U}_f^L H_{\mathrm{AI}}^L \mathcal{U}_f^{L\dagger}. \tag{208}$$

The derivation of the model above largely follows the construction of the bulk models, in that, we first build a model for a 2-group SPT phase, then subsequently gauge the 1-form symmetry and apply the fermionization duality. However, special care is needed at the boundary, and we give the full detail in Appendix K. As a consistency check, notice that when ρ and β are zero, the FDQC $\mathcal{U}_f^L$ reduces to the FDQC $\mathcal{U}_b^L$ for the group cohomology case in Section V A. We also note that H_f^L agrees with the G-symmetric bulk supercohomology model on the interior of M. This is because, away from the boundary of M, the action of $\mathcal{U}_f^L$ is equivalent to that of the bulk circuit $\mathcal{U}_f$.

H_f^L has a global L symmetry, so to recover a supercohomology model with a G symmetry, one can gauge the K subgroup of L. Due to the peculiar L symmetry in Eq. (204), the K gauge fields live only on the boundary of M. Therefore, after gauging the K symmetry, we obtain a G-symmetric supercohomology model with a gapped boundary, hosting a K gauge theory.

VI. DISCUSSION

We have constructed exactly solvable lattice Hamiltonians for supercohomology fermionic SPT (fSPT) phases in (3 + 1)D. Moreover, we have identified finite-depth quantum circuits (FDQCs) that prepare the SPT ground states from symmetric product states. The Hamiltonians are of the simple form:

$$H_f = \mathcal{U}_f H_{\mathrm{AI}}^G \mathcal{U}_f^\dagger, \tag{209}$$

where $\mathcal{U}_f$ is the FDQC that prepares the ground state and H_{AI}^G has a unique unentangled symmetric ground state. With our models, we are able to explicitly compute the supercohomology invariants by gauging the fermion parity symmetry and calculating the symmetry fractionalization on the flux loops. We also generalized the gapped boundary construction for group cohomology models in Ref. [19] to construct gapped boundaries for the supercohomology models through a symmetry extension.

Our construction is based on the correspondence between certain bosonic 2-group SPT phases and the supercohomology fSPT phases, first recognized in Refs. [21] and [32]. By gauging the $\mathbb{Z}_2$ 1-form symmetry of the 2-group SPT phase, we obtain the shadow model – a $\mathbb{Z}_2$ gauge theory with an emergent fermion. The emergent fermion can be interpreted as the gauge charge of an fSPT phase after gauging fermion parity. The supercohomology model results from condensing the emergent fermion, or equivalently, applying the fermionization duality of Ref. [22].

We would like to point out that by adding a disordered or quasiperiodic onsite potential to the Hamiltonian in Eq. (209), the Abelian supercohomology models can in principle exhibit many-body localization, or at least a long-lived pre-thermal regime [41–47]. This is because each eigenstate of the disordered H_f is short-range entangled and can be viewed as a representative ground state of the supercohomology SPT phase.

We also comment further on the relation between our models and the Lagrangian formulation of Ref. [25]. In Ref. [25], it was shown that the shadow theory can be thought of as a G-symmetry-enriched $\mathbb{Z}_2$ gauge theory with a Steenrod square topological term in the action, which transmutes the statistics of the point-like gauge charge. In our case, we built the 2-group SPT model from a 2-group cocycle $\alpha = \nu + \frac{1}{2}\rho \cup_1 \epsilon + \frac{1}{2}\epsilon \cup \epsilon$, described in Section IV B and Appendix J. The cocycle α is cohomologous to $\alpha' \equiv \nu + \frac{1}{2}\epsilon \cup_1 \rho + \frac{1}{2}\epsilon \cup \epsilon$, which can be expressed in terms of the Steenrod square Sq^2 as $\alpha' = \nu + \frac{1}{2}Sq^2\epsilon$. α' is in the same form as the action in Ref. [25], and accordingly, our shadow model Hamiltonians can be understood as the Hamiltonian formulation of the Lagrangians in Ref. [25], for a unitary $G_f = G \times \mathbb{Z}_2^f$.

There are many interesting potential generalizations of our models and avenues for future work. We briefly comment on them below.

Supercohomology models in higher dimensions: We conjecture that supercohomology models in $(n+1)$D can be constructed using a similar approach. In general, the supercohomology data (ρ,ν) belongs to $Z^n(G,\mathbb{Z}_2)\times C^{n+1}(G,\mathbb{R}/\mathbb{Z})$ and satisfies the constraints:

$$\delta\rho = 0, \quad \delta\nu = \frac{1}{2}\rho \cup_{n-2} \rho. \tag{210}$$

Using ρ and ν one can first build an auxiliary bosonic SPT model with an $(n-1)$-group symmetry with the $(n-1)$-group cocycle:

$$\alpha = \nu + \frac{1}{2}\rho \cup_{n-2} \epsilon_{n-1} + \frac{1}{2}\epsilon_{n-1} \cup_{n-3} \epsilon_{n-1}. \tag{211}$$

Here, ϵ_{n-1} can be pulled back to M to give a cochain $\boldsymbol{\epsilon}_{n-1} \in C^{n-1}(M,\mathbb{Z}_2)$ satisfying $\delta\boldsymbol{\epsilon}_{n-1} = \boldsymbol{\rho}$.[20] In principle, one can gauge an $(n-2)$-form $\mathbb{Z}_2$ subgroup to build the shadow model and then apply the fermionization duality of Ref. [30] to construct the fSPT model. We therefore, see no obstruction to finding symmetric FDQCs that prepare the ground states from a symmetric product state, unlike the beyond cohomology model in Ref. [48] and the beyond supercohomology model in Appendix G of Ref. [23].

Time-reversal and nontrivial extensions by fermion parity: Our supercohomology models are protected by unitary symmetries of the form $G_f = G \times \mathbb{Z}_2^f$. An important generalization is to symmetries which may include anti-unitary symmetries, such as time-reversal, and for which G_f is a nontrivial central extension of G by fermion parity. These cases are outside of the supercohomology framework, however, we expect some of our results to apply more broadly.

To include time-reversal symmetries, we can modify ν as in Refs. [15] and [16] so that the homogeneity of ν is replaced with:

$$(-1)^{s(h)}\nu(g_0,g_1,g_2,g_3,g_4) = \nu(hg_0,hg_1,hg_2,hg_3,hg_4), \tag{212}$$

where $s(h) \in \{0,1\}$ is 1 if h includes time-reversal. We expect that, with this modification, the FDQC $\mathcal{U}_f$ will prepare the ground state of the corresponding fSPT model – the symmetry fractionalization on fermion parity flux loops can be generalized to anti-unitary symmetries as described in Appendix B of Ref. [13]. However, the equivalence relation in Eq. (167) relies on the assumption that G is unitary. In fact, the models with time-reversal can be "trivialized" by accounting for the beyond supercohomology data as described in Refs. [17] and [40].

More generally, G_f can take the form $G_f = G \times_\psi \mathbb{Z}_2^f$, where G_f is a nontrivial central extension of G by $\mathbb{Z}_2^f$, specified by a 2-cocycle $\psi \in H^2(G,\mathbb{Z}_2)$. Each element of G_f can be written as $g\Pi^m$, with $g \in G$, $m \in \mathbb{Z}_2$ and Π denoting global fermion parity. The group laws in G_f are defined by:

$$(g\Pi^m)(h\Pi^n) = (gh)\Pi^{m+n+\psi(1,g,gh)}. \tag{213}$$

The supercohomology data (ρ,ν) is modified to satisfy [17]:

$$\delta\rho = 0, \quad \delta\nu = \frac{1}{2}\rho \cup_1 \rho + \frac{1}{2}\psi \cup \rho. \tag{214}$$

We can define a model for the fSPT protected by $G_f = G \times_\psi \mathbb{Z}_2^f$ corresponding to (ρ,ν) in Eq. (214). To do so, we first describe the representation of the symmetry on a Hilbert space with G d.o.f. on vertices and a spinless complex fermion on each tetrahedron. For any $g\Pi^m$ in G_f, the G_f symmetry acts as:

$$\mathbb{V}(g\Pi^m) \equiv \prod_v \mathbb{V}_v(g\Pi^m), \tag{215}$$

with the product over vertices and $\mathbb{V}_v(g\Pi^m)$ the symmetry action associated to v. Here, $\mathbb{V}_v(g\Pi^m)$ is defined as:

$$\mathbb{V}_v(g\Pi^m) \equiv V_v(g) \prod_{t=\langle 1234\rangle | v=\langle 1\rangle} P_t^m, \tag{216}$$

where $V_v(g)$ is the regular representation of g at v, and we have associated the fermionic d.o.f. at the tetrahedra $t = \langle 1234\rangle$ to the vertex $\langle 1\rangle$.

It can be checked that $\mathcal{U}_f$ built with the modified (ρ,ν) is symmetric under the representation of G_f in Eq. (215), so we can define a Hamiltonian H_f as in Eq. (209). Furthermore, it can be shown that the symmetry fractionalizes on the fermion parity flux loops according to ρ as in Section IV C. Finally, using a similar argument as in Ref. [23], it can be verified that the symmetry fractionalization on the fermion parity gauge charges is determined by ψ, in accordance with Ref. [7]. However, in this case, more work is needed to understand both the equivalence relations and the corresponding auxiliary bosonic SPT phases.

Beyond supercohomology models: We showed in Section II C that the ground states of the supercohomology models have $(0+1)$D junctions of symmetry domain walls decorated by complex fermions. The domain wall decoration picture can be extended to the beyond supercohomology phases, where the fixed point wave functions feature $(1+1)$D and

[20] For simplicity, we have suppressed the configuration dependence in the subscript used in Section IV A.

(2 + 1)D junctions of symmetry domains decorated by Majorana wires and $p + ip$ superconductors, respectively [17]. Although exactly-solvable models for beyond supercohomology phases have been constructed in Refs. [20, 21, 32, 49–54], it would be interesting to search for models of the form in Eq. (209) – related to a trivial SPT Hamiltonian by conjugation with a locality preserving unitary. Such a construction might have implications for the classification of fermionic quantum cellular automata, analogous to the beyond group cohomology models in Ref. [48]. It would also be interesting to study the boundaries of the beyond supercohomology models in (3+1)D using exactly-solvable models, similar to Ref. [55].

Acknowledgements – YC thanks Anton Kapustin, Ryohei Kobayashi, Po-Shen Hsin, and Bowen Yang for many useful discussions. YC was supported in part by the US Department of Energy, Office of Science, Office of High Energy Physics, under Award Number DE-SC0011632. TDE would like to acknowledge Sujeet Shukla and Lukasz Fidkowski for their work on a preliminary construction of the $(3+1)$D fSPT models. TDE also thanks Lukasz Fidkowski for carefully explaining the results of Ref. [56], Davide Gaiotto for a useful discussion related to the model in Section III B, and Theo Johnson-Freyd for valuable discussions regarding group supercohomology. TDE is grateful for the hospitality of Perimeter Institute, where much of his work was completed. Perimeter Institute is supported in part by the Government of Canada through the Department of Innovation, Science and Economic Development Canada and by the Province of Ontario through the Ministry of Economic Development, Job Creation and Trade. NT is grateful to Ashvin Vishwanath for helpful discussions and would also like to thank Zheng-Cheng Gu and the participants of the Croucher summer course "Quantum Entanglement and Topological Order" at CUHK for various discussions. NT is supported by NSERC. Part of this work was done during the Simons Collaboration on Ultra Quantum Matter Workshop, which was supported by a grant from the Simons Foundation (651440).

Appendix A: Terminology from cohomology

Here, we compile the cohomology notation used in the main text. This includes the group cohomology notation used to define the supercohomology data as well as the simplicial cohomology notation employed to describe the construction of the supercohomology models. For both, we define group cochains, the coboundary operator, and cup products.

1. Group cohomology

For our purposes, a p-cochain is a homogeneous function from G^{p+1} to A, where G is a finite group and A is either $\mathbb{Z}_2 = \{0, 1\}$ or $\mathbb{R}/\mathbb{Z} = [0, 1)$. By a homogeneous function, we mean that the p-cochain c satisfies:

$$c(g_0, \dots, g_p) = c(hg_0, \dots, hg_p), \quad \forall h \in G. \tag{A1}$$

The collection of p-cochains is denoted as $C^p(G, A)$.

The coboundary operator δ maps a p-cochain to a $(p+1)$-cochain. Explicitly, the coboundary operator maps c to the $(p+1)$-cochain δc, defined as:

$$\delta c(g_0, \dots, g_{p+1}) \equiv \sum_{i=0}^{p+1} (-1)^i c(g_0, \dots, \widehat{g_i}, \dots, g_{p+1}), \tag{A2}$$

where $\widehat{g_i}$ indicates that g_i has been omitted. When $A = \mathbb{Z}_2$, the sign in Eq. (A2) can be ignored. A p-cochain c satisfying $\delta c = 0$ is called a p-cocycle, and we use $Z^p(G, A)$ to denote the set of p-cocycles.

We can impose an equivalence relation on $Z^p(G, A)$ to define the p^{th} group cohomology. We call the p-cocycles c and c' equivalent if there exists a $(p-1)$-cochain $d \in C^{p-1}(G, A)$ such that:

$$c' = c + \delta d. \tag{A3}$$

The set of equivalence classes under the equivalence relation above defines the p^{th} group cohomology, denoted $H^p(G, A)$.

Throughout our calculations, we assume that the cocycles are normalized. That is, the p-cocycle c satisfies:

$$c(1, 1, g_2, \dots, g_p) = 0, \quad \forall g_i, \ i \in \{2, \dots, p\}, \tag{A4}$$

where 1 is the identity in G. This assumption is justified by the fact that every group cohomology equivalence class has a normalized representative.

Lastly, for $A = \mathbb{Z}_2$, we define the cup-n products $\cup_n$ with $n \in \{0, 1, 2\}$. The cup-n product maps a p-cochain c and a q-cochain d to a $(p+q-n)$-cochain $c \cup_n d$. We note that the cup-0 product is referred to as simply the cup product and is denoted by $\cup$. The cup product of the homogeneous group cochains $c \in C^p(G, \mathbb{Z}_2)$ and $d \in C^q(G, \mathbb{Z}_2)$ is the $(p+q)$-cochain given by:

$$c \cup d(g_0, \dots, g_{p+q}) \equiv c(g_0, \dots, g_p) d(g_p, \dots, g_{p+q}). \tag{A5}$$

The cup-1 product of a p-cochain c and a q-cochain d is the $(p+q-1)$-cochain defined by:

$$\begin{aligned} &c \cup_1 d(g_0, \dots, g_{p+q}) = \\ &\sum_{i=0}^{p-1} c(g_0, \dots, g_i, g_{q+i}, \dots, g_{p+q-1}) d(g_i, \dots, g_{q+i}). \end{aligned} \tag{A6}$$

We refer to Ref. [30] for the general formula for the cup-2 product. In the main text, we only ever use the cup-2 product between two group 3-cochains. Hence, we give the explicit cup-2 product of c and d with $c, d \in C^3(G, \mathbb{Z}_2)$:

$$\begin{aligned} c \cup_2 d(g_1, g_2, g_3, g_4, g_5) \equiv\ & c(g_1, g_2, g_3, g_4) d(g_1, g_2, g_4, g_5) \\ &+ c(g_1, g_3, g_4, g_5) d(g_1, g_2, g_3, g_5) \\ &+ c(g_1, g_2, g_3, g_4) d(g_2, g_3, g_4, g_5) \\ &+ c(g_1, g_2, g_4, g_5) d(g_2, g_3, g_4, g_5). \end{aligned} \tag{A7}$$

2. Simplicial cohomology

Simplicial cohomology on M with coefficients in $\mathbb{Z}_2$ was introduced in Section III A in the context of the 1-form SPT model. Here, we summarize the terminology from Section III A and give the cup product relations that are used in the appendices.

Given a triangulation of a manifold M, we denote the vertices, edges, faces, and tetrahedra by v, e, f, and t, respectively. We often denote a p-simplex by its $p+1$ vertices, i.e., $\langle 0,\ldots,p\rangle$. (Elsewhere in the text, we omit the commas between vertices for simplicity.) We define a p-chain as a formal sum (mod 2) of p-simplices in the manifold M.

A p-cochain on M is a linear, $\mathbb{Z}_2$-valued function of p-chains. The set of p-cochains on M is denoted by $C^p(M,\mathbb{Z}_2)$. We use a bold font for cochains on M, e.g., $\boldsymbol{c}\in C^p(M,\mathbb{Z}_2)$.

A cochain labeled by a p-simplex is a p-cochain that evaluates to 1 on the corresponding p-simplex and 0 otherwise. For example, $\boldsymbol{v}$ denotes the 0-cochain dual to the vertex v, i.e.:

$$\boldsymbol{v}(v') = \begin{cases} 1 & v'=v \\ 0 & \text{otherwise.}\end{cases} \tag{A8}$$

Likewise, for an edge e, we have:

$$\boldsymbol{e}(e') = \begin{cases} 1 & e'=e \\ 0 & \text{otherwise,}\end{cases} \tag{A9}$$

and for a face f:

$$\boldsymbol{f}(f') = \begin{cases} 1 & f'=f \\ 0 & \text{otherwise.}\end{cases} \tag{A10}$$

The coboundary operator δ is a linear map from p-cochains to $(p+1)$-cochains:

$$\delta : C^p(M,\mathbb{Z}_2)\to C^{p+1}(M,\mathbb{Z}_2). \tag{A11}$$

The coboundary of a p-cochain $\boldsymbol{c}$ is defined as the $(p+1)$-cochain $\delta\boldsymbol{c}$ such that:

$$\delta\boldsymbol{c}(s) = \boldsymbol{c}(\partial s), \tag{A12}$$

for an arbitrary $(p+1)$-simplex s and ∂s its boundary. Explicitly, ∂s is an equally weighted sum of the p-simplices in s.

A p-cochain $\boldsymbol{c}$ is called closed, if $\delta\boldsymbol{c}=0$. We denote the collection of closed p-cochains on M as $Z^p(M,\mathbb{Z}_2)$. We also note that $\delta\delta=0$, which follows from Eq. (A12) and the fact that $\partial\partial=0$. Therefore, $\delta\boldsymbol{d}$ is a closed p-cochain for any $\boldsymbol{d}\in C^{p-1}(M,\mathbb{Z}_2)$.

The cup product $\cup$ maps a p-cochain and a q-cochain to a $(p+q)$-cochain:

$$\cup : C^p(M,\mathbb{Z}_2)\times C^q(M,\mathbb{Z}_2)\to C^{p+q}(M,\mathbb{Z}_2). \tag{A13}$$

The cup product of $\boldsymbol{c}\in C^p(M,\mathbb{Z}_2)$ and $\boldsymbol{d}\in C^q(M,\mathbb{Z}_2)$ evaluated on a $(p+q)$-simplex $\langle 0\ldots p+q\rangle$ is:

$$\boldsymbol{c}\cup\boldsymbol{d}(\langle 0\ldots p+q\rangle) = \boldsymbol{c}(\langle 0\ldots p\rangle)\boldsymbol{d}(\langle p\ldots p+q\rangle). \tag{A14}$$

The coboundary operator is a derivation, meaning it satisfies:

$$\delta\left(\boldsymbol{c}\cup\boldsymbol{d}\right) = \delta\boldsymbol{c}\cup\boldsymbol{d}+\boldsymbol{c}\cup\delta\boldsymbol{d}. \tag{A15}$$

The cup-1 product $\cup_1$ produces a $(p+q-1)$-cochain from a p-cochain and a q-cochain:

$$\cup_1 : C^p(M,\mathbb{Z}_2)\times C^q(M,\mathbb{Z}_2)\to C^{p+q-1}(M,\mathbb{Z}_2). \tag{A16}$$

For $\boldsymbol{c}\in C^p(M,\mathbb{Z}_2)$ and $\boldsymbol{d}\in C^q(M,\mathbb{Z}_2)$ the cup-1 product $\boldsymbol{c}\cup_1\boldsymbol{d}$ evaluated on the $(p+q-1)$-simplex $\langle 0,\ldots,p+q-1\rangle$ is:

$$\begin{aligned}&\boldsymbol{c}\cup_1\boldsymbol{d}(\langle 0,\ldots,p+q-1\rangle) = \\ &\sum_{i=0}^{p-1}\boldsymbol{c}(\langle 0,\ldots,i,q+i,\ldots,p+q-1\rangle)\boldsymbol{d}(\langle i,\ldots,q+i\rangle).\end{aligned} \tag{A17}$$

Furthermore, the cup-1 product satisfies [57]:

$$\delta(\boldsymbol{c}\cup_1\boldsymbol{d}) = \delta\boldsymbol{c}\cup_1\boldsymbol{d}+\boldsymbol{c}\cup_1\delta\boldsymbol{d}+\boldsymbol{c}\cup\boldsymbol{d}+\boldsymbol{d}\cup\boldsymbol{c}. \tag{A18}$$

Finally, we introduce the cup-2 product

$$\cup_2 : C^p(M,\mathbb{Z}_2)\times C^q(M,\mathbb{Z}_2)\to C^{p+q-2}(M,\mathbb{Z}_2). \tag{A19}$$

The general formula for the cup-2 product is given in Ref. [30]. We provide the explicit formula for the cup-2 product of a 3-cochains $\boldsymbol{c}\in C^3(M,\mathbb{Z}_2)$ and a 4-cochain $\boldsymbol{d}\in C^4(M,\mathbb{Z}_2)$:

$$\begin{aligned}&\boldsymbol{c}\cup_2 d(\langle 1234\rangle)\equiv \\ &\qquad \boldsymbol{c}(\langle 123\rangle)\boldsymbol{d}(\langle 1234\rangle)+\boldsymbol{c}(\langle 134\rangle)\boldsymbol{d}(\langle 1234\rangle),\end{aligned} \tag{A20}$$

for an arbitrary tetrahedron $\langle 1234\rangle$. The cup-2 product satisfies:

$$\delta(\boldsymbol{c}\cup_2\boldsymbol{d}) = \delta\boldsymbol{c}\cup_2\boldsymbol{d}+\boldsymbol{c}\cup_2\delta\boldsymbol{d}+\boldsymbol{c}\cup_1\boldsymbol{d}+\boldsymbol{d}\cup_1\boldsymbol{c}. \tag{A21}$$

To simplify the expressions in the text, we also introduce the notation $\int_N\boldsymbol{c}$ as shorthand for the sum:

$$\int_N\boldsymbol{c} = \sum_s\boldsymbol{c}(s). \tag{A22}$$

Here, N is a p-dimensional manifold, $\boldsymbol{c}$ is a p-cochain, and the sum is over all p-simplices in N. If unspecified, it should be assumed that the integral is over the manifold M.

Appendix B: Explicit 1-form SPT Hamiltonian

In this appendix, we derive the 1-form SPT Hamiltonian H_1 in Eq. (60), i.e.:

$$H_1 = -\sum_e\left(X_e\prod_f W_f^{\int\delta\boldsymbol{e}\cup_1\boldsymbol{f}}\right), \tag{B1}$$

and demonstrate that it is indeed symmetric under the 1-form symmetry in Eq. (30). We begin with H_1 defined in Eq. (34) as:

$$H_1 = -\sum_e \mathcal{U}_1 X_e \mathcal{U}_1^\dagger, \tag{B2}$$

with $\mathcal{U}_1$ given by:

$$\mathcal{U}_1 = \sum_{\boldsymbol{a}_e} \prod_t (-1)^{\boldsymbol{a}_e \cup \delta \boldsymbol{a}_e(t)} |\boldsymbol{a}_e\rangle\langle \boldsymbol{a}_e|. \tag{B3}$$

To compute $\mathcal{U}_1 X_e \mathcal{U}_1^\dagger$ in Eq. (B2) explicitly, we first evaluate $\mathcal{U}_1 X_e$. We find:

$$\begin{aligned}\mathcal{U}_1 X_e &= \sum_{\boldsymbol{a}_e} \prod_t (-1)^{\boldsymbol{a}_e \cup \delta \boldsymbol{a}_e(t)} |\boldsymbol{a}_e\rangle\langle \boldsymbol{a}_e| \sum_{\boldsymbol{a}'_e} |\boldsymbol{a}'_e + \boldsymbol{e}\rangle\langle \boldsymbol{a}'_e| \qquad \text{(B4)}\\ &= \sum_{\boldsymbol{a}_e} \prod_t (-1)^{(\boldsymbol{a}_e + \boldsymbol{e}) \cup \delta(\boldsymbol{a}_e + \boldsymbol{e})(t)} |\boldsymbol{a}_e + \boldsymbol{e}\rangle\langle \boldsymbol{a}_e| \\ &= X_e \sum_{\boldsymbol{a}_e} \prod_t (-1)^{(\boldsymbol{a}_e + \boldsymbol{e}) \cup \delta(\boldsymbol{a}_e + \boldsymbol{e})(t)} |\boldsymbol{a}_e\rangle\langle \boldsymbol{a}_e|\end{aligned}$$

Expanding the cup product in the last line of Eq. (B4), we obtain:

$$\begin{aligned}&\mathcal{U}_1 X_e = \qquad \text{(B5)}\\ &\quad X_e \sum_{\boldsymbol{a}_e} \prod_t (-1)^{(\boldsymbol{e} \cup \delta \boldsymbol{a}_e + \boldsymbol{a}_e \cup \delta \boldsymbol{e} + \boldsymbol{e} \cup \delta \boldsymbol{e})(t)} |\boldsymbol{a}_e\rangle\langle \boldsymbol{a}_e| \mathcal{U}_1\end{aligned}$$

$\boldsymbol{e} \cup \delta \boldsymbol{e}(t)$, in the expression above [Eq. (B5)], is zero for all tetrahedra t. This can be seen by evaluating $\boldsymbol{e} \cup \delta \boldsymbol{e}$ on an arbitrary tetrahedron $\langle 1234\rangle$:

$$\boldsymbol{e} \cup \delta \boldsymbol{e}(\langle 1234\rangle) = \boldsymbol{e}(\langle 12\rangle)\left[\boldsymbol{e}(\langle 23\rangle) + \boldsymbol{e}(\langle 34\rangle) + \boldsymbol{e}(\langle 24\rangle)\right]. \tag{B6}$$

The right hand side is zero if $e \neq \langle 12\rangle$. However, if $e = \langle 12\rangle$, then the term in square brackets must be zero. Hence, we see that $\boldsymbol{e} \cup \delta \boldsymbol{e}(t) = 0$. We then have:

$$\mathcal{U}_1 X_e = X_e \sum_{\boldsymbol{a}_e} \prod_t (-1)^{(\boldsymbol{e} \cup \delta \boldsymbol{a}_e + \boldsymbol{a}_e \cup \delta \boldsymbol{e})(t)} |\boldsymbol{a}_e\rangle\langle \boldsymbol{a}_e| \mathcal{U}_1. \tag{B7}$$

We simplify the right hand side of Eq. (B7) further by employing the identities in Eqs. (A15) and (A18). An application of Eq. (A15) gives us:

$$\mathcal{U}_1 X_e = X_e \sum_{\boldsymbol{a}_e} \prod_t (-1)^{(\delta \boldsymbol{e} \cup \boldsymbol{a}_e + \boldsymbol{a}_e \cup \delta \boldsymbol{e})(t)} |\boldsymbol{a}_e\rangle\langle \boldsymbol{a}_e| \mathcal{U}_1, \tag{B8}$$

where we have also used that M is closed. Then, using Eq. (A18), we see:

$$\mathcal{U}_1 X_e = X_e \sum_{\boldsymbol{a}_e} \prod_t (-1)^{\delta \boldsymbol{a}_e \cup_1 \delta \boldsymbol{e}(t)} |\boldsymbol{a}_e\rangle\langle \boldsymbol{a}_e| \mathcal{U}_1, \tag{B9}$$

where again we have used that M is closed.

We can express the term:

$$\sum_{\boldsymbol{a}_e} \prod_t (-1)^{\delta \boldsymbol{a}_e \cup_1 \delta \boldsymbol{e}(t)} |\boldsymbol{a}_e\rangle\langle \boldsymbol{a}_e| \tag{B10}$$

in Eq. (B9) using Pauli Z operators. To do so, we notice that, for any face $f = \langle 123\rangle$:

$$\sum_{\boldsymbol{a}_e} (-1)^{\delta \boldsymbol{a}_e(f)} |\boldsymbol{a}_e\rangle\langle \boldsymbol{a}_e| = \sum_{\boldsymbol{a}_e} (-1)^{a_{12} + a_{23} + a_{13}} |\boldsymbol{a}_e\rangle\langle \boldsymbol{a}_e| = W_f, \tag{B11}$$

where in the last equality we have defined:

$$W_f \equiv \prod_{e \subset f} Z_e. \tag{B12}$$

Therefore, Eq. (B10) can be written as:

$$\sum_{\boldsymbol{a}_e} \prod_t (-1)^{\delta \boldsymbol{a}_e \cup_1 \delta \boldsymbol{e}(t)} |\boldsymbol{a}_e\rangle\langle \boldsymbol{a}_e| = \prod_t \prod_f W_f^{\boldsymbol{f} \cup_1 \delta \boldsymbol{e}(t)}, \tag{B13}$$

with $\prod_f$ a product over all faces in M. Exchanging the product over tetrahedra for a sum, we see that:

$$\sum_{\boldsymbol{a}_e} \prod_t (-1)^{\delta \boldsymbol{a}_e \cup_1 \delta \boldsymbol{e}(t)} |\boldsymbol{a}_e\rangle\langle \boldsymbol{a}_e| = \prod_f W_f^{\int \boldsymbol{f} \cup_1 \delta \boldsymbol{e}}. \tag{B14}$$

Then, plugging Eq. (B14) into Eq. (B9), we arrive at:

$$\mathcal{U}_1 X_e = X_e \prod_f W_f^{\int \boldsymbol{f} \cup_1 \delta \boldsymbol{e}} \mathcal{U}_1. \tag{B15}$$

Finally, we can compute $\mathcal{U}_1 X_e {\mathcal{U}_1}^\dagger$. From Eq. (B15), we have:

$$\begin{aligned}\mathcal{U}_1 X_e {\mathcal{U}_1}^\dagger &= \left(X_e \prod_f W_f^{\int \boldsymbol{f} \cup_1 \delta \boldsymbol{e}} \mathcal{U}_1\right) {\mathcal{U}_1}^\dagger \qquad \text{(B16)}\\ &= X_e \prod_f W_f^{\int \boldsymbol{f} \cup_1 \delta \boldsymbol{e}}.\end{aligned}$$

The 1-form SPT Hamiltonian is then:

$$H_1 = -\sum_e \left(X_e \prod_f W_f^{\int \boldsymbol{f} \cup_1 \delta \boldsymbol{e}}\right), \tag{B17}$$

as claimed.

Next, we show that H_1 is symmetric under the $\mathbb{Z}_2$ 1-form symmetry. Recall that the symmetry is generated by operators of the form [Eq. (30)]:

$$A_\Sigma \equiv \prod_{e \perp \Sigma} X_e, \tag{B18}$$

for a closed surface Σ of the dual lattice. We prove that H_1 is symmetric by showing that $\mathcal{U}_1$ is symmetric, i.e.:

$$A_\Sigma \mathcal{U}_1 A_\Sigma = \mathcal{U}_1, \tag{B19}$$

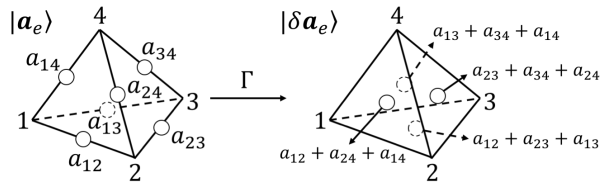

FIG. 23. Γ maps the configuration state $|\boldsymbol{a}_e\rangle$ to the state $|\delta\boldsymbol{a}_e\rangle$. $|\delta\boldsymbol{a}_e\rangle$ is an element of the Hilbert space formed from $\mathbb{Z}_2$ d.o.f. on faces (represented by circles).

for all choices of Σ.

Conjugation of $\mathcal{U}_1$ by an arbitrary generator of the 1-form symmetry A_Σ gives:

$$A_\Sigma \mathcal{U}_1 A_\Sigma = \sum_{\boldsymbol{a}_e} \prod_t (-1)^{\boldsymbol{a}_e \cup \delta\boldsymbol{a}_e(t)} |\boldsymbol{a}_e + \boldsymbol{\Sigma}\rangle\langle \boldsymbol{a}_e + \boldsymbol{\Sigma}|. \tag{B20}$$

Redefining the summation, we have:

$$A_\Sigma \mathcal{U}_1 A_\Sigma = \sum_{\boldsymbol{a}_e} \prod_t (-1)^{(\boldsymbol{a}_e+\boldsymbol{\Sigma}) \cup \delta(\boldsymbol{a}_e+\boldsymbol{\Sigma})(t)} |\boldsymbol{a}_e\rangle\langle \boldsymbol{a}_e|. \tag{B21}$$

Then we expand the exponent and use that $\delta\boldsymbol{\Sigma} = 0$ to obtain:

$$A_\Sigma \mathcal{U}_1 A_\Sigma = \sum_{\boldsymbol{a}_e} \prod_t (-1)^{\boldsymbol{a}_e \cup \delta\boldsymbol{a}_e(t) + \boldsymbol{\Sigma}\cup\delta\boldsymbol{a}_e(t)} |\boldsymbol{a}_e\rangle\langle \boldsymbol{a}_e|. \tag{B22}$$

Finally, we employ the identity in Eq. (A15) and use that M is closed to arrive at:

$$\begin{aligned} A_\Sigma \mathcal{U}_1 A_\Sigma &= \sum_{\boldsymbol{a}_e} \prod_t (-1)^{\boldsymbol{a}_e \cup \delta\boldsymbol{a}_e(t) + \delta(\Sigma\cup\boldsymbol{a}_e)(t)} |\boldsymbol{a}_e\rangle\langle \boldsymbol{a}_e| \qquad \text{(B23)} \\ &= \sum_{\boldsymbol{a}_e} \prod_t (-1)^{\boldsymbol{a}_e \cup \delta\boldsymbol{a}_e(t)} |\boldsymbol{a}_e\rangle\langle \boldsymbol{a}_e| \\ &= \mathcal{U}_1. \end{aligned}$$

Thus, $\mathcal{U}_1$ is symmetric.

Appendix C: Gauging a $\mathbb{Z}_2$ 1-form symmetry at the level of quantum states

In Section III B, we gave a physically motivated description of the gauging procedure and the construction of the twisted toric code. We use this appendix to give a more careful construction of the twisted toric code using a gauging procedure defined at the level of quantum states [33].

We begin by denoting the Hilbert space of the 1-form SPT model as $\mathcal{H}_1$ and the Hilbert space of the twisted toric code as $\mathcal{H}_{\text{ttc}}$. Then, in gauging the $\mathbb{Z}_2$ 1-form symmetry, we map symmetric states from $\mathcal{H}_1$ to a certain constrained subspace of $\mathcal{H}_{\text{ttc}}$. For this purpose, we define the linear map Γ by:

$$\Gamma : |\boldsymbol{a}_e\rangle \mapsto |\delta\boldsymbol{a}_e\rangle, \tag{C1}$$

as shown schematically in Fig. 23. We note that in Eq. (C1), we have omitted a normalization factor for simplicity.[21]

Γ is a many-to-one mapping, since configuration states differing by a 1-form symmetry action are mapped to the same state. Explicitly, for an arbitrary closed 1-cochain $\boldsymbol{\Sigma}$ ($\delta\boldsymbol{\Sigma} = 0$), we have:

$$\Gamma(A_\Sigma|\boldsymbol{a}_e\rangle) = \Gamma(|\boldsymbol{a}_e + \boldsymbol{\Sigma}\rangle) = |\delta\boldsymbol{a}_e + \delta\boldsymbol{\Sigma}\rangle = |\delta\boldsymbol{a}_e\rangle \tag{C2}$$

Thus, $|\boldsymbol{a}_e\rangle$ and $A_\Sigma|\boldsymbol{a}_e\rangle$ map to the same state, namely $|\delta\boldsymbol{a}_e\rangle$.

This observation suggests that a one-to-one mapping of states can be defined by restricting Γ to the subspace of $\mathbb{Z}_2$ 1-form symmetric states $\mathcal{H}_1^{\text{sym}}$, i.e.:

$$\mathcal{H}_1^{\text{sym}} \equiv \{|\Psi\rangle \in \mathcal{H}_1 : A_\Sigma|\Psi\rangle = |\Psi\rangle,\ \forall\Sigma \text{ s.t. } \delta\boldsymbol{\Sigma} = 0\}. \tag{C3}$$

Γ then defines an isomorphism (a duality) between $\mathcal{H}_1^{\text{sym}}$ and its image, where the image of Γ is spanned by the set of configuration states $|\delta\boldsymbol{a}_e\rangle$ for some 1-cochain $\boldsymbol{a}_e$. We denote the image of Γ as $\mathcal{H}_{\text{ttc}}^{\text{con}}$:

$$\mathcal{H}_{\text{ttc}}^{\text{con}} \equiv \{|\Psi\rangle \in \mathcal{H}_{\text{ttc}} : |\Psi\rangle = \sum_{\boldsymbol{a}_e} C_{\boldsymbol{a}_e}|\delta\boldsymbol{a}_e\rangle,\ C_{\boldsymbol{a}_e} \in \mathbb{C}\}. \tag{C4}$$

Alternatively, $\mathcal{H}_{\text{ttc}}^{\text{con}}$ can be expressed as a subspace of $\mathcal{H}_{\text{ttc}}$ with a particular $\mathbb{Z}_2$ 1-form gauge constraint. To motivate this, we notice that any basis state $|\delta\boldsymbol{a}_e\rangle \in \mathcal{H}_{\text{ttc}}^{\text{con}}$ satisfies:

$$\prod_{f\subset\sigma} Z_f|\delta\boldsymbol{a}_e\rangle = |\delta\boldsymbol{a}_e\rangle, \tag{C5}$$

where σ is an arbitrary closed surface ($\partial\sigma = 0$) of the direct lattice, and the product is over faces contained in σ. This follows from the definition of Z_f [Eq. (71)] and the definition of the coboundary [Eq. (47)]:

$$\prod_{f\subset\sigma} Z_f|\delta\boldsymbol{a}_e\rangle = (-1)^{\delta\boldsymbol{a}_e(\sigma)}|\delta\boldsymbol{a}_e\rangle = (-1)^{\boldsymbol{a}_e(\partial\sigma)}|\delta\boldsymbol{a}_e\rangle = |\delta\boldsymbol{a}_e\rangle. \tag{C6}$$

Physically, Eq. (C5) is a statement that $|\delta\boldsymbol{a}_e\rangle$ contains no 1-form gauge fluxes and has a trivial holonomy. It can be checked that an equivalent definition of $\mathcal{H}_{\text{ttc}}^{\text{con}}$ is then the set of constrained states:

$$\mathcal{H}_{\text{ttc}}^{\text{con}} = \{|\Psi\rangle \in \mathcal{H}_{\text{ttc}} : \prod_{f\subset\sigma} Z_f|\Psi\rangle = |\Psi\rangle,\ \forall\sigma \text{ s.t. } \partial\sigma = 0\}. \tag{C7}$$

[21] More precisely, Γ maps: $\Gamma : |\boldsymbol{a}_e\rangle \mapsto \frac{1}{\mathcal{A}}|\delta\boldsymbol{a}_e\rangle$. The normalization factor $\mathcal{A}$ is given by $\mathcal{A} = \sqrt{|Z^1(M,\mathbb{Z}_2)|}$, where $|Z^1(M,\mathbb{Z}_2)|$ is the cardinality of the set of closed 1-cochains on M.

Here, the $\mathbb{Z}_2$ 1-form gauge constraints are:

$$\prod_{f\subset\sigma} Z_f = 1, \tag{C8}$$

for any closed surface σ. We note that the local constraints are generated by the set of operators:

$$W_t \equiv \prod_{f\subset t} Z_f = 1 \tag{C9}$$

for all tetrahedra t.

Γ restricted to $\mathcal{H}_1^{\text{sym}}$ defines a duality at the level of states. However, to apply the duality to H_0 and H_1, we need to extend our understanding of Γ to operators. In particular, we consider operators that preserve the subspace $\mathcal{H}_1^{\text{sym}}$, i.e., commute with A_Σ for all Σ. The local, 1-form symmetric operators can, in fact, be generated by: X_e and W_f. Accordingly, we focus on the image of X_e and W_f under the mapping Γ. For an arbitrary state $|\Psi_{\text{sym}}\rangle$ in $\mathcal{H}_1^{\text{sym}}$, we have:

$$\begin{aligned}\Gamma(X_{e'}|\Psi_{\text{sym}}\rangle) &= \Gamma\left(\sum_{\boldsymbol{a}_e}|\boldsymbol{a}_e+\boldsymbol{e}'\rangle\langle\boldsymbol{a}_e|\Psi_{\text{sym}}\rangle\right) \\ &= \sum_{\boldsymbol{a}_e}|\delta\boldsymbol{a}_e+\delta\boldsymbol{e}'\rangle\langle\boldsymbol{a}_e|\Psi_{\text{sym}}\rangle \\ &= \prod_{f\supset e'}X_f\sum_{\boldsymbol{a}_e}|\delta\boldsymbol{a}_e\rangle\langle\boldsymbol{a}_e|\Psi_{\text{sym}}\rangle \\ &= \prod_{f\supset e'}X_f\Gamma(|\Psi_{\text{sym}}\rangle),\end{aligned} \tag{C10}$$

where the product is over faces containing e' in their boundary. For W_f, on the other hand, we find:

$$\begin{aligned}\Gamma(W_f|\Psi_{\text{sym}}\rangle) &= \Gamma\left(\sum_{\boldsymbol{a}_e}(-1)^{\delta\boldsymbol{a}_e(f)}|\boldsymbol{a}_e\rangle\langle\boldsymbol{a}_e|\Psi_{\text{sym}}\rangle\right) \\ &= \sum_{\boldsymbol{a}_e}(-1)^{\delta\boldsymbol{a}_e(f)}|\delta\boldsymbol{a}_e\rangle\langle\boldsymbol{a}_e|\Psi_{\text{sym}}\rangle \\ &= Z_f\sum_{\boldsymbol{a}_e}|\delta\boldsymbol{a}_e\rangle\langle\boldsymbol{a}_e|\Psi_{\text{sym}}\rangle \\ &= Z_f\Gamma(|\Psi_{\text{sym}}\rangle).\end{aligned} \tag{C11}$$

Therefore, the operators X_e and W_f on $\mathcal{H}_1^{\text{sym}}$ are dual to the operators $\prod_{f\supset e}X_f$ and Z_f on $\mathcal{H}_{\text{ttc}}^{\text{con}}$, respectively:

$$X_e \leftrightarrow \prod_{f\supset e}X_f \tag{C12}$$

$$W_f \leftrightarrow Z_f. \tag{C13}$$

We note that the commutation relations are preserved by the duality. In $\mathcal{H}_1$, X_e anticommutes with W_f if and only if e is in the boundary of f. Likewise, in $\mathcal{H}_{\text{ttc}}$, $\prod_{f\supset e}X_f$ anticommutes with Z_f if and only if e is in the boundary of f.

We are now ready to apply the gauging duality to the models discussed in Section III A. We begin with the 1-form paramagnet. The ground state of the 1-form paramagnet is:

$$|\Psi_0\rangle = \sum_{\boldsymbol{a}_e}|\boldsymbol{a}_e\rangle, \tag{C14}$$

which certainly belongs to the subspace $\mathcal{H}_1^{\text{sym}}$. Applying Γ to $|\Psi_0\rangle$ then yields:

$$|\Psi_{\text{tc}}\rangle \equiv \Gamma\left(|\Psi_0\rangle\right) = \sum_{\boldsymbol{a}_e}|\delta\boldsymbol{a}_e\rangle. \tag{C15}$$

Using Eq. (C12), the 1-form paramagnet Hamiltonian:

$$H_0 = -\sum_e X_e, \tag{C16}$$

is dual to the Hamiltonian $H_{\text{tc}}^{\text{con}}$:

$$H_{\text{tc}}^{\text{con}} = -\sum_e\prod_{f\supset e}X_f, \tag{C17}$$

defined on $\mathcal{H}_{\text{ttc}}^{\text{con}}$. $|\Psi_{\text{tc}}\rangle$ is the unique ground state of $H_{\text{tc}}^{\text{con}}$ in $\mathcal{H}_{\text{ttc}}^{\text{con}}$.

The final step of the gauging procedure is to impose the local constraints [Eq. (C9)] of $\mathcal{H}_{\text{ttc}}^{\text{con}}$ energetically. The resulting Hamiltonian is:[22]

$$H_{\text{tc}} \equiv H_{\text{tc}}^{\text{con}} - \sum_t W_t = -\sum_e\prod_{f\supset e}X_f - \sum_t W_t. \tag{C18}$$

This is the Hamiltonian for the usual 3D toric code (on the dual lattice). Bosonic point-like excitations (1-form gauge fluxes) can be created by the string operators:

$$\prod_{f\perp p}X_f, \tag{C19}$$

where p is a path in the dual lattice, and the product is over faces intersected by p.

Finally, we construct the twisted toric code from the nontrivial $\mathbb{Z}_2$ 1-form SPT Hamiltonian H_1 by gauging the symmetry. The ground state of H_1 is given in Eq. (35) as:

$$|\Psi_1\rangle = \mathcal{U}_1|\Psi_0\rangle = \sum_{\boldsymbol{a}_e}\prod_t(-1)^{\boldsymbol{a}_e\cup\delta\boldsymbol{a}_e(t)}|\boldsymbol{a}_e\rangle. \tag{C20}$$

As shown in Appendix B, $\mathcal{U}_1$ is symmetric, so $|\Psi_1\rangle$ is in $\mathcal{H}_1^{\text{sym}}$. Therefore, we may apply Γ to $|\Psi_1\rangle$:

$$|\Psi_{\text{ttc}}\rangle \equiv \Gamma(|\Psi_1\rangle) = \sum_{\boldsymbol{a}_e}\prod_t(-1)^{\boldsymbol{a}_e\cup\delta\boldsymbol{a}_e(t)}|\delta\boldsymbol{a}_e\rangle. \tag{C21}$$

When viewed as an element of the unconstrained space $\mathcal{H}_{\text{ttc}}$, $|\Psi_{\text{ttc}}\rangle$ is a ground state of the twisted toric code (also see Appendix D).

The twisted toric code Hamiltonian can be derived by applying the operator duality in Eqs. (C12) and (C13) to the 1-form SPT Hamiltonian:

$$H_1 = -\sum_e\left(X_e\prod_f W_f^{\int \boldsymbol{f}\cup_1\delta\boldsymbol{e}}\right). \tag{C22}$$

[22] Strictly speaking, $H_{\text{tc}}^{\text{con}}$ is ill-defined on the unconstrained space. However, we make the non-unique choice to map the operator $\prod_{f\supset e}X_f$ on $\mathcal{H}_{\text{ttc}}^{\text{con}}$ to the operator $\prod_{f\supset e}X_f$ on $\mathcal{H}_{\text{ttc}}$. Importantly, this choice preserves locality and $|\Psi_{\text{tc}}\rangle$ remains a $+1$ eigenstate regardless of the ambient Hilbert space.

This results in $H_{\text{ttc}}^{\text{con}}$ defined in the constrained space $\mathcal{H}_{\text{ttc}}^{\text{con}}$:

$$H_{\text{ttc}}^{\text{con}} = -\sum_e \bar{G}_e, \tag{C23}$$

where $\bar{G}_e$ is defined as:

$$\bar{G}_e \equiv \prod_{f \supset e} X_f \prod_f Z_f^{\int \boldsymbol{f} \cup_1 \delta \boldsymbol{e}}. \tag{C24}$$

Lastly, we impose the local constraints of $\mathcal{H}_{\text{ttc}}^{\text{con}}$ energetically:

$$H_{\text{ttc}} \equiv -\sum_e \bar{G}_e - \sum_t W_t. \tag{C25}$$

H_{ttc} is the Hamilitonian for the twisted toric code with a ground state given by $|\Psi_{\text{ttc}}\rangle$.

Appendix D: A ground state of the twisted toric code

Here, we give a direct proof that the state $|\Psi_{\text{ttc}}\rangle$, defined in Eq. (74) as:

$$|\Psi_{\text{ttc}}\rangle \equiv \sum_{\boldsymbol{a}_e} \prod_t (-1)^{\boldsymbol{a}_e \cup \delta \boldsymbol{a}_e(t)} |\delta \boldsymbol{a}_e\rangle, \tag{D1}$$

is a ground state of the twisted toric code Hamiltonian:

$$H_{\text{ttc}} = \sum_e \bar{G}_e - \sum_t W_t. \tag{D2}$$

In particular, we show that $|\Psi_{\text{ttc}}\rangle$ is a $+1$ eigenstate of both W_t and $\bar{G}_e$. This implies that $|\Psi_{\text{ttc}}\rangle$ is a ground state of H_{ttc}, since W_t and $\bar{G}_e$ have eigenvalues ± 1.[23]

Let us compute $W_t|\Psi_{\text{ttc}}\rangle$ and $\bar{G}_e|\Psi_{\text{ttc}}\rangle$ explicitly. For $W_t|\Psi_{\text{ttc}}\rangle$, we have:

$$\begin{aligned} W_t|\Psi_{\text{ttc}}\rangle &= W_t \sum_{\boldsymbol{a}_e} \prod_t (-1)^{\boldsymbol{a}_e \cup \delta \boldsymbol{a}_e(t)} |\delta \boldsymbol{a}_e\rangle \\ &= \sum_{\boldsymbol{a}_e} (-1)^{\delta \boldsymbol{a}_e(\partial t)} \prod_t (-1)^{\boldsymbol{a}_e \cup \delta \boldsymbol{a}_e(t)} |\delta \boldsymbol{a}_e\rangle \\ &= \sum_{\boldsymbol{a}_e} (-1)^{\boldsymbol{a}_e(\partial\partial t)} \prod_t (-1)^{\boldsymbol{a}_e \cup \delta \boldsymbol{a}_e(t)} |\delta \boldsymbol{a}_e\rangle \\ &= |\Psi_{\text{ttc}}\rangle. \end{aligned} \tag{D3}$$

While for $\bar{G}_e|\Psi_{\text{ttc}}\rangle$, we find:

$$\begin{aligned} \bar{G}_e|\Psi_{\text{ttc}}\rangle &= \bar{G}_e \sum_{\boldsymbol{a}_e} \prod_t (-1)^{\boldsymbol{a}_e \cup \delta \boldsymbol{a}_e(t)} |\delta \boldsymbol{a}_e\rangle \\ &= \sum_{\boldsymbol{a}_e} \prod_t (-1)^{\boldsymbol{a}_e \cup \delta \boldsymbol{a}_e(t) + \delta \boldsymbol{a}_e \cup_1 \delta \boldsymbol{e}(t)} |\delta \boldsymbol{a}_e + \delta \boldsymbol{e}\rangle. \end{aligned} \tag{D4}$$

[23] This follows from the observation that W_t and $\bar{G}_e$ square to the identity

To evaluate this further, we focus on the sign:

$$\prod_t (-1)^{\boldsymbol{a}_e \cup \delta \boldsymbol{a}_e(t) + \delta \boldsymbol{e} \cup_1 \delta \boldsymbol{a}_e(t)}. \tag{D5}$$

Using Eqs. (A18), (A15) and that M is closed, we can write the sign as:

$$\prod_t (-1)^{(\boldsymbol{a}_e + \boldsymbol{e}) \cup \delta(\boldsymbol{a}_e + \boldsymbol{e})(t)}. \tag{D6}$$

Now, we plug this sign into the expression for $\bar{G}_e|\Psi_{\text{ttc}}\rangle$ in Eq. (D4):

$$\begin{aligned} \bar{G}_e|\Psi_{\text{ttc}}\rangle &= \sum_{\boldsymbol{a}_e} \prod_t (-1)^{(\boldsymbol{a}_e + \boldsymbol{e}) \cup \delta(\boldsymbol{a}_e + \boldsymbol{e})(t)} |\delta \boldsymbol{a}_e + \delta \boldsymbol{e}\rangle \\ &= \sum_{\boldsymbol{a}_e} \prod_t (-1)^{\boldsymbol{a}_e \cup \delta \boldsymbol{a}_e(t)} |\delta \boldsymbol{a}_e\rangle \\ &= |\Psi_{\text{ttc}}\rangle. \end{aligned} \tag{D7}$$

Therefore, $|\Psi_{\text{ttc}}\rangle$ is a $+1$ eigenstate of W_t and $\bar{G}_e$ for all t and e, respectively.

Appendix E: Fermion condensation of the twisted toric code

Here, we elaborate on the fermion condensation procedure for the twisted toric code:

$$H_{\text{ttc}} = -\sum_e \bar{G}_e - \sum_t W_t. \tag{E1}$$

We begin by showing that the operators $\bar{G}_e$ are local generators of an anomalous $\mathbb{Z}_2$ 2-form symmetry of the twisted toric code. Then, we apply the prescription for fermion condensation in Section III C to the twisted toric code.

Anomalous 2-form symmetry of the twisted toric code:

We prove the identity in Eq. (83) – for a path p_e intersecting the faces meeting at the edge e:

$$\bar{G}_e = \tilde{\mathcal{S}}_{p_e}, \tag{E2}$$

where for reference, $\bar{G}_e$ is defined as:

$$\bar{G}_e = \prod_{f \supset e} X_f \prod_f Z_f^{\int \boldsymbol{f} \cup_1 \delta \boldsymbol{e}}. \tag{E3}$$

Eq. (E2) says that $\bar{G}_e$ is equal to a small loop of emergent fermion string operator, i.e., it is a local generator of a $\mathbb{Z}_2$ anomalous 2-form symmetry. We prove the equality in Eq. (E2) as follows. First, by definition, $\tilde{\mathcal{S}}_{p_e}$ is:

$$\tilde{\mathcal{S}}_{p_e} \equiv \overline{\prod_{f \in F_{\perp p_e}} \bar{U}_f} \prod_{f \in F_{\perp p_e}} W_{R(f)}. \tag{E4}$$

We simplify the W_t term and $\bar{U}_f$ term independently and then show that their product is $\bar{G}_e$.

To simplify the W_t term, we note that the product $\prod_{f\in F_{\perp p_e}} W_{R(f)}$ can be rewritten as:

$$\prod_t W_t^{\boldsymbol{t}\cup_1 \boldsymbol{e}(t)+\boldsymbol{e}\cup_1 \boldsymbol{t}(t)}. \tag{E5}$$

For $t=\langle 1234\rangle$, the cochain $\boldsymbol{t}\cup_1 \boldsymbol{e}(t)+\boldsymbol{e}\cup_1 \boldsymbol{t}(t)$ evaluates to:

$$\boldsymbol{e}(\langle 12\rangle)+\boldsymbol{e}(\langle 23\rangle)+\boldsymbol{e}(\langle 34\rangle)+\boldsymbol{e}(\langle 14\rangle). \tag{E6}$$

The edges $\langle 12\rangle$, $\langle 23\rangle$, $\langle 34\rangle$, and $\langle 14\rangle$ above are precisely the edges e of t such that, for the two faces of t meeting at e, the orientation of one is towards the center of t, while the orientation of the other is away from the center of t. Therefore, for exactly one of these faces, we have $R(f)=t$. Using the higher cup product relations in Appendix A 2, we can re-express Eq. (E5) in terms of a product over faces as:

$$\prod_t W_t^{\boldsymbol{t}\cup_1 \boldsymbol{e}(t)+\boldsymbol{e}\cup_1 \boldsymbol{t}(t)}=\prod_f Z_f^{\int(\boldsymbol{f}\cup_1 \delta\boldsymbol{e}+\delta\boldsymbol{e}\cup_1 \boldsymbol{f})}. \tag{E7}$$

For the $\bar{U}_f$ term of Eq. (E4), we have:

$$\overline{\prod_{f\in F_{\perp p_e}}}\bar{U}_f=\prod_f Z_f^{\int\delta\boldsymbol{e}\cup_1 \boldsymbol{f}}\prod_{f\supset e} X_f. \tag{E8}$$

By commuting the Pauli Z operators to the right of the Pauli X operators, we find:

$$\overline{\prod_{f\in F_{\perp p_e}}}\bar{U}_f=(-1)^{\int\delta\boldsymbol{e}\cup_1\delta\boldsymbol{e}}\prod_{f\supset e} X_f\prod_f Z_f^{\delta\boldsymbol{e}\cup_1 \boldsymbol{f}(t)}. \tag{E9}$$

Using the cup product relations in Appendix A 2, it can be shown that $\int\delta\boldsymbol{e}\cup_1\delta\boldsymbol{e}=0$. Therefore, the product in Eq. (E4) is:

$$\begin{aligned}\tilde{S}_{p_e}&=\prod_{f\supset e} X_f\prod_f Z_f^{\delta\boldsymbol{e}\cup_1 \boldsymbol{f}(t)}\prod_f Z_f^{\int(\boldsymbol{f}\cup_1\delta\boldsymbol{e}+\delta\boldsymbol{e}\cup_1\boldsymbol{f})}\\&=\prod_{f\supset e} X_f\prod_f Z_f^{\int\boldsymbol{f}\cup_1\delta\boldsymbol{e}}.\end{aligned} \tag{E10}$$

This is exactly $\bar{G}_e$ in Eq. (E2).

Fermion condensation procedure:

Following the steps outlined in Section III C, we first introduce a fermionic d.o.f. at the center of each tetrahedron and impose the gauge constraint:

$$\tilde{U}_f\tilde{S}_f=1, \tag{E11}$$

at each face f. As noted in the main text, the product of $\tilde{U}_f\tilde{S}_f$ over faces adjoined to the edge e is precisely $\bar{G}_e$. Therefore, in the constrained space and after a shift of energy, H_{ttc} becomes:

$$H'_{\text{ttc}}=-\sum_t W_t. \tag{E12}$$

Next, we couple H_{ttc} to the fermionic d.o.f. to make the Hamiltonian gauge invariant. We do so by replacing W_t with W_tP_t:

$$H''_{\text{ttc}}\equiv-\sum_t W_tP_t. \tag{E13}$$

The last step is to fix a gauge in which the eigenvalue of each Z_f is $+1$. Starting with H''_{ttc}, this gives us the atomic insulator Hamiltonian:

$$H_{\text{AI}}=-\sum_t P_t. \tag{E14}$$

Thus, fermion condensation produces the atomic insulator from the twisted toric code Hamiltonian.

For completeness, let us show here that the gauge constraints in Eq. (E11) are all mutually commuting. Using the definition $P_{L(f)}\tilde{S}_f=S_f$ and Eq. (86), the commutation relations between $\tilde{S}_f$ and $\tilde{S}_{f'}$ are:

$$\tilde{S}_f\tilde{S}_{f'}=(-1)^{\int\left(f'\cup_1 f+f\cup_1 f'\right)}(-1)^{\delta\boldsymbol{f}'(L(f))+\delta\boldsymbol{f}(L(f'))}\tilde{S}_{f'}\tilde{S}_f.$$

The expression $\delta\boldsymbol{f}'(L(f))+\delta\boldsymbol{f}(L(f'))$ is 1 when both f and f' share a tetrahedron t and the orientation of only one of the faces points towards the center of t. Otherwise, the expression is 0. This is also true of $\delta\boldsymbol{f}'(R(f))+\delta\boldsymbol{f}(R(f'))$, so we may write:

$$\tilde{S}_f\tilde{S}_{f'}=(-1)^{\int\left(f'\cup_1 f+f\cup_1 f'\right)}(-1)^{\delta\boldsymbol{f}'(R(f))+\delta\boldsymbol{f}(R(f'))}\tilde{S}_{f'}\tilde{S}_f.$$

Given the commutation relations between $\bar{U}_f$ and $\bar{U}_{f'}$ in Eq. (77), for $\tilde{U}_f$ and $\tilde{U}_{f'}$, we have:

$$\tilde{U}_f\tilde{U}_{f'}=(-1)^{\int\left(f'\cup_1 f+f\cup_1 f'\right)}(-1)^{\delta\boldsymbol{f}'(R(f))+\delta\boldsymbol{f}(R(f'))}\tilde{U}_{f'}\tilde{U}_f.$$

Therefore, for all faces f and f':

$$\left(\tilde{U}_f\tilde{S}_f\right)\left(\tilde{U}_{f'}\tilde{S}_{f'}\right)=\left(\tilde{U}_{f'}\tilde{S}_{f'}\right)\left(\tilde{U}_f\tilde{S}_f\right).$$

Appendix F: Bosonization duality in $(3+1)$D and spin structure

In this appendix, we review the operator-level duality between a fermionic theory and a $\mathbb{Z}_2$ lattice gauge theory in three spatial dimensions [22]. The fermion condensation duality in Section III C is functionally equivalent to applying the duality described here. We also elaborate on the spin structure dependent sign in the definition of the hopping operator. We note that the boson-fermion duality in $(2+1)$D is described in Ref. [31], and the duality in arbitrary dimensions is worked out in Ref. [30].

The duality is defined for fermionic systems where each tetrahedron t of the triangulated 3-manifold M hosts a single spinless complex fermion with an operator algebra generated by the Majorana operators γ_t,γ'_t. The fermion parity even algebra is generated by the site fermion parity:

$$P_t=-i\gamma_t\gamma'_t, \tag{F1}$$

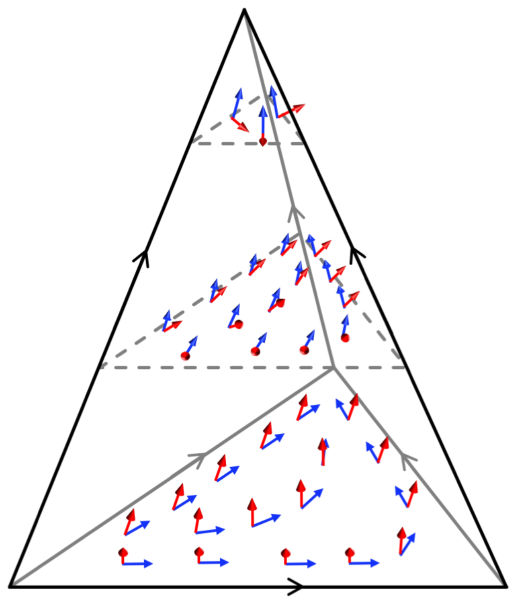

FIG. 24. A coordinate frame field can be constructed from the branching structure. We show cross sections of the frame field above. The x-axes (blue vectors) are given by an interpolation of the edge orientations into the interior of the tetrahedron. The y-axes (red vectors) are an interpolation of the face orientations into the interior of the tetrahedron. The z-axes (not pictured) are chosen with respect to the orientation of the manifold.

and the fermionic hopping operator:

$$S_f = (-1)^{\boldsymbol{f}(E)} i\gamma_{L(f)}\gamma'_{R(f)}. \tag{F2}$$

In the definition of S_f, $L(f)$ and $R(f)$ are the tetrahedra on either side of f, with the orientation of f pointing out of $L(f)$ and into $R(f)$ (Fig. 5). We discuss the spin structure dependent sign $(-1)^{\boldsymbol{f}(E)}$ of S_f in detail below.

The 2-chain $E \in C_2(M, \mathbb{Z}_2)$ in Eq. (F2), is a formal sum of faces, corresponding to a choice of spin structure. E is chosen such that the boundary of E is equal to $w_2 \in C_1(M, \mathbb{Z}_2)$, a representative of the Poincaré dual of the second Stiefel-Whitney cohomology class $\boldsymbol{w}_2(TM)$. For a triangulated 3D manifold, a representative w_2 is given by [17, 30, 58, 59]:

$$w_2 = \sum_e [1 + N_{13}^+(e) + N_{02}^-(e)]_{\mathbf{2}} \cdot e, \tag{F3}$$

where $[\cdots]_{\mathbf{2}}$ denotes that the coefficient of e is taken modulo 2, $N_{13}^+(e)$ is the number of positively oriented tetrahedra $\langle 0123\rangle$ such that $\langle 13\rangle = e$, and $N_{02}^-(e)$ is the number of negatively oriented tetrahedra $\langle 0123\rangle$ such that $\langle 02\rangle = e$.

The set of edges with coefficient 1 in w_2 admits a graphical interpretation, which generalizes the graphical interpretation in Refs. [23] and [60] for a spin structure in 2D. To see this, we use the branching structure of M to define a section of the frame bundle on M - an assignment of a coordinate frame to each point in M. Similar to the 2D case, we first interpolate the branching structure to a vector field on the interior of a tetrahedron of M, as depicted in Fig. 24. These vectors form the x-axes of the coordinate frames. The y-axes are then formed by interpolating the orientations of the faces to a vector field on the interior of the tetrahedron. Finally, the z-axes are determined by the orientation of M. The edges forming w_2 give precisely the singular edges of the frame field, i.e., for any path that encloses an odd number of edges in w_2, the frames along the path rotate by an odd multiple of 2π. Heuristically, a fermion that is moved around a singular edge is rotated by an odd multiple of 2π, and the sign in Eq. (F2) compensates for the rotation via the spin-statistics of fermions (see Fig. 25).

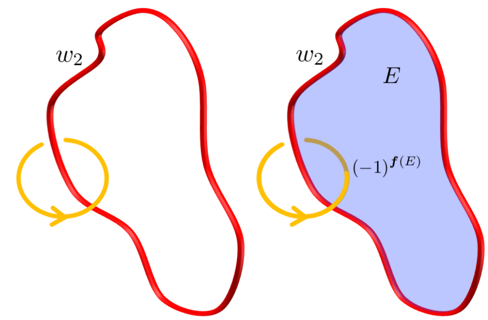

FIG. 25. The frames along a path (yellow) rotate by an odd multiple of 2π when linked with the 1-chain w_2 (red). The 2-chain E (blue) satisfies $\partial E = w_2$. The hopping operators are modified with the sign $(-1)^{\boldsymbol{f}(E)}$ to account for the twisting of the framed path by an odd multiple of 2π.

To describe the bosonization duality, it is convenient to define a product of hopping operators corresponding to a 2-cochain. For a 2-cochain $\boldsymbol{\lambda}$, we define S_λ to be:

$$S_\lambda = \prod_{i,i'|i<i'} (-1)^{\boldsymbol{\lambda}(f_i)\boldsymbol{\lambda}(f_{i'})\int \boldsymbol{f}_i \cup_1 \boldsymbol{f}_{i'}} \prod_f S_f^{\boldsymbol{\lambda}(f)}, \tag{F4}$$

where the faces are arbitrarily ordered $\{f_1, f_2, f_3, \cdots\}$ and the product is $\prod_{f\in\{f_1,f_2,\cdots,f_n\}} S_f = S_{f_n}\cdots S_{f_2}S_{f_1}$. The order dependent sign ensures that the definition of S_λ is independent of the choice of ordering. This follows from the commutation relations of the hopping operators:

$$S_f S_{f'} = (-1)^{\int(\boldsymbol{f}\cup_1\boldsymbol{f}' + \boldsymbol{f}'\cup_1\boldsymbol{f})} S_f S_{f'}. \tag{F5}$$

Given a pair of 2-cochains $\boldsymbol{\lambda}$ and $\boldsymbol{\lambda}'$, we have the identity:

$$S_{\lambda+\lambda'} \equiv (-1)^{\int \boldsymbol{\lambda}\cup_1\boldsymbol{\lambda}'} S_{\lambda'} S_\lambda. \tag{F6}$$

The two generators P_t and S_f satisfy the following constraint at each edge e [30]:

$$S_{\delta \boldsymbol{e}} \prod_t P_t^{\int \boldsymbol{e}\cup_1\boldsymbol{t} + \boldsymbol{t}\cup_1\boldsymbol{e}} = 1 \tag{F7}$$

The physical meaning of this identity is that moving a fermion along a small loop around a edge e is an identity operator. We note that the spin structure dependent sign in the definition of the hopping operator guarantees that the product in Eq. (F7) is 1.

The bosonic dual of this system has $\mathbb{Z}_2$-valued spins on the faces of the triangulation, with an operator algebra generated by X, Z Pauli operators. For every tetrahedron t, we define the flux operator:

$$W_t = \prod_{f \subset t} Z_f, \tag{F8}$$

and for every face f, we define a bosonic hopping operator:

$$\bar{U}_f = \prod_{f'} Z_{f'}^{\int \boldsymbol{f} \cup_1 \boldsymbol{f}'} X_f. \tag{F9}$$

Similar to the fermionic hopping operator, we define a product of $\bar{U}_f$ for any 2-cochain $\boldsymbol{\lambda}$. In this case, $\bar{U}_\lambda$ is defined as:

$$\bar{U}_\lambda = \prod_{f'} Z_{f'}^{\int \boldsymbol{\lambda} \cup_1 \boldsymbol{f}'} \prod_f X_f^{\boldsymbol{\lambda}(f)}. \tag{F10}$$

To define a consistent duality between the even fermionic operator algebra and the algebra generated by W_t and $\bar{U}_f$ operators, we also define $\bar{G}_e$, given by:

$$\bar{G}_e = \prod_{f \supset e} X_f \prod_{f'} Z_{f'}^{\int \boldsymbol{f}' \cup_1 \delta \boldsymbol{e}}. \tag{F11}$$

The duality in Ref. [31], is an isomorphism of the C^* algebras $\mathcal{F}$ and $\mathcal{B}$, where $\mathcal{F}$ is the algebra of even fermion parity operators and $\mathcal{B}$ is the algebra generated by W_t and $\bar{U}_f$ with the constraint $\bar{G}_e = 1$. The mapping of operators is:

$$W_t \leftrightarrow P_t, \quad \bar{U}_f \leftrightarrow S_f. \tag{F12}$$

We note the correspondence above is well-defined since the nontrivial relations map to constraints on the algebra, i.e.:

$$\begin{aligned} \bar{G}_e &\leftrightarrow S_{\delta \boldsymbol{e}} \prod_t P_t^{\int \boldsymbol{e} \cup_1 \boldsymbol{t} + \boldsymbol{t} \cup_1 \boldsymbol{e}} = 1 \\ \prod_t W_t = 1 &\leftrightarrow \prod_t P_t. \end{aligned} \tag{F13}$$

Also, the operators $\bar{U}_\lambda$ and S_λ are defined so that the duality in Eq. (F12) maps:

$$\bar{U}_\lambda \leftrightarrow S_\lambda, \tag{F14}$$

for any 2-cochain $\boldsymbol{\lambda}$. This is because the Pauli X and Pauli Z operators in $\bar{U}_\lambda$ can be commuted past one another to obtain (see Appendix H 2):

$$\bar{U}_\lambda = \prod_{i,i' | i < i'} (-1)^{\boldsymbol{\lambda}(f_i) \boldsymbol{\lambda}(f_{i'}) \int \boldsymbol{f}_i \cup_1 \boldsymbol{f}_{i'}} \prod_f \bar{U}_f^{\boldsymbol{\lambda}(f)}. \tag{F15}$$

Appendix G: Symmetry of the 2-group SPT Hamiltonian

We use this Appendix to prove that the 2-group Hamiltonian $H_2 = \mathcal{U}_2 H_0^G \mathcal{U}_2^\dagger$ in Section IV B is symmetric. Given that H_0^G is invariant under the 2-group symmetry, it suffices to show that $\mathcal{U}_2$ is symmetric. For convenience, we re-write $\mathcal{U}_2$ here as:

$$\mathcal{U}_2 = \sum_{\{g_v\}, \boldsymbol{a}_e} \prod_t e^{2\pi i O_t \overline{\boldsymbol{\alpha}}_{\{g_v\}}(t)} |\{g_v\}, \boldsymbol{a}_e\rangle\langle\{g_v\}, \boldsymbol{a}_e|, \tag{G1}$$

where the 3-cochain $\overline{\boldsymbol{\alpha}}_{\{g_v\}}$ is:

$$\begin{aligned} \overline{\boldsymbol{\alpha}}_{\{g_v\}} =& \overline{\boldsymbol{\nu}}_{\{g_v\}} + \frac{1}{2} \overline{\boldsymbol{\rho}}_{\{g_v\}} \cup_1 \overline{\boldsymbol{\rho}}_{\{g_v\}} \\ &+ \frac{1}{2} \overline{\boldsymbol{\rho}}_{\{g_v\}} \cup_1 \delta \boldsymbol{a}_e + \frac{1}{2} \boldsymbol{a}_e \cup \delta \boldsymbol{a}_e. \end{aligned} \tag{G2}$$

We note that we have expressed the W_f term of $\mathcal{U}_2$ in terms of $\delta \boldsymbol{a}_e$.

First of all, the FDQC $\mathcal{U}_2$ is symmetric under the 1-form symmetry in Eq. (107). The 1-form symmetry only affects the last two terms of $\overline{\boldsymbol{\alpha}}_{\{g_v\}}$, those with $\boldsymbol{a}_e$. The $\frac{1}{2} \boldsymbol{a}_e \cup \delta \boldsymbol{a}_e$ term is invariant, as shown in Appendix B. The $\frac{1}{2} \overline{\boldsymbol{\rho}}_{\{g_v\}} \cup_1 \delta \boldsymbol{a}_e$ term is also symmetric, since it can be written in terms of the 1-form symmetric operators W_f, as in Eq. (115).

Second, we show that $\mathcal{U}_2$ commutes with the 0-form symmetry operator $V_\rho(h)$, for all $h \in G$:

$$V_\rho(h) = V(h) \prod_e X_e^{\hat{\overline{\boldsymbol{\rho}}}^h(e)}. \tag{G3}$$

Specifically, we compute:

$$V_\rho(h) \mathcal{U}_2 V_\rho^\dagger(h). \tag{G4}$$

First, in moving the product of Pauli X operators in Eq. (G3) past $\mathcal{U}_2$, we find:

$$\begin{aligned} &V_\rho(h) \mathcal{U}_2 V_\rho^\dagger(h) = \\ &V(h) \sum_{\{g_v\}, \boldsymbol{a}_e} \prod_t e^{2\pi i O_t \overline{\boldsymbol{\alpha}}'_{\{g_v\}}(t)} |\{g_v\}, \boldsymbol{a}_e\rangle\langle\{g_v\}, \boldsymbol{a}_e| V^\dagger(h), \end{aligned} \tag{G5}$$

where $\overline{\boldsymbol{\alpha}}'_{\{g_v\}}$ is:

$$\begin{aligned} \overline{\boldsymbol{\alpha}}'_{\{g_v\}} =& \overline{\boldsymbol{\nu}}_{\{g_v\}} + \frac{1}{2} \overline{\boldsymbol{\rho}}_{\{g_v\}} \cup_1 \overline{\boldsymbol{\rho}}_{\{g_v\}} \\ &+ \frac{1}{2} \overline{\boldsymbol{\rho}}_{\{g_v\}} \cup_1 \delta (\boldsymbol{a}_e + \overline{\boldsymbol{\rho}}^h_{\{g_v\}}) \\ &+ \frac{1}{2} (\boldsymbol{a}_e + \overline{\boldsymbol{\rho}}^h_{\{g_v\}}) \cup \delta (\boldsymbol{a}_e + \overline{\boldsymbol{\rho}}^h_{\{g_v\}}). \end{aligned} \tag{G6}$$

Then, conjugation by $V(h)$ on the right hand side of Eq. (G5) produces:

$$\begin{aligned} &V_\rho(h) \mathcal{U}_2 V_\rho^\dagger(h) = \\ &\sum_{\{g_v\}, \boldsymbol{a}_e} \prod_t e^{2\pi i O_t \overline{\boldsymbol{\alpha}}'_{\{h^{-1} g_v\}}(t)} |\{g_v\}, \boldsymbol{a}_e\rangle\langle\{g_v\}, \boldsymbol{a}_e|, \end{aligned} \tag{G7}$$

with $\overline{\boldsymbol{\alpha}}'_{\{h^{-1} g_v\}}$ given explicitly by:

$$\begin{aligned} \overline{\boldsymbol{\alpha}}'_{\{h^{-1} g_v\}} =& \overline{\boldsymbol{\nu}}_{\{h^{-1} g_v\}} + \frac{1}{2} \overline{\boldsymbol{\rho}}_{\{h^{-1} g_v\}} \cup_1 \overline{\boldsymbol{\rho}}_{\{h^{-1} g_v\}} \\ &+ \frac{1}{2} \overline{\boldsymbol{\rho}}_{\{h^{-1} g_v\}} \cup_1 \delta (\boldsymbol{a}_e + \overline{\boldsymbol{\rho}}^h_{\{h^{-1} g_v\}}) \\ &+ \frac{1}{2} (\boldsymbol{a}_e + \overline{\boldsymbol{\rho}}^h_{\{h^{-1} g_v\}}) \cup \delta (\boldsymbol{a}_e + \overline{\boldsymbol{\rho}}^h_{\{h^{-1} g_v\}}). \end{aligned} \tag{G8}$$

We now simplify the expression for $\overline{\boldsymbol{\alpha}}'_{\{h^{-1}g_v\}}$ in Eq. (G8). To do so, we make use of the cochain $\widetilde{\boldsymbol{\rho}}^h_{\{g_v\}}$, defined on an arbitrary edge $\langle 12\rangle$ as:

$$\widetilde{\boldsymbol{\rho}}^h_{\{g_v\}}(\langle 12\rangle) = \rho(h,1,g_1,g_2). \tag{G9}$$

It is also useful to introduce $\widetilde{\boldsymbol{\nu}}^h_{\{g_v\}}$:

$$\widetilde{\boldsymbol{\nu}}^h_{\{g_v\}}(\langle 123\rangle) \equiv \nu(h,1,g_1,g_2,g_3), \tag{G10}$$

for an arbitrary face $\langle 123\rangle$. We then employ the following identities:

$$\begin{aligned}\overline{\boldsymbol{\nu}}_{\{h^{-1}g_v\}} =& \overline{\boldsymbol{\nu}}_{\{g_v\}} + \delta\widetilde{\boldsymbol{\nu}}^h_{\{g_v\}} + \frac{1}{2}\delta\widetilde{\boldsymbol{\rho}}^h_{\{g_v\}} \cup_1 \overline{\boldsymbol{\rho}}_{\{g_v\}} \\ &+ \frac{1}{2}\widetilde{\boldsymbol{\rho}}^h_{\{g_v\}} \cup \delta\widetilde{\boldsymbol{\rho}}^h_{\{g_v\}} + \delta(\widetilde{\boldsymbol{\rho}}^h_{\{g_v\}} \cup_1 \overline{\boldsymbol{\rho}}_{\{g_v\}}),\end{aligned} \tag{G11}$$

$$\overline{\boldsymbol{\rho}}_{\{h^{-1}g_v\}} = \overline{\boldsymbol{\rho}}_{\{g_v\}} + \delta\widetilde{\boldsymbol{\rho}}^h_{\{g_v\}}, \tag{G12}$$

$$\overline{\boldsymbol{\rho}}^h_{\{h^{-1}g_v\}} = \widetilde{\boldsymbol{\rho}}^h_{\{g_v\}}. \tag{G13}$$

The first relation, in Eq. (G11), can be derived using the coboundary relation of ν [Eq. (2)], the homogeneity of ν [Eq. (6)], and the cup product relations in Appendix A 2. The second identity, [Eq. (G12)], follows from the fact that ρ is closed [Eq. (2)] as well as the homogeneity of ρ [Eq. (6)]. The final relation, [Eq. (G13)], is a result of the homogeneity of ρ. Plugging Eqs. (G11), (G12), and (G13) into the right hand side of Eq. (G8) and using the cup product relations, we find:

$$\begin{aligned}&\overline{\boldsymbol{\alpha}}'_{\{h^{-1}g_v\}} = \overline{\boldsymbol{\alpha}}_{\{g_v\}} \\ &+ \frac{1}{2}\delta\left[\widetilde{\boldsymbol{\nu}}^h_{\{g_v\}} + \widetilde{\boldsymbol{\rho}}^h_{\{g_v\}} \cup_1 (\overline{\boldsymbol{\rho}}_{\{g_v\}} + \delta\boldsymbol{a}_e) + \boldsymbol{a}_e \cup \widetilde{\boldsymbol{\rho}}^h_{\{g_v\}}\right].\end{aligned} \tag{G14}$$

On a closed manifold, the coboundary term in Eq. (G14) vanishes after taking the product over all tetrahedron in Eq. (G1), by Stokes' theorem. Therefore, for arbitrary $h \in G$:

$$V_\rho(h)\mathcal{U}_2 V_\rho^\dagger(h) = \mathcal{U}_2. \tag{G15}$$

Since $\mathcal{U}_2$ commutes with the symmetry, H_2 must be symmetric under the 2-group symmetry.

Appendix H: Properties of $\mathcal{U}_s$

The goal of this Appendix is to establish the properties of the FDQC $\mathcal{U}_s$ employed in the main text. We first show that $\mathcal{U}_s$ is symmetric up to factors of $\bar{G}_e$. This is used to compute the fractionalization of the G symmetry on the loop-like excitations of the shadow model (see Section IV C). Next, we express $\mathcal{U}_s$ in terms of $\bar{U}_f$ and W_t, as required in Section IV D. As such, $\mathcal{U}_s$ can be straightforwardly fermionized using the fermion condensation duality in Section III B. Lastly, we derive the algebraic composition laws of the FDQCs for different sets of supercohomology data. With this, we determine the stacking laws of the corresponding fSPT phases in Section IV D.

To start, we make a minor simplification to $\mathcal{U}_s$:

$$\begin{aligned}\mathcal{U}_s = \prod_f X_f^{\hat{\bar{\boldsymbol{\rho}}}(f)} \prod_t \left[e^{2\pi i O_t\left[\hat{\bar{\boldsymbol{\nu}}}(t) + \frac{1}{2}\hat{\bar{\boldsymbol{\rho}}}\cup_1\hat{\bar{\boldsymbol{\rho}}}(t)\right]} \prod_{f\subset t} Z_f^{\hat{\bar{\boldsymbol{\rho}}}\cup_1 \boldsymbol{f}(t)}\right] \\ \times \prod_t W_t^{\int \hat{\bar{\boldsymbol{\rho}}}\cup_2 \boldsymbol{t}}.\end{aligned} \tag{H1}$$

We commute the product of X_f operators past the product of Z_f operators. This cancels the sign from $\frac{1}{2}\hat{\bar{\boldsymbol{\rho}}} \cup_1 \hat{\bar{\boldsymbol{\rho}}}(t)$, and we are left with:

$$\mathcal{U}_s = \prod_t e^{2\pi i O_t \hat{\bar{\boldsymbol{\nu}}}(t)} \prod_f Z_f^{\int \hat{\bar{\boldsymbol{\rho}}}\cup_1 \boldsymbol{f}} \prod_f X_f^{\hat{\bar{\boldsymbol{\rho}}}(f)} \prod_t W_t^{\int \hat{\bar{\boldsymbol{\rho}}}\cup_2 \boldsymbol{t}}. \tag{H2}$$

We have also changed the product of Z_f operators to a product over all faces in M. Since the $\cup_1$ product vanishes if f is not contained in the boundary of t, the change of bounds does not affect $\mathcal{U}_s$. We use the form of $\mathcal{U}_s$ in Eq. (H2) for the calculations below.

1. Symmetry variation

Our goal is to show the identity:

$$V(h)\mathcal{U}_s = \mathcal{U}_s\left[\prod_e \bar{G}_e^{\hat{\bar{\boldsymbol{\rho}}}^{h^{-1}}(e)}\right] V(h), \tag{H3}$$

for an arbitrary $h \in G$, used in Section IV C [Eq. (148)]. We compute the action of the symmetry on $\mathcal{U}_s$, i.e., $V(h)\mathcal{U}_s V^\dagger(h)$ by conjugating terms in $\mathcal{U}_s$ one at a time.

First, conjugation of the $\hat{\bar{\boldsymbol{\nu}}}$ term by $V(h)$ produces:

$$V(h)\prod_t e^{2\pi i O_t \hat{\bar{\boldsymbol{\nu}}}(t)} V^\dagger(h) = \phi(h,\{g_v\}) \prod_t e^{2\pi i O_t \hat{\bar{\boldsymbol{\nu}}}(t)}. \tag{H4}$$

$\phi(h,\{g_v\})$ is a phase factor that depends on h and the $\{g_v\}$-configuration. We put constraints on the phase factors that appear during the calculation at the end by using the symmetry of the ground state(s) of H_s.

Next, we conjugate the Pauli X and Pauli Z terms:

$$\prod_f Z_f^{\int \hat{\bar{\boldsymbol{\rho}}}\cup_1 \boldsymbol{f}} \prod_f X_f^{\hat{\bar{\boldsymbol{\rho}}}(f)}. \tag{H5}$$

After conjugation by the symmetry, $\hat{\bar{\boldsymbol{\rho}}}$ becomes:

$$\hat{\bar{\boldsymbol{\rho}}} \to \hat{\bar{\boldsymbol{\rho}}} + \delta\hat{\bar{\boldsymbol{\rho}}}^{h^{-1}}. \tag{H6}$$

Therefore, up to a phase factor $\phi_1'(h,\{g_v\})$, the Pauli X and Z terms of $\mathcal{U}_s$ are mapped by the symmetry action to:

$$\begin{aligned}&\prod_f Z_f^{\int \hat{\bar{\boldsymbol{\rho}}}\cup_1 \boldsymbol{f}} \prod_f X_f^{\hat{\bar{\boldsymbol{\rho}}}(f)} \\ &\quad\times \phi_1'(h,\{g_v\}) \prod_f X_f^{\delta\hat{\bar{\boldsymbol{\rho}}}^{h^{-1}}(f)} \prod_f Z_f^{\int \delta\hat{\bar{\boldsymbol{\rho}}}^{h^{-1}}\cup_1 \boldsymbol{f}}\end{aligned} \tag{H7}$$

Rearranging the last two products in Eq. (H7), we find:

$$\prod_f Z_f^{\int \hat{\bar{\boldsymbol{\rho}}}\cup_1 \boldsymbol{f}} \prod_f X_f^{\hat{\bar{\boldsymbol{\rho}}}(f)} \times \phi_2'(h,\{g_v\}) \prod_e \left(\prod_{f\supset e} X_f \prod_f Z_f^{\int \delta \boldsymbol{e}\cup_1 \boldsymbol{f}} \right)^{\hat{\bar{\boldsymbol{\rho}}}^{g^{-1}}(e)}, \tag{H8}$$

for another phase factor $\phi_2'(h,\{g_v\})$. The term in parentheses in Eq. (H8) is equal to:

$$\prod_{f\supset e} X_f \prod_f Z_f^{\int \delta \boldsymbol{e}\cup_1 \boldsymbol{f}} = \bar{G}_e \prod_t W_t^{\int \delta \boldsymbol{e}\cup_2 \boldsymbol{t}}, \tag{H9}$$

after using a cup product relation from Appendix A 2. Thus, the symmetry action on the Pauli X and Pauli Z terms yields:

$$\prod_f Z_f^{\int \hat{\bar{\boldsymbol{\rho}}}\cup_1 \boldsymbol{f}} \prod_f X_f^{\hat{\bar{\boldsymbol{\rho}}}(f)} \times \phi_2'(h,\{g_v\}) \prod_e \bar{G}_e^{\hat{\bar{\boldsymbol{\rho}}}^{g^{-1}}(e)} \prod_t W_t^{\int \delta \hat{\bar{\boldsymbol{\rho}}}^{h^{-1}} \cup_2 \boldsymbol{t}}. \tag{H10}$$

Lastly, we compute the symmetry action on the W_t term of $\mathcal{U}_s$:

$$\prod_t W_t^{\int \hat{\bar{\boldsymbol{\rho}}}\cup_2 \boldsymbol{t}}. \tag{H11}$$

$\hat{\bar{\boldsymbol{\rho}}}$ is transformed as in Eq. (H6), so we obtain:

$$\prod_t W_t^{\int \hat{\bar{\boldsymbol{\rho}}}\cup_2 \boldsymbol{t}} \prod_t W_t^{\int \delta \hat{\bar{\boldsymbol{\rho}}}^{h^{-1}} \cup_2 \boldsymbol{t}}. \tag{H12}$$

Putting Eqs. (H4), (H10), and (H12) together, we have:

$$V(h)\mathcal{U}_s V^\dagger(h) = \phi''(h,\{g_v\})\mathcal{U}_s \prod_e \bar{G}_e^{\hat{\bar{\boldsymbol{\rho}}}^{h^{-1}}}, \tag{H13}$$

where $\phi''(h,\{g_v\})$ is some yet undetermined phase factor. We note that the equality above differs from Eq. (H3) by precisely $\phi''(h,\{g_v\})$. In what follows, we use the symmetry of the ground state(s) of H_s to argue that $\phi''(h,\{g_v\})$ is indeed 1.

A ground state of the shadow model is given by applying $\mathcal{U}_s$ to a ground state of H^G_{ttc}:

$$|\Psi_s\rangle \equiv \mathcal{U}_s \sum_{\{g_v\},\{\boldsymbol{a}_e\}} (-1)^{\sum_t \boldsymbol{a}_e\cup\delta\boldsymbol{a}_e(t)} |\{g_v\},\{\delta\boldsymbol{a}_e\}\rangle. \tag{H14}$$

Furthermore, the state $|\Psi_s\rangle$ is invariant under the G symmetry, i.e.:

$$V(g)|\Psi_s\rangle = |\Psi_s\rangle. \tag{H15}$$

The symmetry of $|\Psi_s\rangle$ follows from the symmetry of H_s and the fact that it can be prepared from a ground state of H^G_{ttc} by a FDQC.

With this, we argue that the phase factor $\phi''(h,\{g_v\})$ is 1. We apply $V(h)$ to $|\Psi_s\rangle$ to find:

$$\begin{aligned} &V(h)|\Psi_s\rangle \\ &= V(h)\mathcal{U}_s \sum_{\{g_v\},\{\boldsymbol{a}_e\}} (-1)^{\sum_t \boldsymbol{a}_e\cup\delta\boldsymbol{a}_e(t)} |\{g_v\},\{\delta\boldsymbol{a}_e\}\rangle. \\ &= \mathcal{U}_s \sum_{\{g_v\},\{\boldsymbol{a}_e\}} \phi(h,\{g_v\}) (-1)^{\sum_t \boldsymbol{a}_e\cup\delta\boldsymbol{a}_e(t)} |\{g_v\},\{\delta\boldsymbol{a}_e\}\rangle, \end{aligned} \tag{H16}$$

where we have used both Eq. (H13) and that the ground state(s) of H^G_{ttc} are $+1$ eigenstates of $\bar{G}_e$. Now, in comparing Eq. (H15) and the last line of Eq. (H16), we see that $\phi''(h,\{g_v\})$ must be 1 for every $\{g_v\}$. This implies that:

$$V(h)\mathcal{U}_s = \mathcal{U}_s \prod_e \bar{G}_e^{\hat{\bar{\boldsymbol{\rho}}}^{h^{-1}}} V(h), \tag{H17}$$

as claimed.

2. Fermionizability

Here, we show that the FDQC $\mathcal{U}_s$ in Eq. (H2) can be expressed in terms of $\bar{U}_f$ and W_t operators. The fermion condensation duality (Table II) can then be immediately applied to $\mathcal{U}_s$ to construct the the FDQC $\mathcal{U}_f$.

By re-arranging the Pauli X and Pauli Z operators in Eq. (H1):

$$\mathcal{U}_s = \prod_t e^{2\pi i O_t \hat{\bar{\boldsymbol{\nu}}}(t)} \prod_f Z_f^{\int \hat{\bar{\boldsymbol{\rho}}}\cup_1 \boldsymbol{f}} \prod_f X_f^{\hat{\bar{\boldsymbol{\rho}}}(f)} \prod_t W_t^{\int \hat{\bar{\boldsymbol{\rho}}}\cup_2 \boldsymbol{t}}, \tag{H18}$$

we can form $\bar{U}_f$ operators. To show this, we decompose the product of Z_f operators into:

$$\prod_f Z_f^{\int \hat{\bar{\boldsymbol{\rho}}}\cup_1 \boldsymbol{f}} = \prod_f \prod_{f'} Z_{f'}^{\hat{\bar{\boldsymbol{\rho}}}(f)\sum_t \boldsymbol{f}\cup_1 \boldsymbol{f}'(t)}. \tag{H19}$$

We then see that we can form a factor of $\bar{U}_f^{\hat{\bar{\boldsymbol{\rho}}}(f)}$ for each face f:

$$\bar{U}_f^{\hat{\bar{\boldsymbol{\rho}}}(f)} = X_f^{\hat{\bar{\boldsymbol{\rho}}}(f)} \prod_{f'} Z_{f'}^{\hat{\bar{\boldsymbol{\rho}}}(f)\sum_t \boldsymbol{f}\cup_1 \boldsymbol{f}'(t)}. \tag{H20}$$

Given the commutation relations of $\bar{U}_f$ operators, the resulting product of $\bar{U}_f^{\hat{\bar{\boldsymbol{\rho}}}(f)}$ operators will generically depend on a choice of ordering. Hence, we choose an arbitrary ordering of the faces $(f_1 < \cdots < f_i < \cdots)$ of the set F of faces in M. We aim to form a product of $\bar{U}_f^{\hat{\bar{\boldsymbol{\rho}}}(f)}$ according to the ordering on F, i.e.:

$$\prod_{f\in F} \bar{U}_f^{\hat{\bar{\boldsymbol{\rho}}}(f)} = (\cdots \bar{U}_{f_i}^{\hat{\bar{\boldsymbol{\rho}}}(f_i)} \cdots \bar{U}_{f_1}^{\hat{\bar{\boldsymbol{\rho}}}(f_1)}). \tag{H21}$$

We re-order the Pauli X and Pauli Z operators of $\mathcal{U}_s$ into the product in Eq. (H21) by first, ordering the product of Z_f operators by the ordering on F:

$$\prod_{f\in F}\prod_{f'} Z_{f'}^{\hat{\boldsymbol{\rho}}(f)\sum_t \boldsymbol{f}\cup_1 \boldsymbol{f}'(t)} = \Big[\cdots \prod_{f'} Z_{f'}^{\hat{\boldsymbol{\rho}}(f_i)\sum_t \boldsymbol{f}\cup_1 \boldsymbol{f}'(t)} \cdots \prod_{f'} Z_{f'}^{\hat{\boldsymbol{\rho}}(f_1)\sum_t \boldsymbol{f}\cup_1 \boldsymbol{f}'(t)}\Big]. \tag{H22}$$

To form $\bar{U}_{f_i}^{\hat{\boldsymbol{\rho}}(f_i)}$, $X_{f_i}^{\hat{\boldsymbol{\rho}}(f_i)}$ in Eq. (H18) is commuted past the Pauli Z operators of $\bar{U}_{f_{i'}}^{\hat{\boldsymbol{\rho}}(f_{i'})}$ for each $i' < i$. This produces the sign:

$$\prod_{i'<i}(-1)^{\hat{\boldsymbol{\rho}}(f_{i'})\hat{\boldsymbol{\rho}}(f_i)\sum_t \boldsymbol{f}_{i'}\cup_1 \boldsymbol{f}_i(t)}. \tag{H23}$$

In creating the product in Eq (H21), we thus accrue the sign:

$$\xi_\rho(F) = \prod_i \left[\prod_{i'<i}(-1)^{\hat{\boldsymbol{\rho}}(f_{i'})\hat{\boldsymbol{\rho}}(f_i)\int \boldsymbol{f}_{i'}\cup_1 \boldsymbol{f}_i}\right]. \tag{H24}$$

In summary, we have shown that $\mathcal{U}_s$ can be written as:

$$\mathcal{U}_s = \prod_t e^{2\pi i O_t \hat{\boldsymbol{\nu}}(t)}\xi_\rho(F)\prod_{f\in F}\bar{U}_f^{\hat{\boldsymbol{\rho}}(f)}\prod_t W_t^{\int \hat{\boldsymbol{\rho}}\cup_2 \boldsymbol{t}}. \tag{H25}$$

which matches the form of $\mathcal{U}_s$ in Eq. (160). Fermion condensation is implemented by replacing $\bar{U}_f$ with S_f and W_t with P_t. This gives the circuit $\mathcal{U}_f$ in Eq. (165):

$$\mathcal{U}_f \equiv \prod_t e^{2\pi i O_t \hat{\boldsymbol{\nu}}(t)}\xi_\rho(M)\prod_f S_f^{\hat{\boldsymbol{\rho}}(f)}\prod_t P_t^{\int \hat{\boldsymbol{\rho}}\cup_2 \boldsymbol{t}}. \tag{H26}$$

3. Composition laws

As argued in Section II C, the stacking laws of supercohomology phases can be determined by composing the FDQCs $\mathcal{U}_f$ that prepare the supercohomology models. For convenience, we evaluate the composition of the FDQCs $\mathcal{U}_s$ that prepare the shadow model. The composition of $\mathcal{U}_f$ operators follows from this by applying the fermionization duality to the $\mathcal{U}_s$ circuits. For reference, the FDQC $\mathcal{U}_s$ corresponding to the supercohomology data (ρ, ν) is:

$$\mathcal{U}_s^{\rho\nu} = \prod_t e^{2\pi i \hat{\boldsymbol{\nu}}(t) O_t}\prod_{f'} Z_{f'}^{\int \hat{\boldsymbol{\rho}}\cup_1 \boldsymbol{f}'}\prod_f X_f^{\hat{\boldsymbol{\rho}}(f)}\prod_t W_t^{\int \hat{\boldsymbol{\rho}}\cup_2 \boldsymbol{t}}. \tag{H27}$$

Given two sets of supercohomology data (ρ,ν) and (ρ',ν'), we calculate the product of $\mathcal{U}_s^{\rho\nu}$ and $\mathcal{U}_s^{\rho'\nu'}$ directly:

$$\begin{aligned}
&\mathcal{U}_s^{\rho\nu}\mathcal{U}_s^{\rho'\nu'} \\
&= \prod_t e^{2\pi i \hat{\boldsymbol{\nu}}(t) O_t}\prod_{f'} Z_{f'}^{\int \hat{\boldsymbol{\rho}}\cup_1 \boldsymbol{f}'}\prod_f X_f^{\hat{\boldsymbol{\rho}}(f)}\prod_t W_t^{\int \hat{\boldsymbol{\rho}}\cup_2 \boldsymbol{t}} \\
&\times \prod_t e^{2\pi i \hat{\boldsymbol{\nu}}'(t) O_t}\prod_{f'} Z_{f'}^{\int \hat{\boldsymbol{\rho}}'\cup_1 \boldsymbol{f}'}\prod_f X_f^{\hat{\boldsymbol{\rho}}'(f)}\prod_t W_t^{\int \hat{\boldsymbol{\rho}}'\cup_2 \boldsymbol{t}} \\
&= \prod_t e^{2\pi i \hat{\boldsymbol{\nu}}''(t) O_t}\prod_{f'} Z_{f'}^{\int \hat{\boldsymbol{\rho}}''\cup_1 \boldsymbol{f}'}\prod_f X_f^{\hat{\boldsymbol{\rho}}''(f)}\prod_t W_t^{\int \hat{\boldsymbol{\rho}}''\cup_2 \boldsymbol{t}}.
\end{aligned} \tag{H28}$$

In the last line, we have combined the Pauli Z and Pauli X operators and defined $\hat{\boldsymbol{\rho}}'' \equiv \hat{\boldsymbol{\rho}} + \hat{\boldsymbol{\rho}}'$. The operator $\hat{\boldsymbol{\nu}}''$ is a sum of $\hat{\boldsymbol{\nu}}$ and $\hat{\boldsymbol{\nu}}'$ and also incorporates the sign incurred from commuting the Pauli X and Pauli Z operators. In particular, to form the last line in Eq. (H28), we commute the operators:

$$\begin{aligned}
&\prod_{f'}\left(Z_{f'}^{\int \hat{\boldsymbol{\rho}}'\cup_1 f'}\right) \text{ past } \prod_f \left(X_f^{\hat{\boldsymbol{\rho}}(f)}\right), \\
&\prod_f \left(X_f^{\hat{\boldsymbol{\rho}}'(f)}\right) \text{ past } \prod_t \left(W_t^{\hat{\boldsymbol{\rho}}\cup_2 \boldsymbol{t}}\right).
\end{aligned} \tag{H29}$$

This produces the sign:

$$(-1)^{\int \hat{\boldsymbol{\rho}}'\cup_1 \hat{\boldsymbol{\rho}} + \hat{\boldsymbol{\rho}}\cup_2 \delta\hat{\boldsymbol{\rho}}'}, \tag{H30}$$

so we define $\hat{\boldsymbol{\nu}}''$ as:

$$\hat{\boldsymbol{\nu}}'' \equiv \hat{\boldsymbol{\nu}} + \hat{\boldsymbol{\nu}}' + \frac{1}{2}\hat{\boldsymbol{\rho}}'\cup_1 \hat{\boldsymbol{\rho}} + \frac{1}{2}\hat{\boldsymbol{\rho}}\cup_2 \delta\hat{\boldsymbol{\rho}}'. \tag{H31}$$

Now, we recover the supercohomology data corresponding to $\hat{\boldsymbol{\rho}}''$ and $\hat{\boldsymbol{\nu}}''$ from their diagonal matrix elements. For a face $\langle 123\rangle$, the matrix element $\langle\{g_v\}|\hat{\boldsymbol{\rho}}''(\langle 123\rangle)|\{g_v\}\rangle$ is:

$$\langle\{g_v\}|\hat{\boldsymbol{\rho}}''(\langle 123\rangle)|\{g_v\}\rangle = \rho(1,g_1,g_2,g_3) + \rho'(1,g_1,g_2,g_3). \tag{H32}$$

Therefore, $\hat{\boldsymbol{\rho}}''$ corresponds to the function $\rho'' = \rho + \rho'$. For $\hat{\boldsymbol{\nu}}''$, we compute the matrix element $\langle\{g_v\}|\hat{\boldsymbol{\nu}}''(\langle 1234\rangle)|\{g_v\}\rangle$, with an arbitrary tetrahedron $\langle 1234\rangle$:

$$\begin{aligned}
\langle\{g_v\}|\hat{\boldsymbol{\nu}}''(\langle 1234\rangle)|\{g_v\}\rangle = &\\
&\nu(1,g_1,g_2,g_3,g_4) + \nu'(1,g_1,g_2,g_3,g_4) \\
&+\frac{1}{2}\rho(1,g_1,g_2,g_3)\rho'(1,g_1,g_3,g_4) \\
&+\frac{1}{2}\rho(1,g_2,g_3,g_4)\rho'(1,g_1,g_2,g_4) \\
&+\frac{1}{2}\rho(1,g_1,g_2,g_3)\rho'(g_1,g_2,g_3,g_4) \\
&+\frac{1}{2}\rho(1,g_1,g_3,g_4)\rho'(g_1,g_2,g_3,g_4).
\end{aligned} \tag{H33}$$

To obtain the right-hand side of Eq. (H33), we have used the explicit formulas for cup products in Appendix A 2.

The sum of ρ and ρ' terms can be further simplified to $\frac{1}{2}\rho \cup_2 \rho'(1, g_1, g_2, g_3, g_4)$ with Eq. (A7). Thus, $\hat{\boldsymbol{\nu}}''$ corresponds to the function $\nu'' \equiv \nu + \nu'' + \frac{1}{2}\rho \cup_2 \rho'$.

In summary, we have found $\mathcal{U}_s^{\rho\nu}\mathcal{U}_s^{\rho'\nu'} = \mathcal{U}_s^{\rho''\nu''}$, where (ρ'', ν'') is:

$$(\rho'', \nu'') = (\rho + \rho', \nu + \nu'' + \frac{1}{2}\rho \cup_2 \rho'). \tag{H34}$$

Since the composition rules are preserved under fermionization, we have that $\mathcal{U}_f^{\rho\nu}\mathcal{U}_f^{\rho'\nu'} = \mathcal{U}_f^{\rho''\nu''}$. Hence, the stacking rules for supercohomology phases is given by:

$$(\rho, \nu) \boxtimes (\rho', \nu') = (\rho + \rho', \nu + \nu' + \frac{1}{2}\rho \cup_2 \rho'). \tag{H35}$$

Appendix I: Review of (2+1)D supercohomology models

In this appendix, we review the (2+1)D supercohomology fSPT construction with symmetry $G \times \mathbb{Z}_2^f$ in [23]. This is a warm-up for (3+1)D construction described in Appendix K.

1. Bulk construction

We start with the bulk construction, i.e., SPT states on a closed manifold. The (2+1)D supercohomology data is (n, ν) with $n \in H^2(G, \mathbb{Z}_2)$ and $\nu \in C^3(G, \mathbb{R}/\mathbb{Z})$, satisfying the equation [16]:

$$\delta\nu = \frac{1}{2} n \cup n. \tag{I1}$$

Similar to the (3+1)D case described in the main text, we first construct an auxiliary bSPT model from the supercohomology data. The bosonic model is in a 0-form SPT phase protected by a symmetry G' with a normal $\mathbb{Z}_2$ subgroup. By gauging the $\mathbb{Z}_2$ subgroup, we obtain the shadow model, and by subsequently applying the fermionization duality of Ref. [31], we arrive at a fermionic model for the supercohomology phase.

The 2-cocycle $n \in H^2(G, \mathbb{Z}_2)$ corresponds to a central extension of G by $\mathbb{Z}_2$, which we denote as $G' \equiv \mathbb{Z}_2 \times_n G$ given by the short exact sequence:

$$0 \to \mathbb{Z}_2 \to G' \to G \to 1. \tag{I2}$$

The group elements in G' are $g^{(a)}$ with label $g \in G$ and $a \in \mathbb{Z}_2 = \{0, 1\}$, and the group law is

$$g_1^{(a_1)} g_2^{(a_2)} = (g_1 g_2)^{(a_1 + a_2 + n(1, g_1, g_1 g_2))}. \tag{I3}$$

We can define a cocycle in $H^3(G', \mathbb{R}/\mathbb{Z})$ by:

$$\alpha_3 = \nu + \frac{1}{2} n \cup \epsilon_1 \tag{I4}$$

where $\epsilon_1(g_1^{(a_1)}, g_2^{(a_2)}) \equiv a_1 + a_2 + n(1, g_1, g_2)$ is a 1-cochain in G' satisfying $\delta\epsilon_1 = n$ (where n and ν are implicitly pulled back to G'). One can check that ϵ_1 is homogeneous, i.e. $\epsilon_1(h' g_i', h' g_j') = \epsilon(g_i', g_j')$.

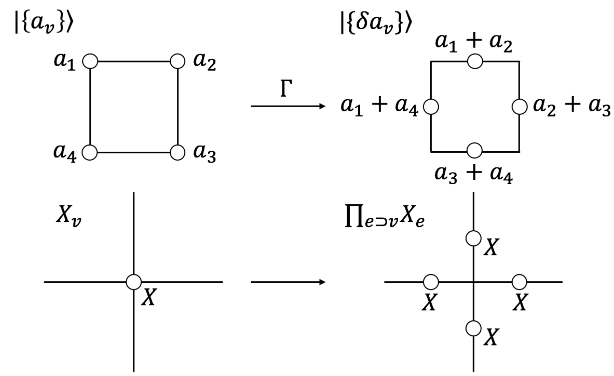

FIG. 26. The gauging map Γ for 0-form $\mathbb{Z}_2$ symmetry. The Hilbert space $\mathcal{H}_1$ on the left contains $\mathbb{Z}_2$ spins at all vertices, with the symmetry constraint $\prod_v X_v = 1$. The Hilbert space $\mathcal{H}_2$ on the right contains $\mathbb{Z}_2$ spins at all edges, with the gauge constraint $\prod_{e \subset f} Z_e = 1$ for each face f. For non simply-connected M_2, there are extra constraints that the product of Z around nontrivial cycles are equal to 1. The gauging map is an isomorphism between $\mathcal{H}_1$ and $\mathcal{H}_2$.

Following the familiar group cohomology construction, we build an auxiliary bSPT state with symmetry G' on a spatial manifold M_2 corresponding to the 3-cocycle α_3:

$$\begin{aligned}
&|\Psi_{\mathrm{b}}\rangle \\
&= \sum_{\{g_v\},\{a_v\}} \prod_{f = \langle 123 \rangle} e^{2\pi i \alpha_3(1, g_1^{(a_1)}, g_2^{(a_2)}, g_3^{(a_3)}) O_f} |\{g_v\}, \{a_v\}\rangle \\
&= \sum_{\{g_v\},\{a_v\}} \prod_{f = \langle 123 \rangle} \Big[e^{2\pi i \nu(1, g_1, g_2, g_3) O_f} \times \\
&\qquad (-1)^{n(1, g_1, g_2)(a_2 + a_3 + n(1, g_2, g_3))} \Big] |\{g_v\}, \{a_v\}\rangle.
\end{aligned} \tag{I5}$$

where O_f denotes the orientation of the face f. This state is invariant under multiplication of constant $h^{(b)}$ on all vertices, i.e $g_v^{(a_v)} \to (h g_v)^{(a_v + b + n(1, h, h g_v))}$. In other words, $|\Psi_{\mathrm{b}}\rangle$ is invariant under the symmetry action:

$$|\{g_v\}, \{a_v\}\rangle \to |\{h g_v\}, \{a_v + b + n(1, h, h g_v)\}\rangle, \tag{I6}$$

for all $h \in G$ and $b \in \mathbb{Z}_2$. By introducing the operators

$$\begin{aligned}
\hat{\boldsymbol{\nu}}(\langle 123 \rangle) |\{g_v\}, \{a_v\}\rangle &= \nu(1, g_1, g_2, g_3) |\{g_v\}, \{a_v\}\rangle \\
\hat{\boldsymbol{n}}(\langle 12 \rangle) |\{g_v\}, \{a_v\}\rangle &= \nu(1, g_1, g_2) |\{g_v\}, \{a_v\}\rangle,
\end{aligned} \tag{I7}$$

and representing $\{a_v\}$ by a 0-cochain $\boldsymbol{a}_v \in C^0(M_2, \mathbb{Z}_2)$, the SPT state can alternatively be written as:

$$|\Psi_{\mathrm{b}}\rangle = \sum_{\{g_v\}, \boldsymbol{a}_v} \prod_f e^{2\pi i \hat{\boldsymbol{\nu}}(f) O_f} (-1)^{\int_{M_2} \hat{\boldsymbol{n}} \cup (\delta \boldsymbol{a}_v + \hat{\boldsymbol{n}})} |\{g_v\}, \boldsymbol{a}_v\rangle. \tag{I8}$$

The next step is to gauge the 0-form $\mathbb{Z}_2$ subgroup. This is a duality mapping $\{a_v\}$ d.o.f. on vertices to $\{a_e\}$ d.o.f.

on the edges, where each $\{a_e\}$ configuration can be labeled by a 1-cochain $\boldsymbol{a}_e \in C^1(M_2, \mathbb{Z}_2)$. Since each configuration $\{a_v\}$ can be represented by the cochain $\boldsymbol{a}_v$, the gauging map is defined as:

$$\Gamma(|\boldsymbol{a}_v\rangle) = |\delta \boldsymbol{a}_v\rangle \tag{I9}$$

where $\delta \boldsymbol{a}_v$ are $\mathbb{Z}_2$ fields living on edges, i.e. $\delta \boldsymbol{a}_v(e_{ij}) = a_i + a_j$, shown in Fig. 26. The ground state of the bosonic shadow model is:

$$\begin{aligned} |\Psi_s\rangle &= \Gamma(|\Psi_{\rm b}\rangle) \\ &= \sum_{\{g_v\},\boldsymbol{a}_v} \prod_f \left[e^{2\pi i \hat{\bar{\boldsymbol{\nu}}}(f) O_f}\right] (-1)^{\int_{M_2} \hat{\bar{\boldsymbol{n}}} \cup (\delta \boldsymbol{a}_v + \hat{\bar{\boldsymbol{n}}})} |\{g_v\}, \delta \boldsymbol{a}_v\rangle. \end{aligned} \tag{I10}$$

Now, we define a new basis of states by a unitary transformation $\mathcal{R} \equiv \prod_e X_e^{\hat{\bar{\boldsymbol{n}}}(e)}$:

$$\begin{aligned} |\{g_v\}, \boldsymbol{a}_e\rangle' &\equiv \mathcal{R} |\{g_v\}, \boldsymbol{a}_e\rangle \\ &= |\{g_v\}, \boldsymbol{a}_e + \bar{\boldsymbol{n}}_{\{g_v\}}\rangle, \end{aligned} \tag{I11}$$

where $\bar{\boldsymbol{n}}_{\{g_v\}}$ is the 1-cochain given by:

$$\bar{\boldsymbol{n}}_{\{g_v\}}(\langle 12\rangle) \equiv n(1, g_1, g_2). \tag{I12}$$

One can check that the symmetry action (I6) acting on this new basis becomes

$$V(h^{(b)}):\ |\{g_v\}, \boldsymbol{a}_e\rangle' \to |\{hg_v\}, \boldsymbol{a}_e\rangle', \tag{I13}$$

which is an onsite symmetry acting only on the vertex variables $\{g_v\}$. Pauli matrices $X_{e'}$ and $Z_{e'}$ are defined to be acting on the second entry of states in the new basis, i.e.,

$$\begin{aligned} X_{e'} |\{g_v\}, \boldsymbol{a}_e\rangle' &= |\{g_v\}, \boldsymbol{a}_e + \boldsymbol{e}'\rangle' \\ Z_{e'} |\{g_v\}, \boldsymbol{a}_e\rangle' &= (-1)^{\boldsymbol{a}_e(e')} |\{g_v\}, \boldsymbol{a}_e\rangle'. \end{aligned} \tag{I14}$$

The bosonic shadow state with an onsite G symmetry is then:

$$\begin{aligned} |\Psi_s\rangle &= \sum_{\{g_v\},\boldsymbol{a}_v} \prod_f e^{2\pi i \hat{\bar{\boldsymbol{\nu}}}(f) O_f} \prod_{e'} Z_{e'}^{\int_{M_2} \hat{\bar{\boldsymbol{n}}} \cup \boldsymbol{e}'} |\{g_v\}, \delta \boldsymbol{a}_v + \hat{\bar{\boldsymbol{n}}}\rangle' \\ &= \sum_{\{g_v\},\boldsymbol{a}_v} \prod_f e^{2\pi i \hat{\bar{\boldsymbol{\nu}}}(f) O_f} \prod_{e'} Z_{e'}^{\int_{M_2} \hat{\bar{\boldsymbol{n}}} \cup \boldsymbol{e}'} \prod_e X_e^{\hat{\bar{\boldsymbol{n}}}(e)} |\{g_v\}, \delta \boldsymbol{a}_v\rangle'. \end{aligned} \tag{I15}$$

Finally, we apply the $(2+1)$D fermionization duality of Refs. [22, 31] to $|\Psi_{\rm b}\rangle$ to find the fSPT state. To apply the duality to $|\Psi_{\rm b}\rangle$, we introduce the notation [similar to Eq. (F10)]:

$$\bar{U}_{\bar{n}} = \prod_{e'} Z_{e'}^{\int \hat{\bar{\boldsymbol{n}}} \cup \boldsymbol{e}'} \prod_e X_e^{\hat{\bar{\boldsymbol{n}}}(e)}. \tag{I16}$$

With this, the shadow state is:

$$|\Psi_{\rm s}\rangle = \sum_{\{g_v\},\{a_v\}} \prod_{f \in M_2} e^{2\pi i \hat{\bar{\boldsymbol{\nu}}}(f) O_f} \bar{U}_{\bar{n}} |\{g_v\}, \delta \boldsymbol{a}_v\rangle', \tag{I17}$$

The operator $\bar{U}_{\bar{n}}$ is dual to the fermionic operator $S_{\bar{n}}$, defined as:

$$S_{\bar{n}} = \xi_n(M_2) \prod_e S_e^{\hat{\bar{\boldsymbol{n}}}(e)}, \tag{I18}$$

where $\xi_n(M_2)$ is a sign that depends on the order of edges in M_2:

$$\xi_n(M_2) = \prod_{e_i, e_{i'} \in M_2 | i < i'} (-1)^{\hat{\bar{\boldsymbol{n}}}(e) \hat{\bar{\boldsymbol{n}}}(e') \int \boldsymbol{e}_i \cup \boldsymbol{e}_{i'}}, \tag{I19}$$

and S_e is the following fermionic hopping operator:

$$S_e = (-1)^{\boldsymbol{e}(E)} i \gamma_{L(e)} \gamma'_{R(e)}. \tag{I20}$$

Here, $E \in C_1(M_2, \mathbb{Z}_2)$ is a choice of spin structure, and $L(e)$,$R(e)$ are the faces to the left and right of the edge e, respectively [22, 23, 30]. The supercohomology state is thus:

$$|\Psi_f\rangle = \sum_{\{g_v\}} \prod_f e^{2\pi i \hat{\bar{\boldsymbol{\nu}}}(f) O_f} S_{\bar{n}} |\{g_v\}, \text{vac}\rangle, \tag{I21}$$

where $|\text{vac}\rangle$ is the fermionic state with trivial fermion occupancy. The toric code ground state is mapped to the fermionic vacuum state, since the toric code Hamiltonian is mapped to the atomic insulator $H_f = -\sum_f P_f$. The symmetry in the fermionic model acts as:

$$V(h): |\{g_v\}, \cdots\rangle \to |\{hg_v\}, \cdots\rangle, \tag{I22}$$

because the symmetry in Eq. (I13) only involves the G degrees of freedom.

2. Boundary construction

In this section, we demonstrate how to construct SPT states for (2+1)D supercohomology phases on a spatial manifold M_2 with boundary ∂M_2. The construction is based on extending the symmetry at the boundary, similar to Section V B and Ref. [19]. In fact, since $\alpha_3 \in H^3(G', \mathbb{R}/\mathbb{Z})$ in Eq. (I4) describes a bSPT phase, we can apply the methods of Ref. [19] to first build a gapped boundary for the auxiliary bSPT. To this end, we identify an extension of G' to G'' that trivializes α_3, i.e., for some μ_2 in $C^2(G'', \mathbb{R}/\mathbb{Z})$, we have $\delta\mu_2 = \alpha_3^*$, where α_3^* is the pullback of α_3. The extension is such that we can then gauge a $\mathbb{Z}_2$ subgroup to construct the shadow model and then fermionize according to Ref. [31] to build the supercohomology state on M_2.

In analogy to Section V B, we find such an extension by composing two central extensions of G. The first trivializes n, so that $n' = \delta\beta'$, where n' is the pullback to an extended group L', and β' belongs to $C^1(L', \mathbb{Z}_2)$. The second extension trivializes the cocycle $\nu' + \frac{1}{2}\beta' \cup \delta\beta'$, with ν' the pullback of ν to L'. The existence of these two extensions is guaranteed by the results of Ref. [39]. Therefore, there is an extension of G to L by K:

$$1 \to K \to L \to G \to 1, \tag{I23}$$

such that the pullback of the supercohomology data (n^*, ν^*) is trivialized:

$$(n^*, \nu^*) = (\delta\beta, \delta\eta + \frac{1}{2}\beta \cup \delta\beta), \tag{I24}$$

for some $\beta \in C^1(L, \mathbb{Z}_2)$ and $\eta \in C^2(L, \mathbb{R}/\mathbb{Z})$. Note that the right-hand side of Eq. (I24) corresponds to a trivial set of supercohomology data [23]. Elements of the group L can be written as $\ell = g^{(k)}$, where g is in G and k is in K. The group law in L is defined by a 2-cocycle $m \in H^2(G, K)$:

$$g_1^{(k_1)} g_2^{(k_2)} = (g_1 g_2)^{(k_1 + k_2 + m(1, g_1, g_1 g_2))}, \tag{I25}$$

with K taken to be an additive group.

We claim that the pullback of α_3 to G'', with G'' defined as:

$$G'' \equiv \mathbb{Z}_2 \times_{n^*} L = K \times_{m^*} G', \tag{I26}$$

is trivial in $H^3(G'', \mathbb{R}/\mathbb{Z})$. In Eq. (I26), we have used $\mathbb{Z}_2 \times_{n^*} L$ to mean the extension of L by $\mathbb{Z}_2$ corresponding to the pullback of n to L, and we have used $K \times_{m^*} G'$ to denote the extension of G' by K corresponding to m pulled back to G'. Using this, we find that the pullback of ϵ_1 is $\epsilon_1^* \in C^1(G'', \mathbb{Z}_2)$:

$$\epsilon_1^*({\ell_1}^{(a_1)}, {\ell_2}^{(a_2)}) = a_1 + a_2 + \beta(\ell_1, \ell_2) + \delta\bar{\beta}(\ell_1, \ell_2), \tag{I27}$$

where ${\ell_1}^{(a_1)}, {\ell_2}^{(a_2)}$ are elments of G'' labeled by ℓ_1, ℓ_2 in L and a_1, a_2 in $\mathbb{Z}_2$, $\bar{\beta}(\ell_1)$ is defined by $\bar{\beta}(\ell_1) \equiv \beta(1, \ell_1)$, and β is implicitly pulled back to G''. Inserting this into the pullback of α_3, we obtain:

$$\begin{aligned} \alpha_3^* &= \delta\eta + \frac{1}{2}\beta \cup \delta\beta + \frac{1}{2}\delta\beta \cup \epsilon_1^* \\ &= \delta(\eta + \frac{1}{2}\beta \cup \epsilon_1^*). \end{aligned} \tag{I28}$$

Hence, we can define:

$$\mu_2 \equiv \eta + \frac{1}{2}\beta \cup \epsilon_1^*, \tag{I29}$$

such that $\alpha_3^* = \delta\mu_2$.

Following the discussion for bosonic SPT phases in Section V A, we extend the symmetry on the boundary to G'' by adding extra degrees of freedom $k_{v_\partial} \in K$ to each boundary vertex $v_\partial \in \partial M_2$. We see that the symmetry action for each $h^{(k)} \in L$ is

$$\begin{aligned} V(h^{(k)}) : & g_v \to h g_v, \quad \forall v \in M_2, \\ & k_v \to k + k_v + m(h^{-1}, 1, g), \quad \forall v \in \partial M_2, \\ & a_v \to a_v + n(h^{-1}, 1, g_i), \quad \forall v \in M_2. \end{aligned} \tag{I30}$$

There is also a 0-form $\mathbb{Z}_2$ symmetry (analogous to the 1-form symmetry in the $(3+1)$D construction):

$$A : a_v \to a_v + 1, \quad \forall v \in M_2. \tag{I31}$$

The symmetric wave function on M_2 is then:

$$\begin{aligned} |\Psi_\text{b}\rangle = \sum_{\{g_v, a_v, k_{v_\partial}\}} & \prod_{e_{12} \in \partial M_2} e^{-2\pi i \mu_2(1, g_1^{(k_1)}, g_2^{(k_2)}) O_{e_{12}}} \\ & \prod_{f = \langle 123 \rangle \in M_2} e^{2\pi i \alpha_3(1, g_1', g_2', g_3') O_f} |\{g_v\}, \{k_{v_\partial}\}, \boldsymbol{a}_v\rangle, \end{aligned} \tag{I32}$$

where $O_{e_{12}}$ is the orientation of the boundary edge e_{12}. Using the operators introduced in the previous section, $|\Psi_\text{b}\rangle$ can be written as:

$$\begin{aligned} |\Psi_\text{b}\rangle = & \\ & \sum_{\{g_v\}, \{k_{v_\partial}\}, \boldsymbol{a}_v} \prod_{e \in \partial M_2} \left[e^{-2\pi i \hat{\bar{\boldsymbol{\eta}}}(e) O_e} (-1)^{\int_{\partial M_2} \hat{\bar{\boldsymbol{\beta}}} \cup (\delta \boldsymbol{a}_v + \hat{\bar{\boldsymbol{n}}})} \right] \\ & \prod_{f \in M_2} \left[e^{2\pi i \hat{\bar{\boldsymbol{\nu}}}(f) O_f} \right] (-1)^{\int_{M_2} \hat{\bar{\boldsymbol{n}}} \cup (\delta \boldsymbol{a}_v + \hat{\bar{\boldsymbol{n}}})} |\{g_v\}, \{k_{v_\partial}\}, \boldsymbol{a}_v\rangle, \end{aligned} \tag{I33}$$

where $\hat{\bar{\boldsymbol{\eta}}}$ and $\hat{\bar{\boldsymbol{\beta}}}$ are defined as:

$$\begin{aligned} & \hat{\bar{\boldsymbol{\eta}}}(\langle 12 \rangle) |\{g_v\}, \{k_{v_\partial}\}, \boldsymbol{a}_v\rangle = \\ & \qquad \eta(1, g_1^{(k_1)}, g_2^{(k_2)}) |\{g_v\}, \{k_{v_\partial}\}, \boldsymbol{a}_v\rangle, \\ & \hat{\bar{\boldsymbol{\beta}}}(\langle 1 \rangle) |\{g_v\}, \{k_{v_\partial}\}, \boldsymbol{a}_v\rangle = \beta(1, g_1^{(k_1)}) |\{g_v\}, \{k_{v_\partial}\}, \boldsymbol{a}_v\rangle. \end{aligned} \tag{I34}$$

We now gauge the $\mathbb{Z}_2$ symmetry in Eq. (I31) to obtain the bosonic shadow model. To do so, we consider the manifold $\overline{M}_2$, formed by connecting all boundary vertices of M_2 to an additional vertex 0. In other words, $\overline{M}_2$ is $M_2 \coprod C(\partial M_2)$, where the cone of ∂M_2, $C(\partial M_2)$, is attached to M_2. We define $a_0 = 0$ for this extra vertex and apply the gauging map Γ on the simply connected manifold $\overline{M}_2$. The bosonic shadow state is $|\Psi_s\rangle \equiv \Gamma(|\Psi_\text{b}\rangle)$, defined on a Hilbert space with $\{a_e\}$-configurations on edges labeled by a 1-cochain $\boldsymbol{a}_e \in C^1(\overline{M}_2, \mathbb{Z}_2)$.

As in the bulk construction, we perform a change of basis to make the symmetry onsite. Including the edges $e = \langle 0i \rangle$, for all $\langle i \rangle \in \partial M_2$, the basis transformation is:

$$|\{g_v\}, \{k_{v_\partial}\}, \boldsymbol{a}_e\rangle' \equiv |\{g_v\}, \{k_{v_\partial}\}, \boldsymbol{a}_e + \boldsymbol{B}_e\rangle, \tag{I35}$$

where $\boldsymbol{B}_e$ is defined as:

$$\begin{aligned} \boldsymbol{B}_e(\langle ij \rangle) &= n(1, g_i, g_j) \\ \boldsymbol{B}_e(\langle 0i \rangle) &= \beta(1, g_i''). \end{aligned} \tag{I36}$$

We define Pauli operators in the new basis by:

$$\begin{aligned} X_{e'} |\{g_v\}, \{k_{v_\partial}\}, \boldsymbol{a}_e\rangle' &\equiv |\{g_v\}, \{k_{v_\partial}\}, \boldsymbol{a}_e + \boldsymbol{e}'\rangle' \\ Z_{e'} |\{g_v\}, \{k_{v_\partial}\}, \boldsymbol{a}_e\rangle' &\equiv (-1)^{\boldsymbol{a}_e(e')} |\{g_v\}, \{k_{v_\partial}\}, \boldsymbol{a}_e\rangle'. \end{aligned} \tag{I37}$$

After applying the basis transformation in Eq. (I35), the bosonic shadow state is:

$$\begin{aligned} |\Psi_s\rangle = \sum_{\{g_v\}, \{k_{v_\partial}\}, \boldsymbol{a}_v} & \prod_{e \in \partial M_2} \left[e^{-2\pi i \hat{\bar{\boldsymbol{\eta}}}(e) O_e} \right] \bar{U}_{\bar{\beta}} \\ & \prod_{f \in M_2} \left[e^{2\pi i \hat{\bar{\boldsymbol{\nu}}}(f) O_f} \right] \bar{U}_{\bar{n}} |\{g_v\}, \{k_{v_\partial}\}, \delta \boldsymbol{a}_v\rangle'. \end{aligned} \tag{I38}$$

Above, $\bar{U}_{\bar{n}}$ is the product of Pauli Z and Pauli X operators:

$$\bar{U}_{\bar{n}} = \prod_{e'} Z_{e'}^{\int_{M_2} \hat{\bar{\boldsymbol{n}}} \cup \boldsymbol{e}'} \prod_{e \in M_2} X_e^{\hat{\bar{\boldsymbol{n}}}(e)}, \tag{I39}$$

and $\bar{U}_{\bar{\beta}}$ is the operator:

$$\bar{U}_{\bar{\beta}} = \prod_{\langle 12 \rangle \in \partial M_2} Z_{12}^{\hat{\bar{\boldsymbol{\beta}}}(\langle 1 \rangle)} \prod_{v_\partial \in \partial M_2} X_{0 v_\partial}^{\hat{\bar{\boldsymbol{\beta}}}(v_\partial)}. \tag{I40}$$

The operators $\bar{U}_{\bar{n}}$ and $\bar{U}_{\bar{\beta}}$ in the expression for the shadow state can be fermionized following Refs. [22, 31]. $\bar{U}_{\bar{n}}$ maps to the product of hopping operators $S_{\bar{n}}$ in Eq. (I18):

$$S_{\bar{n}} = \xi_n(M_2) \prod_{e \in M_2} S_e^{\hat{\bar{\boldsymbol{n}}}(e)}, \tag{I41}$$

while $\bar{U}_{\bar{\beta}}$ fermionizes to:

$$\prod_{v_\partial \in \partial M_2} S_{v_\partial}^{\hat{\bar{\boldsymbol{\beta}}}(v_\partial)}. \tag{I42}$$

Here, S_{v_∂} is shorthand for the operator $S_{0 v_\partial}$, and we note that there is no order dependence of the product of S_{v_∂} operators, since the S_{v_∂} are all commuting.

The (2+1)D boson-fermion duality maps the bosonic shadow state to the supercohomology state:

$$|\Psi_f\rangle = \sum_{\{g_v\},\{k_{v_\partial}\}} \prod_{e \in \partial M_2} \left[e^{-2\pi i \hat{\bar{\boldsymbol{\eta}}}(e) O_e}\right] \prod_{v_\partial \in \partial M_2} S_{v_\partial}^{\hat{\bar{\boldsymbol{\beta}}}(v_\partial)} \prod_{f \in M_2} \left[e^{2\pi i \hat{\bar{\boldsymbol{\nu}}}(f) O_f}\right] \xi_n(M_2) \prod_{e \in M_2} S_e^{\hat{\bar{\boldsymbol{n}}}(e)} |\{g_v\},\{k_{v_\partial}\},\mathrm{vac}\rangle. \tag{I43}$$

$|\Psi_f\rangle$ is defined on M_2 with a spinless complex fermion at each face f and at each edge $e \in \partial M_2$.

Appendix J: 2-groups and 2-gauge theories

The goal of this appendix is to define 2-groups and 2-gauge theory [32]. In Section J 1, we give a formal definition of strict 2-groups and argue that certain equivalence classes of strict 2-groups, i.e., weak 2-groups, can be labeled by a 3-cocycle. In Section J 2, we describe 2-gauge theories [32], built from 2-groups. The machinery of 2-gauge theory is used to derive the 2-group SPT model and symmetric gapped boundaries of supercohomology models in the subsequent appendix, Appendix K.

1. Definition of 2-groups

We first define strict 2-groups before describing the notion of weak 2-groups, also simply referred to as 2-groups, which are used directly in the definition of 2-gauge theory in the next section. Following Ref. [32], a strict 2-group is given by $\mathbb{G} = (G', A', t', \alpha')$, where G' and A' are groups, $t' : A' \to G'$ is a group homomorphism, and $\alpha' : G' \to \mathrm{Aut}(A')$ is an action of G' on A'. Furthermore, for any $g' \in G'$ and $a', a'_1, a'_2 \in A'$, the maps t' and α' satisfy:

$$t'(\alpha'[g'](a')) = g' t'(a') g'^{-1}, \quad \alpha'[t'(a'_1)](a'_2) = a'_1 a'_2 a'^{-1}_1. \tag{J1}$$

Weak 2-groups, on the other hand, correspond to certain equivalence classes of strict 2-groups sharing the same $\ker t'$ and $\mathrm{coker}\, t' = G'/\,\mathrm{Im}\, t'$. Given any strict 2-group (G', A', t', α') with $\ker t' = A$ and $\mathrm{coker}\, t' = G$, it can be organized into the short exact sequence:

$$1 \to A \xrightarrow{\iota} A' \xrightarrow{t'} G' \xrightarrow{\pi} G \to 1, \tag{J2}$$

also known as a double extension of G by A. The double extensions of G by A can be labeled by an action of G on A given by a map $\alpha : G \to \mathrm{Aut}(A)$ (induced from α') and a cocycle $\varrho \in H^3(G, A)$. A weak 2-group is specified by the quadruple (G, A, α, ϱ).

We find the prescription, described below, for determining the cocycle ϱ associated to the double extension illuminating. For example, we take A to be $\mathbb{Z}_2$, in which case, α is trivial, and consider the double extension of G by $\mathbb{Z}_2$:

$$1 \to \mathbb{Z}_2 \xrightarrow{\iota} A' \xrightarrow{t'} G' \xrightarrow{\pi} G \to 1, \tag{J3}$$

with the action $\alpha' : G' \to \mathrm{Aut}(A')$. First, any section $s : G \to G'$ satisfies the group law projectively:

$$s(g)s(h) = f(g,h)s(gh) \tag{J4}$$

with $f : G \times G \to \ker \pi$. Furthermore, by the associative property, f must obey:

$$[s(g)f(h,k)s(g)^{-1}]f(g,hk) = f(g,h)f(gh,k). \tag{J5}$$

Finally, since $\mathrm{Im}\, t' = \ker \pi$, we can lift f to $F : G \times G \to A'$, where Eq. (J5) is satisfied projectively:

$$(\alpha'[s(g)]F(h,k))F(g,hk) = \iota(\varrho(g,h,k))F(g,h)F(gh,k). \tag{J6}$$

It can be shown that ϱ is a 3-cocycle, whose cohomology class is independent on the choice of s and F, and therefore the double extension can be labeled by $H^3(G, A)$. We point out that the calculation of ϱ here is analogous to the calculation of the G-symmetry fractionalization on loop-like excitations of the shadow model in Section IV C [12].

2. Review of 2-gauge theory

We now define a 2-gauge theory, using the data (G, A, α, ϱ) described in the previous section [32]. For our purposes, we consider A to be $\mathbb{Z}_2$, in which case, only a trivial α exists. The 2-gauge theory is defined on a discrete spacetime manifold

N with a branching structure, and the field configurations are given by an assignment of an element $g_e \in G$ to each edge and an element $b_f \in \mathbb{Z}_2$ to each face. We denote a configuration of $\{g_e\}$ and $\{b_f\}$ fields by $(\bar{g}, \bar{b})$, where $\bar{g}$ and $\bar{b}$ are shorthand for $\{g_e\}$ and $\{b_f\}$, respectively. The allowable field configurations must satisfy the following "flatness condition". First, for every face $f = \langle 012 \rangle$, $\bar{g}$ must satisfy:

$$g_{01} g_{12} = g_{02}. \tag{J7}$$

Second, on each tetrahedron, $(\bar{g}, \bar{b})$ has to satisfy:

$$\delta b = b_{012} + b_{013} + b_{023} + b_{123} = \varrho(g_{01}, g_{12}, g_{23}). \tag{J8}$$

The 0-form gauge transformations are parameterized by $\bar{h} = \{h_v\}$, i.e., a choice of $h_v \in G$ for every vertex v, and are defined by:

$$\begin{aligned} \bar{g} &\to \bar{g}^h = \{g_{ij}^h\} = \{h_i^{-1} g_{ij} h_j\} \\ \bar{b} &\to \bar{b}^h = \{b_{ijk}^h\} = \{b_{ijk} + \zeta(g_{ij}, g_{jk}, h_i, h_j, h_k)\} \end{aligned} \tag{J9}$$

where ζ is a $\mathbb{Z}_2$-valued 2-cochain on N with the property:

$$\delta\zeta(\bar{g}, \bar{h}) = \rho(\bar{g}^h) - \rho(\bar{g}). \tag{J10}$$

Here and below, we use the homogeneous notation ρ for the cocycle ϱ, i.e. $\rho(1, g, gh, ghk) = \varrho(g, h, k)$. Heuristically, one can show that a solution for ζ in Eq. (J10) always exists by considering ρ as a label for a "Dijkgraaf-Witten-type" theory (see Section J 3). Therefore, the 0-form gauge transformation only changes the values of ϱ in Eq. (J8) by coboundary terms. In what follows, we take ζ to be:

$$\begin{aligned} &\zeta(g_{12}, g_{23}, h_1, h_2, h_3) = \rho(1, g_{12}, g_{12}g_{23}, g_{12}g_{23}h_3) + \\ &\rho(1, g_{12}, g_{12}h_2, g_{12}g_{23}h_3) + \rho(1, h_1, g_{12}h_2, g_{12}g_{23}h_3), \end{aligned} \tag{J11}$$

derived in Section J 3. In particular, we note that for the trivial G configuration $g_e = 1$, $\forall e$, the gauge transformation on the $\bar{b}$ fields yields:

$$\zeta(1, 1, h_1, h_2, h_3) = \rho(1, h_1, h_2, h_3). \tag{J12}$$

The 1-form symmetry depends on a $\mathbb{Z}_2$-valued 1-cochain $\bar{\lambda} = \{\lambda_e\}$. The transformation is as usual:

$$\begin{aligned} g_e &\to g_e \\ b_f &\to b_f + \delta\lambda_e. \end{aligned} \tag{J13}$$

The classifying space of a 2-group $\mathbb{G}$, denoted as $B\mathbb{G}$ allows us to define a 2-gauge theory via the map $M \to B\mathbb{G}$. It can be described by a Δ-complex structure. $B\mathbb{G}$ contains one vertex and edges labeled by $g \in G$. Its 2-simplices $\langle 012 \rangle$ are labeled by $(g_{01}, g_{12}, g_{02}, b_{012})$ such that $g_{01}g_{12} = g_{02}$ and $b_{012} = 0, 1$. Its 3-simplices $\langle 0123 \rangle$ contains boundary 2-simplices $\langle 012 \rangle$, $\langle 013 \rangle$, $\langle 023 \rangle$, and $\langle 123 \rangle$ such that

$$\begin{aligned} \varrho(g_{01}, g_{12}, g_{23}) =& \rho(1, g_{01}, g_{01}g_{12}, g_{01}g_{12}g_{23}) \\ =& b_{012} + b_{013} + b_{023} + b_{123} \end{aligned} \tag{J14}$$

For $n \geq 4$, we glue n-simplices to $(n-1)$-cycles to eliminate all higher homotopy groups. According to Dijkgraaf and Witten [61], topological gauge theories with gauge group G in $(n+1)$ spacetime dimensions are classified by $H^{d+1}(G, \mathbb{R}/\mathbb{Z}) \equiv H^{n+1}(BG, \mathbb{R}/\mathbb{Z})$. This was generalized to 2-group gauge theories by Kapustin and Thorngren [32]: 2-gauge theories with 2-group $\mathbb{G}$ in $(n+1)$D are classified by $H^{n+1}(B\mathbb{G}, \mathbb{R}/\mathbb{Z})$.

3. Derivation of ζ

Here, we derive the choice of ζ in (J11). Consider a tetrahedron $\langle 0123 \rangle$ with group elements g, h, k on edges $\langle 01 \rangle, \langle 12 \rangle, \langle 23 \rangle$. The value of cocycle ρ on this tetrahedron is expressed as $\rho(1, g, gh, ghk)$. First, we perform a gauge transformation on vertex 0 by group element c_0 (and identity element on all other vertices); g, h, k becomes $c_0^{-1}g, h, k$ and the value of cocycle is (using the homogeneity of ρ):

$$\begin{aligned} \rho(c_0, g, gh, ghk) = &\rho(1, c_0, g, ghk) - \rho(1, c_0, g, gh) \\ &- \rho(1, c_0, gk, ghk) + \rho(1, g, gh, ghk) \end{aligned} \tag{J15}$$

To satisfy (J10), we can define the gauge transformation of b_{ijk} by c_0 at the vertex i of a face $\langle ijk \rangle$ as $\rho(1, c_0, g_{ij}, g_{ij}g_{jk})$, or explicitly $\zeta(g_{ij}, g_{jk}, c_0, 1, 1) = \rho(1, c_0, g_{ij}, g_{ij}g_{jk})$.

Secondly, we perform a gauge transformation on vertex 1 by group element c_1. g, h, k becomes $gc_1, c_1^{-1}h, k$ and the value of the cocycle is

$$\begin{aligned} \rho(1, gc_1, gh, ghk) = &\rho(1, g, gc_1, gh) - \rho(1, g, gc_1, ghk) \\ &+ \rho(g, gc_1, gh, ghk) + \rho(1, g, gh, ghk) \\ = &\rho(1, g, gc_1, gh) - \rho(1, g, gc_1, ghk) \\ &+ \rho(1, c_1, h, hk) + \rho(1, g, gh, ghk). \end{aligned} \tag{J16}$$

The first two terms after the last equality indicate that the gauge transformation on the vertex j of a face $\langle ijk \rangle$ is $\rho(1, g_{ij}, g_{ij}c_1, g_{jk})$, or $\zeta(g_{ij}, g_{jk}, 1, c_1, 1) = \rho(1, g_{ij}, g_{ij}c_1, g_{jk})$, and the third term after the second equality is consistent with the previous case.

Similarly for the gauge transformation on the vertex 2 by group element c_2, we have

$$\begin{aligned} \rho(1, g, ghc_2, ghk) = &\rho(g, gh, ghc_2, ghk) - \rho(1, g, gh, ghc_2) \\ &+ \rho(1, g, ghc_2, ghk) + \rho(1, g, gh, ghk) \\ = &\rho(1, h, hc_2, hk) - \rho(1, g, gh, ghc_2) \\ &+ \rho(1, g, ghc_2, ghk) + \rho(1, g, gh, ghk). \end{aligned} \tag{J17}$$

The term $\rho(1, g, gh, ghc_2)$ after the last equality implies $\zeta(g_{ij}, g_{jk}, 1, 1, c_2) = \rho(1, g_{ij}, g_{ij}g_{jk}, g_{ij}g_{jk}c_2)$; the remaining terms are consistent with the previous cases.

We can check the gauge transformation on the 3 vertex of the tetrahedron. However, it just gives us a consistency check. The previous three cases specify the gauge transformation.

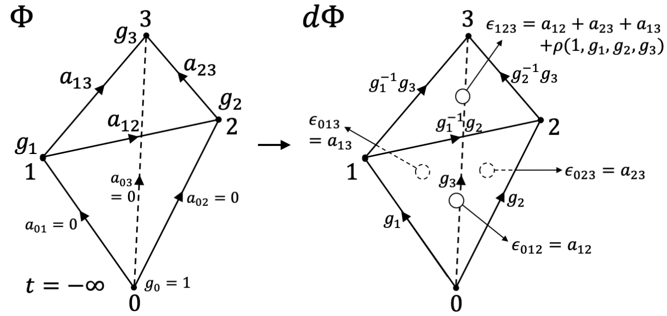

FIG. 27. For a representative tetrahedron including the 0 vertex, we show the mapping of the configuration Φ (left) to the configuration $d\Phi$ (right). In general, ϵ_{ijk} is $a_{ij} + a_{ik} + a_{jk} + \rho(1, g_i, g_j, g_k)$, with the labels determined by Φ. We have assumed that ρ is normalized, i.e., $\rho(1, 1, g, h) = 0$. Notice that $d\Phi$ can be interpreted as applying gauge transformation specified by the configuration Φ on the trivial configuration of a 2-gauge theory.

Now, we combine the three cases and apply the three gauge transformations h_3, h_2, h_1 on vertices $3, 2, 1$ of a face $\langle 123\rangle$ in sequence. First, we add $\rho(1, g_{12}, g_{12}g_{23}, g_{12}g_{23}h_3)$ to b_{123} and g_{12}, g_{23} is mapped to $g_{12}, g_{23}h_3$. Second, we gain a factor of $\rho(1, g_{12}, g_{12}h_2, g_{12}g_{23}h_3)$ and $g_{12}, g_{23}h_3$ becomes $g_{12}h_2, h_2^{-1}g_{23}h_3$. Finally, we add $\rho(1, h_1, g_{12}h_2, g_{12}g_{23}h_3)$. In total, the gauge transformation on b_{123} is

$$\zeta(g_{12}, g_{23}, h_1, h_2, h_3) = \rho(1, g_{12}, g_{12}g_{23}, g_{12}g_{23}h_3) + \rho(1, g_{12}, g_{12}h_2, g_{12}g_{23}h_3) + \rho(1, h_1, g_{12}h_2, g_{12}g_{23}h_3). \tag{J18}$$

Appendix K: Spacetime construction of the 2-group SPT model and supercohomology models with a boundary

We use the language of 2-gauge theory, summarized in Appendix J, to describe a 2-gauge theory dual to the 2-group SPT models of Section IV B. We then provide the details behind the construction of the topologically ordered symmetric gapped boundaries of the supercohomology models from Section V B. We start by constructing the partition function for the 2-group model on a manifold without boundary from the corresponding 2-gauge theory in Section K 1. Then, in Section K 2, we describe the construction of the supercohomology models on a manifold with boundary starting with the spacetime description of the 2-group model.

1. 2-gauge theory interpretation of the bulk 2-group SPT model

2-group SPT phases are dual to 2-gauge theories, similar to the familiar duality between ordinary 0-form SPT phases and conventional Dijkgraaf-Witten gauge theories [1, 9, 16]. To see this, we consider a triangulated spatial 3-manifold M along with the spacetime manifold CM formed by connecting each vertex of M to a vertex 0, sometimes referred to as the spacetime infinity vertex. We define a configuration $\Phi = \{\{g_v\}, \{a_e\}\}$ on CM by assigning a $g_v \in G$ to each vertex $v \in M$ and an $a_e \in \mathbb{Z}_2$ to each edge $e \in M$; the temporal edges (connected to the 0 vertex) are labeled with $0 \in \mathbb{Z}_2$ and the 0 vertex is labeled with $1 \in G$. Furthermore, we define a map d from a configuration Φ to a configuration $d\Phi$ on CM. The configuration $d\Phi$ consists of a set of G labels g_{ij} for all edges in CM and $\mathbb{Z}_2$ labels a_{ijk} for all faces in CM. Specifically, for a configuration $\Phi = \{\{g_v\}, \{a_e\}\}$, the associated configuration $d\Phi$ is:

$$d\Phi = \{\{g_i^{-1}g_j\}, \{a_{ij} + a_{ik} + a_{jk} + \bar{\rho}(1, g_i, g_j, g_k)\}\}, \tag{K1}$$

depicted in Fig. 27. One can verify that this $d\Phi$ satisfies the constraint (J8) and therefore is an allowed configuration for a 2-gauge theory.

Given a 2-group cocycle $\alpha \in H^4(B\mathbb{G}, \mathbb{R}/\mathbb{Z})$ we can now define the corresponding 2-group SPT state. We first pull back α to a cocycle on CM. In a slight abuse of the notation introduced in the main text, for a configuration $d\Phi$, we denote the pullback of α to CM as $\alpha_{d\Phi} \in Z^4(CM, \mathbb{R}/\mathbb{Z})$. When it is clear from context, we also omit the subscript $d\Phi$. A ground state in the associated 2-group SPT phase can then be written as:

$$|\Psi_{\text{SPT}}\rangle \equiv \sum_{\Phi} \prod_{t=\langle 1234\rangle \in M} e^{2\pi i \alpha_{d\Phi}(01234) O_t} |\Phi\rangle \tag{K2}$$

Here, the product in Eq. (K2) is over all 4-simplices in CM, O_t is the orientation of t, and we have omitted the angled brackets around the 4-simplex $\langle 01234\rangle$. In what follows, to simplify the notation, we often omit the angled brackets.

We recover the 2-group SPT states from Section IV B, by considering the 2-gauge theory corresponding to the weak 2-group $(G, \mathbb{Z}_2, 0, \rho)$[24] and the choice of 2-group 4-cocycle α:

$$\alpha = \nu + \frac{1}{2}\rho \cup_1 \epsilon + \frac{1}{2}\epsilon \cup \epsilon, \tag{K3}$$

described in Section IV B. We use the remainder of this section to verify that the SPT state associated to this choice of α is indeed symmetric. The calculation will prove useful in the construction of supercohomology models on a manifold with boundary in the next section.

The 2-group symmetry contains two types of symmetry actions: 0-form and 1-form. The 0-form part is:

$$\begin{aligned} V_\rho(h): &g_v \to hg_v, && \forall v \in M \\ &a_{ij} \to a_{ij} + \rho(1, h^{-1}, g_i, g_j), && \forall \langle ij\rangle \in M, \end{aligned} \tag{K4}$$

and the local 1-form symmetry at the vertex $v \in M$ is:

$$A_{\delta \boldsymbol{v}}: \; a_{ij} \to a_{ij} + \delta \boldsymbol{v}(\langle ij\rangle), \quad \forall \langle ij\rangle \in M. \tag{K5}$$

[24] Here, 0 denotes the trivial action of G on A.

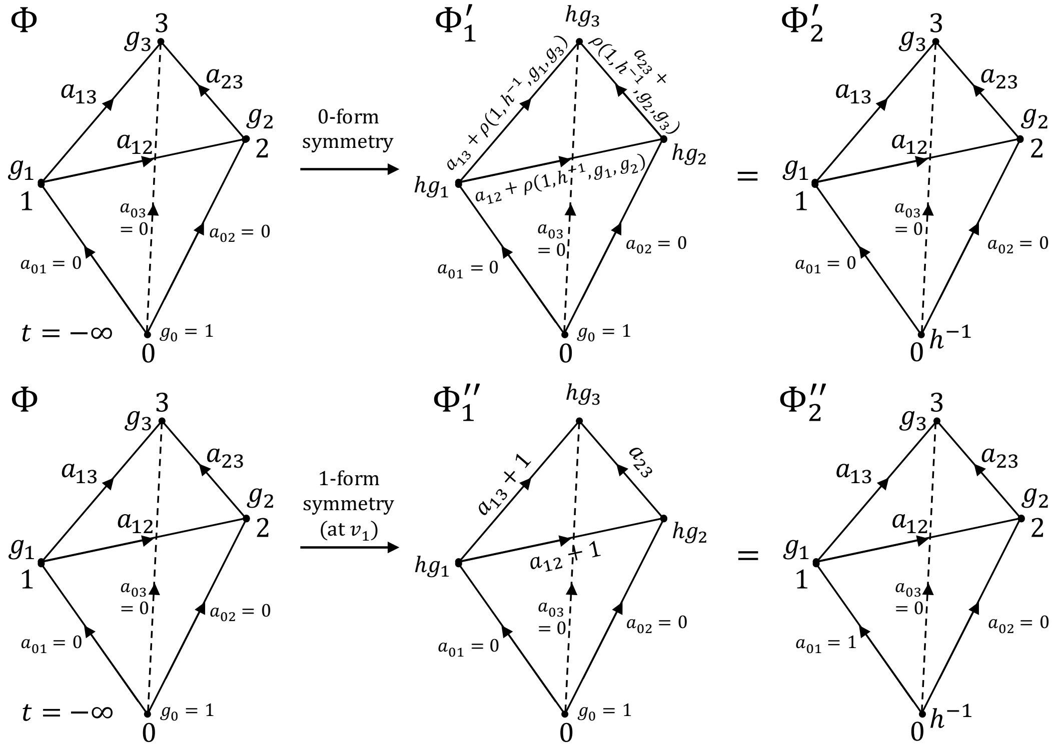

FIG. 28. The first row represents the 0-form symmetry action [represented by $V_\rho(h)$]. Acting on the configuration Φ, it multiplies h on spatial vertices $v \in M$ and modifies spatial edges $e_{ij} \in M$ by $\rho(1, h^{-1}, g_i, g_j)$. The resulting configuration is Φ'_1. Given that α depends only on $d\Phi'_1$, we can consider this configuration to be equivalent to Φ'_2, which is generated from Φ by changing $g_0 = 1$ to h^{-1}. The second row represents the 1-form symmetry action at the vertex 1. The labels on the edges joined at 1 change by $+1$. With respect to α, this is equivalent to only changing the temporal edge a_{01} by $+1$, i.e., $d\Phi''_1 = d\Phi''_2$.

These two symmetries are explicitly demonstrated in Fig. 28. Notice that the symmetry actions in Eq. (K4) and Eq. (K5) only change the spatial d.o.f., i.e., those belonging to M.

To simplify the symmetry analysis, we use that the amplitude of the SPT state depends only on the configuration $d\Phi$ and not on the configuration Φ. As such, we can consider two configurations Φ_1 and Φ_2 equivalent, with respect to the amplitude, if $d\Phi_1 = d\Phi_2$. In Fig. 28, the configuration Φ is mapped to the configuration Φ'_1 by the 0-form symmetry action. Furthermore, Φ'_1 is equivalent to a configuration Φ'_2 obtained from Φ by simply changing $g_0 = 1$ to $g_0 = h^{-1}$, see Fig. 29. Similarly, the 1-form symmetry action by $A_{\delta \boldsymbol{v}}$ is equivalent to changing $a_{0v} = 0$ to $a_{0v} = 1$ for all the temporal edges $\langle 0v \rangle$. This is analogous to the homogeneous property of 0-form group cocycles. More generally, the total 2-group symmetry can be labeled by $(h, \{y_v\})$ with $h \in G$ and $y_v = 0, 1, \forall v \in M$:

$$V_2(h, \{y_v\}) \equiv V_\rho(h) \prod_v A_{\delta \boldsymbol{v}}^{y_v}, \tag{K6}$$

and with respect to the amplitude of $|\Psi_{\text{SPT}}\rangle$, this is effectively equivalent to mapping $g_0 = 1$ to $g_0 = h^{-1}$ at the 0 vertex and $a_{0v} = 0$ to $a_{0v} = y_v$ on all temporal edges $\langle 0v \rangle$.

To show that the 2-group state is invariant under the 2-group symmetry, we consider the affect of the symmetry action on

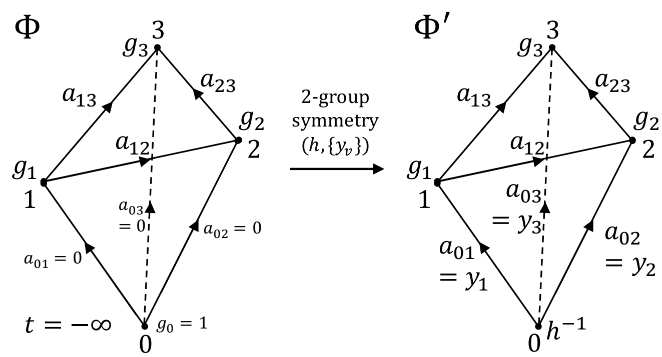

FIG. 29. The (local) 2-group symmetry is parameterized by $(h, \{y_v\})$. The configuration Φ is mapped by the symmetry to a configuration $\tilde{\Phi}$ that is equivalent to Φ', in the sense that $d\Phi'_1 = d\Phi'$. Φ' differs from Φ on the temporal links, where $a_{0v} = y_v$, for $v \in M$, and at the 0 vertex, where g_0 is $g_0 = h^{-1}$.

the amplitude of the state. The symmetry action maps a configuration Φ to a configuration equivalent to Φ', depicted in Fig. 29. We thus need to compare $\alpha_{d\Phi'}$ to $\alpha_{d\Phi}$. To do so, it is useful to append a vertex 0^h to CM by connecting each vertex of CM to 0^h. We assign a configuration on any 4-simplices of the form $\langle 01234 \rangle$ with $\langle 1234 \rangle$ in M according to Φ, and we assign a configuration to any 4-simplices $\langle 0^h 1234\rangle$ according to Φ'. (We also fix $a_{00^h}=0$.) We can then consider the difference:

$$\begin{aligned}\alpha(0^h1234)-\alpha(01234)=&\alpha(00^h123)-\alpha(00^h124)\\&\alpha(00^h134)-\alpha(00^h234),\end{aligned} \tag{K7}$$

where the equality comes from the cocycle condition $\delta\alpha(00^h1234)=0$. The change in the amplitude depends on the sum over all tetrahedra in M:

$$\sum_{t=\langle 1234\rangle\in M}[\alpha(0^h1234)-\alpha(01234)]O_t. \tag{K8}$$

Inserting the right-hand side of Eq. (K7) into the expression above, we find that each term appears exactly twice and with the opposite sign. This can be seen by noting that every term can be associated to a face, e.g., $\alpha(00^h123)$ corresponds to $f=\langle 123\rangle$. Thus, the sum in Eq. (K8) vanishes, and the 2-group SPT state in Eq. (K2) is invariant under 2-group symmetry action in Eq. (K6).

2. Derivation of the supercohomology models with a boundary

We now describe the construction of the supercohomology models on a manifold with boundary, introduced in Section V B, starting from a spacetime model for the 2-group SPT phase. For a spatial manifold M with boundary ∂M, the 2-group SPT model is defined on the cone CM, and has a modified 2-group symmetry action on the boundary of CM. With this spacetime 2-group SPT model, we follow the prescription for the bulk construction of the supercohomology models, i.e., gauging the 1-form symmetry followed by applying the fermionization duality.

As described in Section V B, the symmetry G can be extended by K to L such that the supercohomology data is trivialized:

$$(\rho^*,\nu^*)=(\delta\beta,\delta\eta+\frac{1}{2}\beta\cup_1\delta\beta+\frac{1}{2}\beta\cup\beta), \tag{K9}$$

for some $\beta\in C^2(L,\mathbb{Z}_2)$ and $\eta\in C^3(L,\mathbb{R}/\mathbb{Z})$. The elements of L can be written as $\ell=g^{(k)}$ with $g\in G$ and $k\in K$. If we let m be the 2-cocycle $m\in H^2(G,K)$ corresponding to the extension of G by K, then the group law in L is specified by:

$$g_1^{(k_1)}g_2^{(k_2)}=(g_1g_2)^{(k_1+k_2+m(1,g_1,g_1g_2))}. \tag{K10}$$

To define the spacetime 2-group SPT models, we first describe the configurations Φ on CM. A configuration Φ is specified by a G label on each vertex, a K label on the vertices v_∂ in ∂M, and a $\mathbb{Z}_2$ label on every edge in the boundary of CM, which we denote as $\overline{M}$. Unless otherwise specified, we fix the label at 0 to be $1\in L$ and the labels at the temporal edges $e\notin\overline{M}$ to be $0\in\mathbb{Z}_2$. We write such a configuration Φ as $\Phi=\{\{g_v\},\{k_{v_\partial}\},\{a_e\}\}$. We note that, since each vertex in the boundary of M is labeled by an element $g\in G$ and a $k\in K$, one can consider the boundary vertices to be labeled by an element of L.

The SPT model has a 0-form symmetry parameterized by an element $h^{(k)}\in L$ as well as a $\mathbb{Z}_2$ 1-form symmetry. The 0-form symmetry action is:

$$\begin{aligned}V_B(h^{(k)}):\ & g_v\to hg_v && \forall v\in M\\ & k_v\to k+k_v+m(1,h,hg), && \forall v\in\partial M\\ & a_{ij}\to a_{ij}+B_{ij}^{h^{(k)}}, && \forall\langle ij\rangle\in\overline{M},\end{aligned} \tag{K11}$$

where $B_{ij}^{h^{(k)}}$ is defined as:

$$B_{ij}^{h^{(k)}}=\begin{cases}\rho(1,h^{-1},g_i,g_j) & i\neq 0\\ \beta(1,{h^{(k)}}^{-1},g_j^{(k_j)}) & i=0.\end{cases} \tag{K12}$$

The local 1-form symmetry action, for $v\in\overline{M}$, is given by:

$$A_{\delta\boldsymbol{v}}:\ a_{ij}\to a_{ij}+\delta\boldsymbol{v}(\langle ij\rangle),\quad\forall\langle ij\rangle\in\overline{M}. \tag{K13}$$

Note that, unlike the symmetry action in the previous section, the symmetry acts on some of the temporal links of CM as well. A more general 2-group symmetry action is specified by a choice $(h^{(k)},\{y_v\})$ with $h\in G$, $k\in K$, and $y_v=0,1$, $\forall v\in\overline{M}$, and is represented by:

$$V_2(h^{(k)},\{y_v\})\equiv V_B(h^{(k)})\prod_v A_{\delta\boldsymbol{v}}^{y_v}. \tag{K14}$$

We now (naively) follow the prescription for building a 2-group SPT state - described in Section K 1 - using the 2-group cocycle α^*, the pullback of α to $H^4(B\mathbb{L},\mathbb{R}/\mathbb{Z})$. The amplitude of the state in Eq. (K2) depends on the configuration $d\Phi$ as opposed to Φ. We use this fact to analyze the symmetry (or lack thereof) of the state constructed using α^*.

In particular, the symmetry action corresponding to $(h^{(k)},\{y_v\})$ on a configuration Φ maps it to a configuration $\tilde{\Phi}$ according to the maps in Eqs. (K11) and (K13). $d\tilde{\Phi}$ is equivalent to $d\Phi'$, where Φ' (pictured in Fig. 30) is obtained from Φ by changing the label on the 0 vertex to $(h^{(k)})^{-1}$ and adding $\beta(1,{h^{(k)}}^{-1},g_v^{(k_v)})$ to any temporal link connected to a boundary vertex $v\in\partial M$.

Similar to the argument in the previous section, we can introduce a vertex 0^h and use $\delta\alpha=0$ to evaluate the difference:

$$\sum_{t=\langle 1234\rangle\in M}[\alpha^*(0^h1234)-\alpha^*(01234)]O_t. \tag{K15}$$

Here, we have assigned the configuration Φ (Φ') to 4-simplices formed from a tetrahedron in M and the 0 (0^h) vertex. Unlike the case in Section K 1, where M had no boundary, the sum in Eq. (K15) does not vanish. Instead, we have:

$$\begin{aligned}\sum_{t=\langle 1234\rangle\in M}&[\alpha^*(0^h1234)-\alpha^*(01234)]O_t\\&=\sum_{f=\langle 123\rangle\in\partial M}\alpha^*(00^h123)O_f,\end{aligned} \tag{K16}$$

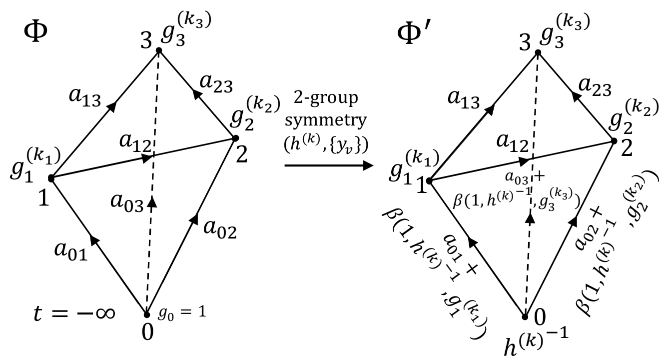

FIG. 30. When M has a boundary, the 2-group symmetry action is modified to act on the temporal links connected to vertices $v_\partial \in \partial M$. In the figure above, $\langle 123\rangle$ is a face in ∂M. The (local) 2-group symmetry, parameterized by $(h^{(k)},\{y_v\})$, maps Φ to a configuration $\tilde{\Phi}$, which satisfies: $d\tilde{\Phi} = d\Phi'$. Φ' is equivalent to changing Φ so that $g_0 = 1$ goes to $g_0 = {h^{(k)}}^{-1}$ and a_{0v_∂} goes to $a_{0v_\partial} + \beta(1,{h^{(k)}}^{-1}, g_{v_\partial}^{k_{v_\partial}})$. Acting on Φ with the local 1-form symmetry at a vertex in ∂M does not affect Φ'.

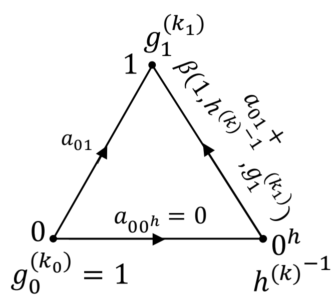

FIG. 31. To determine the effect of the 0-form symmetry action $V_B(h^{(k)})$ on α, we append a vertex 0^h, labeled by ${h^{(k)}}^{-1}$, to CM. The edges connected to 0^h and a vertex $v \in \partial M$ are labeled by $a_{0v} + \beta(1,{h^{(k)}}^{-1}, g_v^{(k_v)})$. The vertex 0 and 0^h are connected by the edge $\langle 00^h\rangle$, labeled by $a_{00^h} = 0$. When pulled back to this manifold, $(\epsilon+\beta)$ evaluates to zero on the face $\langle 00^h1\rangle$, as shown in Eq. (K18).

where $O_f \in \{-1,+1\}$ is the orientation of the face f with respect to the orientation of the boundary. Thus, the state constructed using α^* [Eq. (K2)] is not invariant under the symmetry in Eq. (K14).

To remedy this, we first observe that the cocycle $\alpha^* \in H^4(B\mathbb{L},\mathbb{R}/\mathbb{Z})$ can be written as:

$$\begin{aligned}\alpha^* &= \nu^* + \frac{1}{2}\rho^* \cup_1 \epsilon^* + \frac{1}{2}\epsilon^* \cup \epsilon^* \\ &= \delta\mu + \frac{1}{2}(\epsilon^*+\beta)\cup(\epsilon^*+\beta)\end{aligned} \tag{K17}$$

where μ is defined as $\mu \equiv \eta + \frac{1}{2}\beta \cup_1 \epsilon$. The leftover factor $\alpha^*(00^h123)$ in Eq. (K16) is equivalent to $\delta\mu(00^h123)$. This is because $(\epsilon+\beta)(00^h1)$ is trivial (Fig. 31):

$$\begin{aligned}(\epsilon+\beta)(00^h1) &= (\delta\boldsymbol{a}+\bar{\rho}+\beta)(00^h1) \\ &= 2\times\beta(1,{h^{(k)}}^{-1},g_1^{(k_1)}) + \rho(1,1,h^{-1},g_1) \\ &= 0,\end{aligned} \tag{K18}$$

where we have implicitly pulled back functions to cochains on the manifold with 0^h, and we have used that ρ is normalized. Therefore, the phase difference in Eq. (K16) is:

$$\begin{aligned}&\sum_{f=\langle 123\rangle\in\partial M} \alpha^*(00^h123)O_f \\ &\quad= \sum_{f=\langle 123\rangle\in\partial M} [\mu(0^h123)-\mu(0123)]O_f.\end{aligned} \tag{K19}$$

To form a symmetric wave function, we can include a factor of $-\mu(0ijk)$ for each face $f=\langle ijk\rangle$ in the boundary of M. According to Eq. (K19), the change in this factor under the symmetry action will precisely cancel the change from the α^* terms. Consequently, the following state is invariant under the symmetry action:

$$\begin{aligned}|\Psi_\mathrm{b}\rangle = \sum_{\Phi} \prod_{f_\partial=\langle 123\rangle\in\partial M} & e^{-2\pi i\mu(0123)O_f} \\ &\prod_{t=\langle 1234\rangle\in M} e^{2\pi i\alpha^*(01234)O_t}|\Phi\rangle,\end{aligned} \tag{K20}$$

where the sum is over all configurations Φ with the label for the 0 vertex fixed as $1\in L$ and the labels for the temporal edges $e\notin\overline{M}$ set to $0\in\mathbb{Z}_2$. By replacing the configurations $\{a_e\}$ on the edges in $\overline{M}$ with a 1-cochain $\boldsymbol{a}_e$ and using the notation introduced in the main text, we can write the state $|\Psi_\mathrm{b}\rangle$ more explicitly as:

$$\begin{aligned}|\Psi_\mathrm{b}\rangle = &\sum_{\{g_v,k_{v_\partial}\},\,\boldsymbol{a}_e} \prod_{f_\partial=\langle 123\rangle\in\partial M} e^{-2\pi i O_{f_\partial}\hat{\bar{\boldsymbol{\eta}}}(123)}(-1)^{\hat{\bar{\boldsymbol{\beta}}}(23)\delta\boldsymbol{a}(012)}(-1)^{\hat{\bar{\boldsymbol{\beta}}}(13)[\delta\boldsymbol{a}(123)+\hat{\bar{\boldsymbol{\rho}}}(123)]} \\ &\prod_{t=\langle 1234\rangle} e^{2\pi i O_t\hat{\bar{\boldsymbol{\nu}}}(1234)}(-1)^{\delta\boldsymbol{a}(012)\delta\boldsymbol{a}(234)}(-1)^{\hat{\bar{\boldsymbol{\rho}}}(134)[\delta\boldsymbol{a}(123)+\hat{\bar{\boldsymbol{\rho}}}(123)]+\hat{\bar{\boldsymbol{\rho}}}(124)[\delta\boldsymbol{a}(234)+\hat{\bar{\boldsymbol{\rho}}}(234)]}|\{g_v\},\{k_{v_\partial}\},\boldsymbol{a}_e\rangle.\end{aligned} \tag{K21}$$

The next steps in the construction of the supercohomology models on a manifold with boundary are to gauge the 1-form symmetry of $|\Psi_\mathrm{b}\rangle$ and to apply the fermionization duality. The 1-form symmetry can be gauged by applying the linear map Γ defined in Appendix C, which, up to a normalization factor, acts on a configuration state as:

$$\Gamma\big(|\{g_v\},\{k_{v_\partial}\},\boldsymbol{a}_e\rangle\big) = |\{g_v\},\{k_{v_\partial}\},\delta\boldsymbol{a}_e\rangle. \tag{K22}$$

A ground state of the bosonic shadow model is then simply $|\Psi_\mathrm{s}\rangle = \Gamma\big(|\Psi_\mathrm{b}\rangle\big)$.

Similar to the bulk construction in Section IV, we make a change of basis to ensure that the L symmetry is onsite. Here, the temporal edges in $\overline{M}$ are also included in the basis transformation. The basis change is implemented by the operator $\mathcal{R}$:

$$\mathcal{R} \equiv \prod_{e=\langle ij\rangle\in\partial M} X_{\langle 0ij\rangle}^{\hat{\overline{\boldsymbol{\beta}}}(e)} \prod_{f\in M} X_f^{\hat{\overline{\boldsymbol{\rho}}}(f)}. \tag{K23}$$

Letting $\boldsymbol{a}_f$ denote a 2-cochain on $\overline{M}$, the action of $\mathcal{R}$ on a configuration state is:

$$\mathcal{R}|\{g_v\},\{k_{v_\partial}\},\boldsymbol{a}_f\rangle = |\{g_v\},\{k_{v_\partial}\},\boldsymbol{a}_f+\boldsymbol{B}_f\rangle, \tag{K24}$$

where $\boldsymbol{B}_f$ is the 2-cochain satisfying:

$$\begin{aligned}\boldsymbol{B}_f(\langle ijk\rangle) &= \rho(1,g_i,g_j,g_k), && \forall\langle ijk\rangle\in M\\ \boldsymbol{B}_f(\langle 0ij\rangle) &= \beta(1,g_i^{(k_i)},g_j^{(k_j)}), && \forall\langle ij\rangle\in\partial M.\end{aligned} \tag{K25}$$

Further, we define a new basis by the identification:

$$\begin{aligned}|\{g_v\},\{k_{v_\partial}\},\boldsymbol{a}_f\rangle' &\equiv \mathcal{R}|\{g_v\},\{k_{v_\partial}\},\boldsymbol{a}_f\rangle\\ &= |\{g_v\},\{k_{v_\partial}\},\boldsymbol{a}_f+\boldsymbol{B}_f\rangle.\end{aligned} \tag{K26}$$

In this basis, the 0-form L symmetry is onsite:

$$\begin{aligned}&V(h^{(k)})|\{g_v\},\{k_{v_\partial}\},\boldsymbol{a}_f\rangle'\\ &\quad= |\{hg_v\},\{k+k_{v_\partial}+m(1,h,hg_{v_\partial})\},\boldsymbol{a}_f\rangle'.\end{aligned} \tag{K27}$$

We also re-define the Pauli operators in this basis so that:

$$\begin{aligned}X_{f'}|\{g_v\},\{k_{v_\partial}\},\boldsymbol{a}_f\rangle' &= |\{g_v\},\{k_{v_\partial}\},\boldsymbol{a}_f+\boldsymbol{f'}\rangle'\\ Z_{f'}|\{g_v\},\{k_{v_\partial}\},\boldsymbol{a}_f\rangle' &= (-1)^{\boldsymbol{a}_f(f')}|\{g_v\},\{k_{v_\partial}\},\boldsymbol{a}_f\rangle'.\end{aligned} \tag{K28}$$

Finally, the shadow model ground state $|\Psi_\mathrm{s}\rangle$ can be written as:

$$\begin{aligned}|\Psi_s\rangle = &\sum_{\{g_v,k_{v_\partial}\},\,\boldsymbol{a}_e} \prod_{f_\partial=\langle 123\rangle\in\partial M} e^{-2\pi i[\hat{\overline{\boldsymbol{\eta}}}(123)+\frac{1}{2}\hat{\overline{\boldsymbol{\beta}}}(12)\hat{\overline{\boldsymbol{\beta}}}(23)]O_{f_\partial}} Z_{012}^{\hat{\overline{\boldsymbol{\beta}}}(23)} Z_{123}^{\hat{\overline{\boldsymbol{\beta}}}(13)}\\ &\prod_{t=\langle 1234\rangle} e^{2\pi i\,\hat{\overline{\boldsymbol{\nu}}}(1234)O_t}(-1)^{\delta\boldsymbol{a}(012)\delta\boldsymbol{a}(234)} Z_{123}^{\hat{\overline{\boldsymbol{\rho}}}(134)} Z_{234}^{\hat{\overline{\boldsymbol{\rho}}}(124)}|\{g_v\},\{k_{v_\partial}\},\delta\boldsymbol{a}_e+\boldsymbol{B}_f\rangle'.\end{aligned} \tag{K29}$$

Next, we write $|\Psi_\mathrm{s}\rangle$ in a form that can be more readily fermionized using the duality in Appendix F or equivalently Ref. [22]. First, the $\boldsymbol{B}_f$ factor in Eq. (K29) can be expressed using X_f operators:

$$\begin{aligned}|\Psi_s\rangle = &\sum_{\{g_v,k_{v_\partial}\},\boldsymbol{a}_e} \prod_{f_\partial=\langle 123\rangle\in\partial M} e^{-2\pi i[\hat{\overline{\boldsymbol{\eta}}}(123)+\frac{1}{2}\hat{\overline{\boldsymbol{\beta}}}(12)\hat{\overline{\boldsymbol{\beta}}}(23)]O_{f_\partial}} Z_{012}^{\hat{\overline{\boldsymbol{\beta}}}(23)} Z_{123}^{\hat{\overline{\boldsymbol{\beta}}}(13)} \prod_{\langle ij\rangle\in\partial M} X_{0ij}^{\hat{\overline{\boldsymbol{\beta}}}(ij)}\\ &\prod_{t=\langle 1234\rangle\in M} e^{2\pi i\,\hat{\overline{\boldsymbol{\nu}}}(1234)O_t}(-1)^{\delta\boldsymbol{a}(012)\delta\boldsymbol{a}(234)} Z_{123}^{\hat{\overline{\boldsymbol{\rho}}}(134)} Z_{234}^{\hat{\overline{\boldsymbol{\rho}}}(124)} \prod_{f\in M} X_f^{\hat{\overline{\boldsymbol{\rho}}}(f)}|\{g_v\},\{k_{v_\partial}\},\delta\boldsymbol{a}_e\rangle'\end{aligned} \tag{K30}$$

Then, the Pauli X and Pauli Z operators can be commuted to form the fermionizable operators $\bar{U}_{\bar{\beta}}$ and $\bar{U}_{\bar{\rho}}$, defined as:

$$\bar{U}_{\bar{\beta}} \equiv \prod_{f'\in\overline{M}} Z_{f'}^{\int_{\overline{M}}\hat{\boldsymbol{\beta}}\cup_1\boldsymbol{f'}} \prod_{\langle ij\rangle\in\partial M} X_{0ij}^{\hat{\overline{\boldsymbol{\beta}}}(ij)}, \qquad \text{and} \qquad \bar{U}_{\bar{\rho}} \equiv \prod_{f'\in\overline{M}} Z_{f'}^{\int_M\hat{\boldsymbol{\rho}}\cup_1\boldsymbol{f'}} \prod_{f\in M} X_f^{\hat{\overline{\boldsymbol{\rho}}}(f)}, \tag{K31}$$

where $\hat{\boldsymbol{\beta}}(\langle ijk\rangle)|\{g_v\},\{k_{v_\partial}\},\boldsymbol{a}_e\rangle = \beta(g_i^{(k_i)},g_j^{(k_j)},g_k^{(k_k)})|\{g_v\},\{k_{v_\partial}\},\boldsymbol{a}_e\rangle$ for $i,j,k\in\partial M\cup\{0\}$. With this, the shadow state $|\Psi_\mathrm{s}\rangle$ can be written as:

$$\begin{aligned}|\Psi_s\rangle = &\prod_{f_\partial=\langle 123\rangle\in\partial M} e^{-2\pi i[\hat{\overline{\boldsymbol{\eta}}}(123)+\frac{1}{2}\hat{\overline{\boldsymbol{\beta}}}(12)\hat{\overline{\boldsymbol{\beta}}}(23)]O_{f_\partial}}\bar{U}_{\bar{\beta}} \prod_{t=\langle 1234\rangle} e^{2\pi i\,\hat{\overline{\boldsymbol{\nu}}}(1234)O_t}\bar{U}_{\bar{\rho}}\\ &\sum_{\{g_v,k_{v_\partial}\},\boldsymbol{a}_e} \prod_{f_\partial=\langle 123\rangle\in\partial M}(-1)^{\boldsymbol{a}(01)\delta\boldsymbol{a}(123)} \prod_{t=\langle 1234\rangle}(-1)^{\boldsymbol{a}(12)\delta\boldsymbol{a}(234)}|\{g_v\},\{k_{v_\partial}\},\delta\boldsymbol{a}_e\rangle'.\end{aligned} \tag{K32}$$

To write Eq. (K32), we have also used Stokes' theorem:

$$\int_{CM}\delta\boldsymbol{a}\cup\delta\boldsymbol{a} = \int_{\overline{M}}\boldsymbol{a}\cup\delta\boldsymbol{a}. \tag{K33}$$

The state in Eq. (K32) can be fermionized straightforwardly. First of all, the second line in Eq. (K32) is precisely a ground state of the twisted toric code on $\overline{M}$. Therefore, it is dual to the ground state of an atomic insulator. Furthermore, according to Appendix F, the operators $\bar{U}_{\bar{\beta}}$ and $\bar{U}_{\bar{\rho}}$ can be fermionized to the product of hopping operators:

$$\bar{U}_{\bar{\beta}} \to \xi_\beta(\partial M) \prod_{\langle 0ij\rangle} S_{0ij}^{\hat{\bar{\boldsymbol{\beta}}}(ij)}, \text{ and } \bar{U}_{\bar{\rho}} \to \xi_\rho(M) \prod_{f\in M} S_f^{\hat{\bar{\boldsymbol{\rho}}}(f)}. \tag{K34}$$

Here, $\xi_\beta(\partial M)$ is a sign that depends on an ordering of the faces $\langle 0ij\rangle$, where $\langle ij\rangle$ is some edge in ∂M. It compensates for the order dependence of the product of hopping operators and is explicitly:

$$\xi_\beta(\partial M) \equiv \prod_{e_i,e_{i'}\in\partial M | i<i'} (-1)^{\hat{\bar{\boldsymbol{\beta}}}(e_i)\hat{\bar{\boldsymbol{\beta}}}(e_{i'}) \int_{\partial M} \boldsymbol{e}_{i'}\cup\boldsymbol{e}_i}. \tag{K35}$$

$\xi_\rho(M)$ is defined in Section IV D and Appendix H 2. Fermionization thus results in the supercohomology state:

$$|\Psi_f\rangle = \prod_{f_\partial} e^{-2\pi i O_{f_\partial}[\hat{\bar{\boldsymbol{\eta}}}(f_\partial)+\frac{1}{2}\hat{\bar{\boldsymbol{\beta}}}\cup\hat{\bar{\boldsymbol{\beta}}}(f_\partial)]} \xi_\beta(\partial M) \prod_{e_\partial} S_{e_\partial}^{\hat{\bar{\boldsymbol{\beta}}}(e_\partial)} \prod_t e^{2\pi i O_t \hat{\bar{\boldsymbol{\nu}}}(t)} \xi_\rho(M) \prod_f S_f^{\hat{\bar{\boldsymbol{\rho}}}(f)} \sum_{\{g_v\},\{k_{v_\partial}\}} |\{g_v\},\{k_{v_\partial}\},\text{vac}\rangle, \tag{K36}$$

where the second product is over edges e_∂ in ∂M, S_{e_∂} is the hopping operator associated to the face formed by e_∂ and the 0 vertex, and $|\text{vac}\rangle$ is the fermionic state with zero fermion occupancy at each site. The fermionic d.o.f. on the tetrahedra in $\overline{M}\setminus M$ can be associated to faces in ∂M as in Section V B.

From Eq. (K36), we see that the supercohomology state $|\Psi_f\rangle$ can be prepared from a symmetric product state by the FDQC:

$$\tilde{\mathcal{U}}_f^L \equiv \prod_{f_\partial} e^{-2\pi i O_{f_\partial}[\hat{\bar{\boldsymbol{\eta}}}(f_\partial)+\frac{1}{2}\hat{\bar{\boldsymbol{\beta}}}\cup\hat{\bar{\boldsymbol{\beta}}}(f_\partial)]} \xi_\beta(\partial M) \prod_{e_\partial} S_{e_\partial}^{\hat{\bar{\boldsymbol{\beta}}}(e_\partial)} \prod_t e^{2\pi i O_t \hat{\bar{\boldsymbol{\nu}}}(t)} \xi_\rho(M) \prod_f S_f^{\hat{\bar{\boldsymbol{\rho}}}(f)} \tag{K37}$$

However, $\tilde{\mathcal{U}}_f^L$ is not symmetric. A symmetric FDQC can be formed by multiplying on the right by a product of parity operators:

$$\prod_t P_t^{\int_{\overline{M}} \boldsymbol{B}_f \cup_2 \boldsymbol{t}}. \tag{K38}$$

This is analogous to the product of parity operators in the definition of $\mathcal{U}_f$ on a manifold without boundary in Eq. (165). The product of parity operators does not change the state produced by $\tilde{\mathcal{U}}_f^L$, since $|\text{vac}\rangle$ is a $+1$ eigenstate of the parity operators. Using the definition of $\boldsymbol{B}_f$ in Eq. (K25) and the explicit formulas for the cup products, the product of parity operators in Eq. (K38) can be decomposed into:

$$\prod_t P_t^{\int_{\overline{M}} \boldsymbol{B}_f \cup_2 \boldsymbol{t}} = \prod_t P_t^{\int_M \hat{\bar{\boldsymbol{\rho}}}\cup_2 \boldsymbol{t}} \prod_{f\in\partial M} P_f^{\int_{\partial M} \boldsymbol{f}\cup_1 \hat{\bar{\boldsymbol{\beta}}}}. \tag{K39}$$

Thus, the FDQC $\mathcal{U}_f^L$ in the main text is produced by composing $\tilde{\mathcal{U}}_f^L$ with the product of parity operators above:

$$\mathcal{U}_f^L = \prod_{f_\partial} e^{-2\pi i O_{f_\partial} \hat{\bar{\boldsymbol{\eta}}}(f_\partial)} \chi_\beta(\partial M) \prod_{e_\partial} S_{e_\partial}^{\hat{\bar{\boldsymbol{\beta}}}(e_\partial)} \prod_{f_\partial} P_{f_\partial}^{\int_{\partial M} \boldsymbol{f}_\partial \cup_1 \hat{\bar{\boldsymbol{\beta}}}} \times \prod_t e^{2\pi i O_t \hat{\bar{\boldsymbol{\nu}}}(t)} \xi_\rho(M) \prod_f S_f^{\hat{\bar{\boldsymbol{\rho}}}(f)} \prod_t P_t^{\int_M \hat{\bar{\boldsymbol{\rho}}}\cup_2 \boldsymbol{t}}. \tag{K40}$$

Here, we have absorbed the sign from commuting parity operators and the $\frac{1}{2}\hat{\bar{\boldsymbol{\beta}}}\cup\hat{\bar{\boldsymbol{\beta}}}$ factor into $\chi_\beta(\partial M)$, defined as:

$$\chi_\beta(\partial M) \equiv (-1)^{\int_{\partial M} \left(\hat{\bar{\boldsymbol{\beta}}}\cup_1\hat{\bar{\boldsymbol{\beta}}} + \delta\hat{\bar{\boldsymbol{\beta}}}\cup_1\hat{\bar{\boldsymbol{\beta}}} + \hat{\bar{\boldsymbol{\beta}}}\cup\hat{\bar{\boldsymbol{\beta}}}\right)} \xi_\beta(\partial M). \tag{K41}$$

Appendix L: Trivialization of supercohomology data: $G_f = \mathbb{Z}_2 \times \mathbb{Z}_4 \times \mathbb{Z}_2^f$

In this appendix, we give an example of using a symmetry extension to trivialize the supercohomology data, as described in the construction of the gapped boundaries of supercohomology models in Section V. We consider a fSPT phase protected by a $G_f = \mathbb{Z}_2 \times \mathbb{Z}_4 \times \mathbb{Z}_2^f$ symmetry, and we identify two possible symmetry extensions that trivialize the supercohomology data. We note that a gapped boundary for the particular $G_f = \mathbb{Z}_2 \times \mathbb{Z}_4 \times \mathbb{Z}_2^f$ phase has been found in Refs. [56] and [62].

To get started, we describe the supercohomology data (ρ,ν) corresponding to our phase of interest. We represent a generic group element as $(g,h) \in \mathbb{Z}_2 \times \mathbb{Z}_4$ where $g = 0,1$ and $h = 0,1,2,3$, and use the notation $[\cdots]_{\boldsymbol{N}}$ to denote modulo N. The cocycle ρ can be obtained from a decorated domain-wall picture. Namely, a $(2+1)$D $\mathcal{N}=2$ supercohomology SPT with $\mathbb{Z}_2$ symmetry is decorated on the $\mathbb{Z}_4$ domain walls. The supercohomology data for the $(2+1)$D phase (in homogeneous variables) is given by[16]:

$$n_2(g_0,g_1,g_2) = [g_0-g_1]_{\boldsymbol{2}}[g_1-g_2]_{\boldsymbol{2}}, \tag{L1}$$

$$\nu_3(g_0,g_1,g_2,g_3) = \frac{1}{4}[g_0-g_1]_{\boldsymbol{2}}[g_1-g_2]_{\boldsymbol{2}}[g_2-g_3]_{\boldsymbol{2}}. \tag{L2}$$

Therefore, the cocycle $\rho \in Z^3(\mathbb{Z}_2\times\mathbb{Z}_4,\mathbb{Z}_2)$ takes the form:

$$\rho = n_2 \cup \phi_1 \tag{L3}$$

where the class of ϕ_1 is the generator of $H^1(\mathbb{Z}_4,\mathbb{Z}_2)$ given by $\phi_1(h_0,h_1) = [h_0-h_1]_{\boldsymbol{2}}$, and both cocycles are implicitly pulled back via the projection map to each subgroup. Explicitly, the supercohomology data can be chosen to be:

$$\rho((g_0,h_0),(g_1,h_1),(g_2,h_2),(g_3,h_3)) = [g_0-g_1]_{\boldsymbol{2}}[g_1-g_2]_{\boldsymbol{2}}[h_2-h_3]_{\boldsymbol{2}}, \tag{L4}$$

$$\nu((g_0,h_0),(g_1,h_1),(g_2,h_2),(g_3,h_3),(g_4,h_4)) = \frac{1}{4}[g_0-g_1]_{\boldsymbol{2}}[g_1-g_2]_{\boldsymbol{2}}[g_2-g_3]_{\boldsymbol{2}}[h_3-h_4]_{\boldsymbol{4}} \tag{L5}$$

One can verify that they indeed satisfy the supercohomology equations in Eq. (2).

To construct a symmetric gapped boundary, we perform two symmetry extensions to trivialize the supercohomology data. First, we extend by $\mathbb{Z}_2$ to trivialize ρ_3. The extension is given by:

$$1 \to \mathbb{Z}_2 \to \mathbb{Z}_4 \times \mathbb{Z}_4 \xrightarrow{\pi_1} \mathbb{Z}_2 \times \mathbb{Z}_4 \to 1 \tag{L6}$$

where π_1 is the projector $\pi_1\big((g,h)\big) = ([g]_{\mathbf{2}}, h)$. The pulled-back cocycle ρ^* is a coboundary of the cochain:

$$\beta_2\big((g_0, g_1), (g_1, h_1), (g_2, h_2)\big) = \left\lfloor \frac{g_0 - g_1}{2} \right\rfloor [h_1 - h_2]_{\mathbf{2}}. \tag{L7}$$

The next step is to trivialize the following cocycle:

$$\omega \equiv \nu^* + \frac{1}{2}\beta \cup \beta + \frac{1}{2}\beta \cup_1 \delta\beta \tag{L8}$$

which was defined in Eq. (200). However, because ω has a very complicated closed form, we instead identify the cohomology class of ω in $H^4(\mathbb{Z}_4 \times \mathbb{Z}_4, \mathbb{R}/\mathbb{Z}) \cong \mathbb{Z}_4^2$ by using topological invariants that completely distinguish the elements of the above cohomology group [9, 59]. In particular, for inhomogeneous cocycles, the invariants of the cohomology group $H^4(\mathbb{Z}_{N_i} \times \mathbb{Z}_{N_j}, \mathbb{R}/\mathbb{Z}) \cong \mathbb{Z}^2_{\gcd(N_i,N_j)}$ are given by:

$$\begin{aligned}
\mathcal{I}_1 &= \sum_{n=0}^{N_j-1} i_{(1,0)}\omega\big((0,1),(0,n),(0,1)\big), \\
\mathcal{I}_2 &= \sum_{n=0}^{N_i-1} i_{(0,1)}\omega\big((1,0),(n,0),(1,0)\big).
\end{aligned}$$

where $i_g\omega$ is called the slant product of g and ω and is defined as

$$\begin{aligned}
i_g\omega(a,b,c) = \omega(g,a,b,c) - \omega(a,g,b,c) \\
+ \omega(a,b,g,c) - \omega(a,b,c,g).
\end{aligned} \tag{L9}$$

We stress that the quantities above are invariant under adding a coboundary to ω.

In our case, the topological invariants are valued in $\mathbb{R}/\mathbb{Z}$ and are multiples of $\frac{1}{4}$:

$$\mathcal{I}_1 = \sum_{n=0}^{3} i_{(1,0)}\omega\big((0,n+2),(0,n+1),(0,1),(0,0)\big), \tag{L10}$$

$$\mathcal{I}_2 = \sum_{n=0}^{3} i_{(0,1)}\omega\big((n+2,0),(n+1,0),(1,0),(0,0)\big). \tag{L11}$$

where the equations above are now using homogeneous cocycles Computing the invariants for the cocycle ω given in Eq. (L8), we find $\mathcal{I}_1 = 0$ and $\mathcal{I}_2 = \frac{1}{2}$.

One can also check that the following "canonical" cocycle

$$\begin{aligned}
&\omega^{\text{can}}\big((g_0,h_0),(g_1,h_1),(g_2,h_2),(g_3,h_3),(g_4,h_4)\big) \\
&= \frac{1}{8}[g_0 - g_1]_{\mathbf{4}}[h_3 - h_4]_{\mathbf{4}} \\
&\times \big([g_1 - g_2]_{\mathbf{4}} + [g_2 - g_3]_{\mathbf{4}} - [g_1 - g_3]_{\mathbf{4}}\big)
\end{aligned} \tag{L12}$$

has the same topological invariants, and therefore is in the same cohomology class as the previous cocycle. It follows that the two must differ by a coboundary

$$\omega = \omega^{\text{can}} + \delta\lambda \tag{L13}$$

For some group 3-cochain λ. Although we do not have a closed form for λ, it can in principle be obtained by numerically solving linear equations $\delta\lambda = \omega - \omega^{\text{can}}$ using the Smith decomposition. We refer to Appendix G of Ref. [59] for further details.

We can now perform a second symmetry extension. Here, we present two possible extensions. The first is given by

$$1 \to \mathbb{Z}_2 \to \mathbb{Z}_8 \times \mathbb{Z}_4 \xrightarrow{\pi_2} \mathbb{Z}_4 \times \mathbb{Z}_4 \to 1, \tag{L14}$$

where, $\pi_2\big((g,h)\big) = ([g]_{\mathbf{4}}, h)$, and the second is given by

$$1 \to \mathbb{Z}_2 \to \mathbb{Z}_4 \times \mathbb{Z}_8 \xrightarrow{\pi_3} \mathbb{Z}_4 \times \mathbb{Z}_4 \to 1, \tag{L15}$$

where $\pi_3\big((g,h)\big) = (g, [h]_{\mathbf{4}})$. One can check that the pulled back canonical cocycles are trivialized in both cases by computing similar topological invariants of cocycles in the extended groups. This means that $\pi^*\omega^{\text{can}} = \delta\eta^{\text{can}}$ for some choice of η, where $\pi = \pi_2 \circ \pi_1$ or $\pi = \pi_3 \circ \pi_1$ depending on the choice of extension. It follows that we can choose

$$\eta = \eta^{\text{can}} + \lambda, \tag{L16}$$

so that $\delta\eta = \pi^*\omega$, as desired.

We have two extensions that trivialize the supercohomology data, one is an extension by $K = \mathbb{Z}_2 \times \mathbb{Z}_2$ and the other is by $K = \mathbb{Z}_4$. To build the gapped boundary, we gauge the K symmetry, these give a $\mathbb{Z}_2 \times \mathbb{Z}_2$ gauge theory and a $\mathbb{Z}_4$ gauge theory, respectively. It would be interesting to compare the $\mathbb{Z}_4$ anomalous topological order here with that found in Refs. [56] and [62]. It would also be interesting to study the anomalous $\mathbb{Z}_2 \times \mathbb{Z}_2$ topological order.

[1] Michael Levin and Zheng-Cheng Gu, "Braiding statistics approach to symmetry-protected topological phases," Phys. Rev. B **86**, 115109 (2012).

[2] Anton Kapustin, "Bosonic topological insulators and paramagnets: a view from cobordisms," (2014), arXiv:1404.6659.

[3] Anton Kapustin, Ryan Thorngren, Alex Turzillo, and Zitao Wang, "Fermionic symmetry protected topological phases and cobordisms," Journal of High Energy Physics **2015**, 1–21 (2015).

[4] Xiao-Gang Wen, "Construction of bosonic symmetry-protected-trivial states and their topological invariants via $G \times SO(\infty)$ nonlinear σ models," Phys. Rev. B **91**, 205101 (2015).

[5] Charles Zhaoxi Xiong, "Minimalist approach to the classification of symmetry protected topological phases," Journal of Physics A: Mathematical and Theoretical **51**, 445001 (2018).

[6] Davide Gaiotto and Theo Johnson-Freyd, "Symmetry protected topological phases and generalized cohomology," Journal of High Energy Physics **2019**, 7 (2019).

[7] Meng Cheng, Nathanan Tantivasadakarn, and Chenjie Wang, "Loop braiding statistics and interacting fermionic symmetry-protected topological phases in three dimensions," Phys. Rev. X **8**, 011054 (2018).

[8] Chenjie Wang, Chien-Hung Lin, and Zheng-Cheng Gu, "Interacting fermionic symmetry-protected topological phases in two dimensions," Phys. Rev. B **95**, 195147 (2017).

[9] Chenjie Wang and Michael Levin, "Topological invariants for gauge theories and symmetry-protected topological phases," Phys. Rev. B **91**, 165119 (2015).

[10] Chenjie Wang, "Braiding statistics and classification of two-dimensional charge-$2m$ superconductors," Phys. Rev. B **94**, 085130 (2016).

[11] Jing-Ren Zhou, Qing-Rui Wang, Chenjie Wang, and Zheng-Cheng Gu, "Non-Abelian Three-Loop Braiding Statistics for 3D Fermionic Topological Phases," arXiv e-prints , arXiv:1912.13505 (2019), arXiv:1912.13505 [cond-mat.str-el].

[12] Dominic V. Else and Chetan Nayak, "Classifying symmetry-protected topological phases through the anomalous action of the symmetry on the edge," Phys. Rev. B **90**, 235137 (2014).

[13] Meng Cheng, "Symmetry Fractionalization in Three-Dimensional $\mathbb{Z}_2$ Topological Order and Fermionic Symmetry-Protected Phases," arXiv e-prints , arXiv:1511.02563 (2015), arXiv:1511.02563 [cond-mat.str-el].

[14] Lukasz Fidkowski and Ashvin Vishwanath, "Realizing anomalous anyonic symmetries at the surfaces of three-dimensional gauge theories," Phys. Rev. B **96**, 045131 (2017).

[15] Xie Chen, Zheng-Cheng Gu, Zheng-Xin Liu, and Xiao-Gang Wen, "Symmetry protected topological orders and the group cohomology of their symmetry group," Phys. Rev. B **87**, 155114 (2013).

[16] Zheng-Cheng Gu and Xiao-Gang Wen, "Symmetry-protected topological orders for interacting fermions: Fermionic topological nonlinear σ models and a special group supercohomology theory," Phys. Rev. B **90**, 115141 (2014).

[17] Qing-Rui Wang and Zheng-Cheng Gu, "Towards a complete classification of symmetry-protected topological phases for interacting fermions in three dimensions and a general group supercohomology theory," Phys. Rev. X **8**, 011055 (2018).

[18] Xie Chen, Zheng-Cheng Gu, and Xiao-Gang Wen, "Local unitary transformation, long-range quantum entanglement, wave function renormalization, and topological order," Phys. Rev. B **82**, 155138 (2010).

[19] Juven Wang, Xiao-Gang Wen, and Edward Witten, "Symmetric gapped interfaces of spt and set states: Systematic constructions," Phys. Rev. X **8**, 031048 (2018).

[20] Anton Kapustin and Ryan Thorngren, "Fermionic spt phases in higher dimensions and bosonization," Journal of High Energy Physics **2017**, 80 (2017).

[21] Lakshya Bhardwaj, Davide Gaiotto, and Anton Kapustin, "State sum constructions of spin-tfts and string net constructions of fermionic phases of matter," Journal of High Energy Physics **2017**, 96 (2017).

[22] Yu-An Chen and Anton Kapustin, "Bosonization in three spatial dimensions and a 2-form gauge theory," Phys. Rev. B **100**, 245127 (2019).

[23] Tyler D. Ellison and Lukasz Fidkowski, "Disentangling interacting symmetry-protected phases of fermions in two dimensions," Phys. Rev. X **9**, 011016 (2019).

[24] Nathanan Tantivasadakarn and Ashvin Vishwanath, "Full commuting projector hamiltonians of interacting symmetry-protected topological phases of fermions," Phys. Rev. B **98**, 165104 (2018).

[25] Tian Lan, Chenchang Zhu, and Xiao-Gang Wen, "Fermion decoration construction of symmetry-protected trivial order for fermion systems with any symmetry and in any dimension," Phys. Rev. B **100**, 235141 (2019).

[26] Ryohei Kobayashi, Kantaro Ohmori, and Yuji Tachikawa, "On gapped boundaries for spt phases beyond group cohomology," Journal of High Energy Physics **2019**, 131 (2019).

[27] Andreas P Schnyder, Shinsei Ryu, Akira Furusaki, and Andreas WW Ludwig, "Classification of topological insulators and superconductors in three spatial dimensions," Physical Review B **78**, 195125 (2008).

[28] Alexei Kitaev, "Periodic table for topological insulators and superconductors," in *AIP conference proceedings*, Vol. 1134 (American Institute of Physics, 2009) pp. 22–30.

[29] Shinsei Ryu, Andreas P Schnyder, Akira Furusaki, and Andreas WW Ludwig, "Topological insulators and superconductors: tenfold way and dimensional hierarchy," New Journal of Physics **12**, 065010 (2010).

[30] Yu-An Chen, "Exact bosonization in arbitrary dimensions," (2019), arXiv:1911.00017.

[31] Yu-An Chen, Anton Kapustin, and Djordje Radicevic, "Exact bosonization in two spatial dimensions and a new class of lattice gauge theories," Annals of Physics **393**, 234 – 253 (2018).

[32] Anton Kapustin and Ryan Thorngren, "Higher symmetry and gapped phases of gauge theories," in *Algebra, Geometry, and Physics in the 21st Century: Kontsevich Festschrift*, edited by Denis Auroux, Ludmil Katzarkov, Tony Pantev, Yan Soibelman, and Yuri Tschinkel (Springer International Publishing, Cham, 2017) pp. 177–202.

[33] Beni Yoshida, "Topological phases with generalized global symmetries," Phys. Rev. B **93**, 155131 (2016).

[34] Lokman Tsui and Xiao-Gang Wen, "Lattice models that realize $\mathbb{Z}_n$-1 symmetry-protected topological states for even n," Phys. Rev. B **101**, 035101 (2020).

[35] Michael Levin and Xiao-Gang Wen, "Fermions, strings, and gauge fields in lattice spin models," Phys. Rev. B **67**, 245316 (2003).

[36] Kyle Kawagoe and Michael Levin, "Microscopic definitions of anyon data," Phys. Rev. B **101**, 115113 (2020).

[37] David Aasen, Ethan Lake, and Kevin Walker, "Fermion con-

densation and super pivotal categories," Journal of Mathematical Physics **60**, 121901 (2019).

[38] Chris Heinrich, Fiona Burnell, Lukasz Fidkowski, and Michael Levin, "Symmetry-enriched string nets: Exactly solvable models for set phases," Phys. Rev. B **94**, 235136 (2016).

[39] Yuji Tachikawa, "On gauging finite subgroups," arXiv e-prints , arXiv:1712.09542 (2017), arXiv:1712.09542 [hep-th].

[40] Qing-Rui Wang, Yang Qi, and Zheng-Cheng Gu, "Anomalous Symmetry Protected Topological States in Interacting Fermion Systems," Phys. Rev. Lett. **123**, 207003 (2019).

[41] Andrew C. Potter and Romain Vasseur, "Symmetry constraints on many-body localization," Phys. Rev. B **94**, 224206 (2016).

[42] David A. Huse, Rahul Nandkishore, Vadim Oganesyan, Arijeet Pal, and S. L. Sondhi, "Localization-protected quantum order," Phys. Rev. B **88**, 014206 (2013).

[43] Yasaman Bahri, Ronen Vosk, Ehud Altman, and Ashvin Vishwanath, "Localization and topology protected quantum coherence at the edge of hot matter," Nat. Commun. **6** (2015).

[44] Arijeet Pal and David A. Huse, "Many-body localization phase transition," Phys. Rev. B **82**, 174411 (2010).

[45] Anushya Chandran, Vedika Khemani, C. R. Laumann, and S. L. Sondhi, "Many-body localization and symmetry-protected topological order," Phys. Rev. B **89**, 144201 (2014).

[46] Bela Bauer and Chetan Nayak, "Area laws in a many-body localized state and its implications for topological order," Journal of Statistical Mechanics: Theory and Experiment **2013**, P09005 (2013).

[47] Dominic V. Else, Bela Bauer, and Chetan Nayak, "Prethermal phases of matter protected by time-translation symmetry," Phys. Rev. X **7**, 011026 (2017).

[48] Jeongwan Haah, Lukasz Fidkowski, and Matthew B. Hastings, "Nontrivial Quantum Cellular Automata in Higher Dimensions," arXiv e-prints , arXiv:1812.01625 (2018), arXiv:1812.01625 [quant-ph].

[49] Lukasz Fidkowski, Xie Chen, and Ashvin Vishwanath, "Non-abelian topological order on the surface of a 3d topological superconductor from an exactly solved model," Phys. Rev. X **3**, 041016 (2013).

[50] Nicolas Tarantino and Lukasz Fidkowski, "Discrete spin structures and commuting projector models for two-dimensional fermionic symmetry-protected topological phases," Phys. Rev. B **94**, 115115 (2016).

[51] Zitao Wang, Shang-Qiang Ning, and Xie Chen, "Exactly solvable model for two-dimensional topological superconductors," Phys. Rev. B **98**, 094502 (2018).

[52] Qing-Rui Wang and Zheng-Cheng Gu, "Construction and classification of symmetry protected topological phases in interacting fermion systems," arXiv e-prints , arXiv:1811.00536 (2018), arXiv:1811.00536 [cond-mat.str-el].

[53] Jun Ho Son and Jason Alicea, "Commuting-projector hamiltonians for two-dimensional topological insulators: Edge physics and many-body invariants," Phys. Rev. B **100**, 155107 (2019).

[54] Ryohei Kobayashi, "Commuting projector models for (3+1)d topological superconductors via string net of (1+1)d topological superconductors," arXiv e-prints , arXiv:2006.00159 (2020), arXiv:2006.00159 [cond-mat.str-el].

[55] Max A Metlitski, "A 1d lattice model for the boundary of the quantum spin-hall insulator," arXiv preprint arXiv:1908.08958 (2019).

[56] Lukasz Fidkowski, Ashvin Vishwanath, and Max A. Metlitski, "Surface Topological Order and a new 't Hooft Anomaly of Interaction Enabled 3+1D Fermion SPTs," arXiv e-prints , arXiv:1804.08628 (2018), arXiv:1804.08628 [cond-mat.str-el].

[57] N. E. Steenrod, "Products of cocycles and extensions of mappings," Annals of Mathematics **48**, 290–320 (1947).

[58] Richard Z Goldstein and Edward C Turner, "A formula for stiefel-whitney homology classes," Proceedings of the American Mathematical Society **58**, 339–342 (1976).

[59] Nathanan Tantivasadakarn, "Dimensional reduction and topological invariants of symmetry-protected topological phases," Phys. Rev. B **96**, 195101 (2017).

[60] Davide Gaiotto and Anton Kapustin, "Spin tqfts and fermionic phases of matter," International Journal of Modern Physics A **31**, 1645044 (2016).

[61] Robbert Dijkgraaf and Edward Witten, "Topological Gauge Theories and Group Cohomology," Commun. Math. Phys. **129**, 393 (1990).

[62] Meng Cheng, "Fermionic lieb-schultz-mattis theorems and weak symmetry-protected phases," Phys. Rev. B **99**, 075143 (2019).